Scientific Research and Essays

Volume 9 Number 8 30 April 2014

ISSN 1992-2248

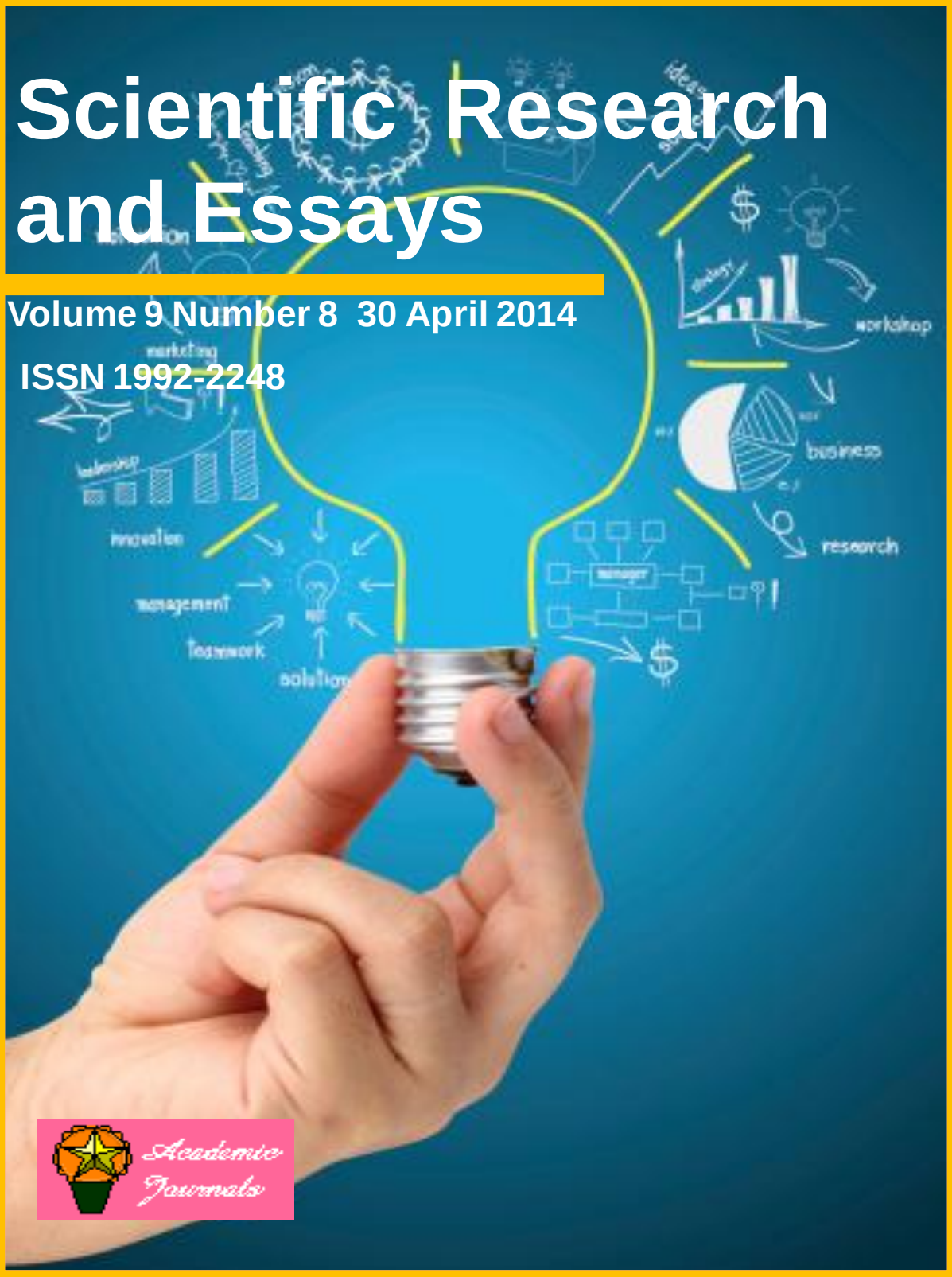

Academic Journals

ABOUT SRE

The **Scientific Research and Essays (SRE)** is published weekly (one volume per year) by Academic Journals.

Scientific Research and Essays (SRE) is an open access journal with the objective of publishing quality research articles in science, medicine, agriculture and engineering such as Nanotechnology, Climate Change and Global Warming, Air Pollution Management and Electronics etc. All papers published by SRE are blind peer reviewed.

Submission of Manuscript

Submit manuscripts as e-mail attachment to the Editorial Office at: sre@academicjournals.org. A manuscript number will be mailed to the corresponding author shortly after submission.

The Scientific Research and Essays will only accept manuscripts submitted as e-mail attachments.

Please read the **Instructions for Authors** before submitting your manuscript. The manuscript files should be given the last name of the first author.

Editors

Fees and Charges: Authors are required to pay a $550 handling fee. Publication of an article in the Scientific Research and Essays is not contingent upon the author's ability to pay the charges. Neither is acceptance to pay the handling fee a guarantee that the paper will be accepted for publication. Authors may still request (in advance) that the editorial office waive some of the handling fee under special circumstances.

Submission of a manuscript implies: that the work described has not been published before (except in the form of an abstract or as part of a published lecture, or thesis) that it is not under consideration for publication elsewhere; that if and when the manuscript is accepted for publication, the authors agree to automatic transfer of the copyright to the publisher.

Scientific Research and Essays

Table of Contents: Volume 9 Number 8 4 April, 2014

ARTICLES

Review

Research Articles

Scientific Research and Essays

Table of Contents: Volume 9 Number 8 30 April, 2014

academicJournals

Vol. 9(8), pp. 213-223, 30 April, 2014
DOI: 10.5897/SRE2013.5704
Article Number: B64161044179
ISSN 1992-2248 © 2014

http://www.academicjournals.org/SRE

Scientific Research and Essays

Review

A review on nanotechnology as a tool of change in Nigeria

M. T. Bankole[1,2], Jimoh O. Tijani[2]*, I. A. Mohammed[1,3] and A. S. Abdulkareem[1,3]

[1]Centre for Genetic Engineering and Biotechnology, Federal University of Technology, P. M. B. 65, Minna, Nigeria.
[2]Department of Chemistry, Federal University of Technology, P. M. B. 65, Minna, Nigeria.
[3]Department of Chemical Engineering, Federal University of Technology, P. M. B. 65, Minna, Nigeria.

Received 7 October, 2013; Accepted 10 March, 2014

Nanotechnology has generated diverse awareness and attentions nowadays and stand as one of the foremost alternative modern clean technologies of the 21st century. In spite of the essential benefits of nanoscience and technology, Nigeria is yet to key into nanotechnology initiative and strategy towards improving her socio-economic development as well as transformation of important sectors. The benefits and opportunities these evolving technology offers are enormous, and have led to high expectations in the academics, industries and even government. As a consequence of the uniqueness of this technology in science and engineering, quite a vast numbers of nanomaterials are now been synthesized, characterized and fabricated to solve societal immediate problems. This is because nanoscience or nanotechnology have control over the properties of matter and therefore have the ability to create materials with specific properties that can be utilized for specific functions. Therefore, nanotechnological approach offer hopes of reshaping humanity and redefine human condition vis-a-vis reduction of pressure on the existing natural resources. Thus, this review focus on nanotechnology, its emergence, importance and perhaps its applications, most especially the significant contributions to policy makers, non-governmental organizations and the general public as a whole. This serves as one of the viable emergent technology for socio- economic growth most especially in developing countries like Nigeria.

Key words: Application, matter, nanotechnology, novel, socio-economic

INTRODUCTION

The word “Nano” means dwarf in Greek and it is exemplified as length of hydrogen atom line up in a row. A material at nano scale is one billionth of the material (10^{-9}). In nature, nanotechnology has been in existence ever since the inception of the earth, through evolution, mutation, and adaptation in which plant passed through a photosynthesis route through the aid of tiny structures called ‘chloroplasts’ which are of nanoscale (Roco, 1999). Another natural phenomenon of nanotechnology is in the area of chemical catalysis (catalysts) or bioscience (enzymes) involving catalyst or enzymes catalyse of a chemical reaction (Smith, 1997). The first to carry out an

*Corresponding author. E-mail: jimohtijani@futminna.edu.ng

experiment on a molecule using nanoscale is a man called James Clerk Maxwell in 1867. Zsigmondy in 1914 was the first to characterize particle in sizes on nanoscale using nanometer, with the advancement of Langmuir and Blodgett (1920s) through the introduction of mono layer in characterization of particle sizes.

Derjaguin (1954) also reported the first measurement of surface force and in 1959, Richard Feymann proposed a technique for the manipulation of atoms and molecules using some specific tools (Gribbin, 1997). With several improvements, Taniguchi (1974) proposed the definition of Nano-technology as a method comprises processing, separation, consolidation and deformation of a molecule by the usage of manipulating particulate matter at nanoscale. The tools used in the 1980s then were scanning tunneling microscope (STM), atomic force microscopy (AFM), scanning probe microscopes (SPMs) and molecular beam epitaxy (MBE) (Roco, 1999). Presently, with recent advancement in science and technology latest modern analytical equipment are now being used to identify, quantify the phase composition, morphological and surface structure, elemental composition as well as crystal size of a nanosample. Some of these facilities are X-ray diffraction (XRD), high resolution scanning electron microscopy-electron diffraction spectroscopy (HRSEM-EDS), high resolution transmission electron microscopy-electron diffraction spectroscopy (HRTEM-EDS), X-ray photoelectron spectroscopy (XPS), Atomic force microscopy (AFM), to mention but a few.

Nanotechnology is the engineering and art of manipulating matter at the nanoscale (1 to 100 nm), at this level, materials are characterized by difference in its chemical, physical and biological properties than its normal size equivalent (Davies, 2006). This technology can easily merge with other technology on modification based on scientific concept and that is why nanotechnology is referred to as 'Platform' technology (Schmidt, 2007). The application of nanotechnology as it involves environmental remediation, industrial application, reduction in energy consumption which translate to lower production cost thereby increasing the production efficiencies cannot be overemphasized. This technology might not be the total solution to our problem in the world today, but it would surely alleviate some of the social-economic challenges confronting the developing countries especially Africa. Examples of the social problems include; the need for clean water, treatment of epidemic diseases (Fleischer and Grunwald, 2008), numerous industrial applications (Theron et al., 2008), energy and several scientific innovation (Binks, 2007). While government of developed countries such as Europe, United States, China even South Africa have continued to prioritize technologies through massive investment in nanotechnology with sole aim of strengthen economic growth. Today, there is no official gazette released by the Government of Nigeria prioritizing nanotechnology applications battered toward solving any societal problems confronting over 170 million people living in the country. Thus, the potentials of nanotechnology could be explored so as to solve the immediate but critical developmental problems of the country. This paper therefore focuses on the review of nanotechnology application as it related to water treatment, nanomedicine and energy development.

NIGERIA LINGERING PROBLEM: QUEST FOR POTABLE WATER

Water, energy and poverty are closely related, this has made access to water resources affect basic human needs. Everybody in the world depend directly on water and energy for their livelihoods (Amalu, 2011). Water, an essential resources needed in daily activities; its usability depends on the state of its cleanliness which comes as a result of sanitation of the environment. Unclean water and unsanitary practices are at the root causes of many health problems in the developing world with resultant adverse effect on international global health efforts (Tiaji, 2012a).

According to UNICEF and WHO (2013) close to one billion people do not have access to uncontaminated drinking water globally and above 2.5 billion people are without adequate sanitation facilities. The World Health Organization (WHO) estimates that 6.3% of all deaths are caused by limited access to safe drinking water, improved sanitation facilities, hygiene practices, and better water management practices. According to the United Nations (2005), more than 14,000 people die every day due to consumption of contaminated water. The bulk of these deaths were related to a number of infections, including 2 billion cases of intestinal worms, 5 million cases of lymphatic filariasis and trachoma, 1.4 million children died of diarrheal deaths; and 500,000 deaths from malaria (United Nations report, 2005).

The importance of good quality drinking water for the socio-economic benefit of any nations could not be underestimated. However inadequate access to potable water and better sanitary facilities coupled with high abject poverty ultimately affects many aspects of the society such as health, agriculture, economic growth, education, conflict etc. In health, diseases like diarrhea and several neglected tropical diseases are contracted through contact with bacteria infested water and soil and cause millions of deaths and illnesses annually (Tiaji, 2012b). Good sewerage and drainage systems can eliminate breeding grounds and water can be treated to remove bacteria found in tainted water. Effect of growth in agriculture and economic, parasitic worms afflict more than 1 billion people annually and cause a variety of ailments, like stunting, malnutrition, and anemia.

Water would be a scarce resource due to the impact of global climate change and high population growth,

Table 1. Global trend on fresh water crisis including Nigeria.

884 million people lack access to safe water supplies - approximately one in eight people
6 km is the average distance African and Asian women walk to fetch water
3.6 million people die each year from water-related diseases
98% of water-related deaths occur in the developing world
84% of water-related deaths are in children ages 0-14
43% of water-related deaths are due to diarrhoea
65 million people are at risk of arsenic poisoning in the Bangladesh, India and Nepal area
70 million Nigerians lack access to safe drinking

Source: (Pruss-Ustin et al., 2008; UNICEF/WHO, 2013)

especially in developing regions. But its availability still procure safety in the usage; often unsafe for drinking. Moreover, the current statistics shows more than three billion people globally will lack access to safe drinking water by 2050. Presently a third of the world's population lives in water-stressed countries, and by 2025, this is expected to rise to two-thirds (Amalu, 2011). The quest to ensure that all people have access to clean drinking water is now enshrined in the UN's Millennium Development Goals, which aims to halve the proportion of people without sustainable access to safe drinking water by 2015 (Belgiorno et al., 2007; UNICEF and WHO, 2012, 2013). But despite these efforts, getting the water clean is also a major challenge facing the African continent, including Nigeria.

Nigeria is blessed with abundant water resources but largely unused. In spite of the abundant water resources, the governments (Federal, State and Local) have been unsuccessful in their effort to harness these resources to sustainability and equitable scale (www.onlinenigeria.com). Nigeria, the eight most populous countries in the world, is being faced with challenge ranging from non-availability of portable water across number of its states; decay infrastructure and long term sustainability questions. The recent joint report by UNICEF/WHO, (2013) placed Nigeria as the third country with most people without access to safe water. In Nigeria, accessibility to improved water supply is prejudiced in favour of urban centres, which was originated from the colonial administration in an attempt to use improved water supply as a means of controlling the spread of diseases in urban centre. Abeokuta was the first to be supplied with pipe-borne water in 1911, followed by Lagos (1914), Enugu (1925), Kaduna (1930), Akure (1931), Jos (1935), Okene (1936), and Port Harcourt (1937). By 1953, 29 towns already has potable water and, by 1960, the number had risen to 67 which later rose to 261 by 1977 (Krebs, 2010).

Establishment of the River Basin Development Authorities (RBDAs) in 1976 and the Directorate of Foods, Roads and Rural Infrastructure (DFRRI) in 1986 later improved the situation. In 1997, all settlements were taken into account irrespective of sizes; about 24.74% of all households in Nigeria had access to pipe-borne water. DFRRI succeeded at providing 5,054 communities in all states of the federation with potable water mainly through boreholes, and by the end of 1999 it raised the proportion of access to pipe-borne water to about 13.63% for rural households, 68.50% for urban and 42.45% for semi-urban centre (www.onlinenigeria.com). Cumulatively, the households that depended on boreholes, wells and stream/ponds were 15.41, 27.62 and 32.23%, respectively. Thus, the provisions of potable water still demands government's rapid and sustainable attention (www.onlinenigeria.com). Scarcity of potable water is considerably looking unachievable in the face of conventional technologies used in water purification due to large infrastructure requirement, high capital investment and of course high population growth where less than 30% have access to portable water (Krebs, 2010). Table 1 shows the global trend on the scarcity of clean water Nigeria inclusive. The common cleansing agent normally used is alum to get dirty water clean. Even, the normal pipe borne water popularly known as tap water did not meet up with the expectation of the teeming populace. Recently, nanotechnology has proved to be one of the best options globally among other technologies, but making this new innovation accessible and affordable to the global poor looks unattainable especially in Nigeria (Amalu, 2011). According to United Nations Industrial Development Organization (UNIDO) and the United Nations Educational, Scientific and Cultural Organization (UNESCO), nanotechnology may offer promising solutions to water problems in developing countries, but the challenges cannot be underestimated, the two organizations have agreed to work together on a number of joint actions to search for more potential of nanotechnology in water purification and wastewater treatment (UNESCO and UNIDO, 2013).

APPLICATION OF NANOTECHNOLOGY FOR WATER TREATMENT

Because nanoparticles have a high surface area to volume ratio that could be chemically controlled, this is an indication of the technology great potential; as sorbents,

materials that latch on to pollutants and pull them out of solution. For instance, multi-walled carbon nanotubes have been shown to take up lead, cadmium and copper more effectively than activated carbon, a commonly used sorbent (Savage and Mamadou, 2005). Some nanoparticles such as zero valent nano iron, titania nanoparticles also act as potent catalysts and could be used to degrade recalcitrant organic pollutants into harmless compounds. For instance, zerovalent nano iron could detoxify halogenated organic compounds, such as trichloroethylene and triclosan. Other nanoparticles that are bioactive, such as silver and magnesium oxide, can kill bacteria and might be used in place of chlorine to disinfect water (Schmidt, 2007).

Nano-engineered membranes and filtration devices could be used to detect and remove viruses and other pollutants that are difficult to trap using current technologies (Theron et al., 2008). For instance, a preliminary technique employs imprinted polymer nanospheres to detect contaminants of emerging concern, a kind of pollution recently discovered at ng/L to µg/L in various water sources posing serious public health challenges (Binks, 2007). Such nanoscale sensors might be helpful for real-time monitoring of these pollutants everything from chemicals in Prozac to hormones in birth control pills at water-treatment plants and industrial sites. Membranes with nanopores are designed to both detect and remove such pollutants. With greater ability to filter out unwanted materials, industrial wastewater and even the ocean could become available to boost the supply of clean water. One of the most promising examples is zero-valent nano-iron, which is being tested for use in removing solvents from pumped groundwater. Titanium dioxide nanoparticles could potentially be sprinkled into a contaminated body of water, where they would be activated by sunlight to degrade quite a large number of organic pollutants such as PCBs and dioxins under the influence of the generated hydroxyl radicals (Schmidt, 2007; Klavarioti et al., 2009; Chong et al., 2010; Gupta et al., 2013).

Nanotechnology is expected to have an impact on water treatment beginning with nanosorbents and bioactive nanoparticles that could be integrated into existing purification systems. These first hybrid technologies would eventually be replaced by entirely new kinds of devices that use nanotechnology to improve the efficiency of filtration, remove more kinds of contaminants and add functions, such as water-quality sensors. Research groups are currently investigating a wide variety of nanomaterials—including carbon nanotubes, zeolites, dendrimers, metal-oxide nanoparticles and immobilized semiconductor nanocomposites for use in such devices (Savage and Mamadou, 2005). Nanosorbents, nanocatalysts, smart membranes, nanosensors and other kinds of nanotechnology could serve as the basis for new, small scale water treatment systems.

Unfortunately, new kinds of pollutants are being continually discovered in water resources, even while we still deal with old problems such as lead, pesticides and *Escherichia. coli*. Nano-enhanced water filtration could be developed to target these contaminants (Liu and Yang, 2003; Schmidt, 2007; Kiran et al., 2013). Nanotechnology is being applied for water purification through a material normally referred to as nanomaterial. According to Theron et al. (2008), there are nanomaterials that serve as water filtration membrane; nanoparticles, carbon nanotubes, metal nanoparticles. These nanomaterials offer a novel potential for the treatment of surface water, groundwater and wastewater contaminated by toxic metal ions, organic and inorganic solutes and microorganisms (Cloete et al., 2010).

Nanomaterials are very effective as a separation medium for water purification: they contain a number of key physicochemical properties (Savage and Mamadou, 2005), they are also known for their high surface area to mass ratio which occurs as a result of decreasing the size of the adsorbent particle from bulk to nanoscale dimensions (Pradeep, 2009), thereby making adsorption to be considered as an efficient, effective and more economical technique for the treatment of unclean water (Jiuhui, 2008). This property of nanomaterials leads to the availability of a high number of atoms or molecules on the surface of contaminants thereby enhancing the adsorption capacities of sorbent materials (Tiwari et al., 2008; Pradeep, 2009).

Moreover, this large surface area coupled with their size, electronic and catalytic properties provide unparalleled opportunities to develop more efficient water purification catalysts and redox active media which is really gaining popularity today, especially disinfection of water using UV light mediated semiconductor photocatalyst, such as TiO_2 (Chong et al., 2010; Manoj et al., 2012). The photocatalytic activity of TiO_2 nanoparticles synthesized using hydrothermal, sol-gel, chemical precipitation etc is a well-known phenomenon in the literature. Among the heterogeneous semiconductor photocatalysts, TiO_2 has received interest in research and development to solve global water pollution problem, aside that, the treatment technique is considered to be less-expensive, environmental friendly and sustainable in the water industry without necessarily generate toxic sludge (Chong et al., 2010). Table 2 shows the photocatalytic water treatment using nano synthesised TiO_2. These advanced nanomaterials can also be immobilized with various chemical groups to increase their affinity toward a given compound.

NIGERIA PROTRACTED PROBLEM: QUEST FOR UNSEASONED ENERGY

Nigeria is blessed with energy resources; crude oil, natural gas, coal, tar sand, biomass and other renewable energy resources such as tidal and wind power, and solar

Table 2. Recent examples of pollutants photocatalytically degraded by nano heterogeneous photocatalysts (TiO_2).

Contaminant	Photocatalytic system	References
Dyes		
Reactive violet 5	UV/Anatase	Chung and Chen (2009)
Blue 9, Red 51 and Yellow 23	Solar/TiO_2 (Degussa P_{25})	Dias and Azevedo (2009)
Methyl orange	UV/TiO_2 on glass	Lopez et al. (2010)
Methyl blue	UV/TiO_2	Esparza et al. (2010)
Rhodamine B	UV/TiO_2 bilayer	Zhuang et al. (2010)
Pesticides and herbicides		
Organophosphate and Phosphonoglycine	UV/TiO_2 immobilsed on glass	Echavia et al. (2009)
Azimsulfuron Swep residues	UV/TiO_2 coated on glass rings	Pelentridou et al. (2009)
Pharmaceuticals and cosmetics	Electrocoagulation and UV/TiO_2/H_2O_2	Fabbri et al. (2009)
Benzylparaben	UV/TiO_2(Aeroxide P_{25})	Boroski et al. (2009)
	TiO_2/Fe_3O_4 and TiO_2/SiO_2/Fe_3O_4	Choina et al. (2010)
	UV/TiO_2 (Degussa P_{25})	Alvarez et al. (2010)
Drugs		Lin et al. (2011)
Oxolinic acid	UV/TiO_2 (Degussa P_{25})	Giraldo et al. (2010)
Atenolol and Propranolol	UV/TiO_2 commercial	Hapeshi et al. (2010)
Ciprofloxacin, Ofloxacin, Norfloxacin and Enrofloxacin	Solar/TiO_2 (six commercial samples)/H_2O_2	Ioannou et al. (2011)
Lamivudine	UV/TiO_2 (Degussa P_{25})	An et al. (2010)
Oxytetracycline	Simulated solar/TiO_2 P_{25}	Li et al. (2012)
	UV/TiO_2 (Degussa P_{25})	Pereira et al. (2011)
	UV/TiO_2 (Degussa P_{25})	Adams and Impellitteri (2009).
Others		
N,*N*-diethyl-*m*-toluamide	UV/TiO_2 (Degussa P_{25})	Qourzal et al. (2009)
ß-naphthol	UV/TiO_2-SiO_2	Miranda-Garcia et al. (2010)
15 emerging micropollutants	Solar UV/TiO_2 coated on glass spheres	Antoniou et al. (2008)
Grey water	UV/TiO_2 (Aeroxide P_{25})	Sharma et al. (2012)
Microcystins (Cyanotoxin)	UV/TiO_2 film	Graham et al. (2010)
	UV/Doped TiO_2	Triantis et al. (2012)
	UV/ Nitrogen doped TiO_2	Dalrymple et al. (2011)
Lipid vesicles and E.colli cells	UV/TiO_2 (Degussa P_{25})	Amarjargal et al. (2012)
Bacterial colony	UV/TiO_2 on Titanium beads	Li et al. (2011)
	UV/TiO_2-coated bio-film	Zhang et al. (2012)
Paper mill wastewater	Solar/TiO_2	Wang et al. (2011)
Endocrine disrupting compounds	UV/TiO_2 (Degussa P_{25})	Wang et al. (2009)
Municipal waste water		Montoya et al. (2009)
Contaminated soil	Solar/sol-gel $TiO_{22}$and Degussa P_{25}	Tasseroul et al. (2012)
	Plasma/TiO_2 (Degussa P_{25})	Emeline et al. (2005)

Source: Lazar et al., (2012).

energy. It has been established that crude oil reserves stand at about 40 billion barrels, and it is expected to cubic metre while tar sand deposits stands at about 31 reach about 55 million barrels in the nearest future. Natural gas resource, currently stands at about 2.7 billion billion tons, and coal resource are estimated to be

between 2 and 10 billion tons (Nigeria Study Report, 2005).

Despite the large quantity of oil and gas and high potential for electricity, Nigeria still depends to a large extent on traditional energy sources such as fuel wood, bagasse and crop residue for its domestic energy needs while the fuel wood consumption is about 80 million cubic meters (about 25 million tonnes) mainly used for cooking, heating, cottage industrial applications and food processing industries (Nigeria Study Report, 2005). Harnessing these resources is one of the major challenges in the country; only 20% of the nation's hydro-power potential is tapped for use and the amount of solar radiation in the country is about 5.5 KW-h/m^2-day, but not fully used, making the country to lose huge prospect for energy generation ((ECNUNDP, 2005). With the country's four refineries which produce about 30% of installed capacity of 445,000 bpd and lost, so many away through bunkering and pipeline vandalism affecting not only the consumption but has also paralysed the country's industrial and socio-economic development, according to the National Bureau of Statistics (NBS) who revealed that "electricity and oil production challenges have slowed down the growth of Nigeria's Gross Domestic Product, GDP" (Adeola, 2013).

The Nigerian government has currently implemented public sector reform plans geared towards reducing poverty, corruption eradication, and empowering the private sector to become the engine for economic growth in the country. This reform initiative called the National Economic Empowerment and Development Strategy (NEEDS) has identified the deregulation of the downstream oil sector as a key aspect of the reform plan. The major work of NEEDS is the commercialisation and privatisation of the energy sector. This will make energy products more readily available to all, although at a higher price (Nigeria Study Report, 2005). Although, this energy sector reforms would lead to improve access to clean and affordable energy but the consequence of this could be detrimental to the poor masses since income per day is less than one US dollar. Therefore, a scientific innovation would be needed to raise people's awareness about the comparative advantages of more efficient energy sources through nanotechnology than previously used options.

APPLICATION OF NANOTECHNOLOGY FOR ENERGY DEVELOPMENT

Energy is around us all, though not accessible, therefore there will be a need to convert it into a usable form. Currently, we extract chemical energy from coal, oil and natural gas because these energy-rich materials come in convenient forms. These are also relatively easy to transform into a range of products, including formulated fuels, and into electricity which can be widely distributed by power lines. As fossil fuels grow scarce and increase in value, nanotechnology could be used to reduce losses during energy conversion. For instance, nano-engineered catalysts could improve the conversion of crude oil into various petroleum products, as well as the conversion of coal into clean fuels for generating electricity (Schmidt, 2007). In oil and gas applications, nanotechnology is used to increase opportunities to develop geothermal resources by enhancing thermal conductivity, improving down hole separation, and aiding in the development of non-corrosive materials that could be used for geothermal-energy production. Nanomaterials that are metallic in nature can be used to delineate ore deposits for geochemical exploration. Nanotechnology can also be used to improve the drilling process. Some specialized petroleum laboratory has developed an advanced fluid mixed with nanoparticles and superfine powder that significantly improve drilling speed. This blend eliminates damage to the reservoir rock in the well, making it possible to extract more oil (Abdollah, 2009).

Nanotechnology is used to enhance the development of unconventional and stranded gas resources. Near-term challenges focus on liquefied-natural-gas (LNG) infrastructure and efficiency, LNG quality, and developing gas-to-liquids (GTL) technology. Nanotechnology can address the problems associated with accessing stranded natural-gas resources by developing nanocatalysts and nanomembranes for GTL production and creating nanomaterials for compressed-natural-gas transport or long-distance electricity transmission (Abdollah, 2009).

Another application is in terms of electricity, novel electrical generating method includes electrokinetic power generation where fluids with charged ions are forced through a nanosized channel creating current. This process is similar to the electro-chemical process of action potential generation in animal neurons (nerve cells). Though not useful for large volumes of power production, the technology is still useful in powering other nano applications such as Lab-on-a-Chip. For energy conversion, the increased surface area to volume ratio of nanoparticles enhances solar energy collection and efficiency by exposing more conducting surfaces to the sunlight. The research and development of solar cells using nanotechnology is probably the most promising for alternative energy production (Gardner, 2008).

Carbon nanotubes (CNT), fullerenes and quantum dots are used to make solar cells lighter, cheaper, and more efficient. For example, constructing photovoltaics with vertical laying CNTs greatly increases the amount of light that can be collected. Notre Dame Researchers are utilizing quantum dots with the ability to absorb different wavelengths of light that result in dynamic solar cells in the near future. Another arena that nanotechnology will impact is increasing photovoltaic efficiency through the use of materials like lead-selenide. These materials cause more electrons (and therefore more electricity) to

be released when hit by a photon of light. Additionally, structural properties of photovoltaics can be modified using nanotechnology.

The ASTAR Institute of Microelectronics has constructed photovoltaics out of nanowires that give solar cells extreme enhanced flexibility not seen in many silicon-based cells. In terms of energy storage, it must be stored so that it can be used as needed. In the near term, nanotechnology could be used to create appliances and other products that can store energy more efficiently, that is, take up charge and hold it over time. Many research groups are working on better batteries, often using engineered nanomaterials (Schmidt, 2007). When batteries are constructed with nanoscale materials, this property will increase power density to battery size (Gardner, 2008). The efficiency of battery power is partially dependent on the diffusion distance between oppositely charged nodes. Nanomaterials can reduce this diffusion distance, coupled with hydrophilic electrolyte polymers, and battery efficiency is poised to increase dramatically. Altair Technologies has developed a prototype battery that has three times the capacity of existing batteries and can be fully charged in six minutes. Presently, scientists are trying to address the final two concerns in lithium-ion batteries. They have created batteries that prevent electrode contact prior to battery activation. This gives the product an almost limitless shelf life and an active life of 25 years (as opposed to two years).

In addition, reserve cells within the battery release chemicals during disposal that neutralize the normally toxic output from typical batteries (Baxter et al., 2009). Nanotechnology in battery production should revolutionize the industry of hybrid cars. The Micro-Vett Fiat Doblo powered by an AltairNano lithium ion NanoSafe battery has travelled 186 miles between chargings (that can take less than 10 min). Phoenix Motorcars will sell about 500 nano-powered Sports Utility Trucks featuring Altair technology in the coming years as well. Interesting areas being explored to assist battery technology is using CNTs to produce “printable” sheets of batteries and using viruses to self-assemble battery components (Gardner, 2008).

Similarly, nanotechnology will offer exciting advances in hydrogen energy production, storage, and distribution. In hydrogen production, similar processes to the photovoltaics are being utilized. Splitting water with light could get rid of the reliance on fossil fuels and other hydrocarbons. This process requires precision, and at the moment, research into this production method is in the early stages. One of the most exciting areas for nanotechnology to impact hydrogen energy is efficient hydrogen storage (Abdollah, 2009). There is currently no viable technology to store large volumes of hydrogen fuel because it is either too bulky or expensive. This is a severe limitation to implementing hydrogen as an alternative energy source (Baxter et al., 2009).

Researchers at Rensselaer have developed “nanoblades” that are extremely thin, uniform, and have high surface areas. Also, scientists have found that fullerenes can hold large volumes of hydrogen (equivalent to the density of hydrogen at the center of Jupiter). The efficiency of hydrogen transport could be further enhanced by the use of carbon nanotube wiring in place of traditional pipelines. These lines would have increased strength, conductivity, and stability at high temperatures. Researchers at Rice University are examining CNT wiring for just this purpose. Nanoparticle monitors are also being developed at New Mexico Tech to be placed in hydrogen transport pathways to detect potential impurities (Gardner, 2008).

For efficient energy transmission, nanotechnology could be used to create new kinds of conductive materials that lose very little energy as electricity moves down the line. Many research groups are investigating whether nanowires and nanocoatings could reduce losses in electrical-transmission lines. And for efficient energy use, nanotechnology could lead to breakthroughs that indirectly conserve large amounts of fossil fuels. Nanomanufacturing might also enable us to make all kinds of products using less energy. For instance, nanosensors might be used to track energy use and help minimize waste (Schmidt, 2007).

NIGERIA PROLONGED MENACE: SEARCH FOR INNOVATIVE MEDICINE

In Nigeria, the health condition of the populace is highly deplorable. Common diseases plaguing the country are malaria, guinea worm, pneumonia, measles, gonorrhea, schistosomiasis, typhoid, tuberculosis, chicken pox, diarrhea, HIV/AIDS (Oyebanji, 2013). The Federal and State Governments are the major providers of basic health facilities and services in Nigeria, providing significant funding to various aspects of the health sector in the country. WHO, UNICEF, UNDP, and the Carter Foundation have aided also in the control and eradication of communicable/infectious diseases like guinea worm, tuberculosis, cholera, river blindness, schistosomiasis and HIV/AIDS (Oyebanji, 2013).

There are three major public health diseases that are of great challenge in Nigeria; tuberculosis, malaria and HIV/AIDS. Tuberculosis (TB) as a major public health problem in the country is an air-borne infectious disease caused by bacteria, which primarily affects the lungs. WHO declared TB a global emergency in 1993 and it remains one of the world’s major causes of illness and death (United States Embassy in Nigeria, 2012). According to WHO, the country is ranked 5th among the 22 high TB burden countries, bearing 80% of the global burden of TB (WHO, 2013). The number of TB cases in 2002 increased from 31,264 to 90,307 in 2008 in the country. Though, more than 450,000 TB cases have

been successfully treated in the past 5 years in Nigeria, the challenge is still on the emergence of multi-drug resistant tuberculosis (MDR-TB) (WHO, 2013).

In Nigeria, malaria is the most prevalent public health problem. Malaria is a risk for 97% of country's populace while the remaining 3% live in the malaria-free environment. The disease is a major cause of maternal mortality and poor child development (United States Embassy in Nigeria, 2011). It is estimated that there exist about 100 million malaria cases with over 300,000 deaths annually in Nigeria. It account for about 11% of maternal mortality and about 50% death in children aged 6 to 59 months (South West, North Central, and North West regions) with least occurrence of 27.6%, in children of same age in the South East region of the country (United States Embassy in Nigeria, 2011). The new malaria treatment is Artemisinin-based combination therapies (ACTs) which have replaced chloroquine but has not still met the requirement needed for malaria total eradication (Nigeria MDG, 2013). Roll Back Malaria is a new means of preventing malaria in Nigeria (global strategies for malaria control) which includes the use of insecticide-treated nets, indoor residual spraying and environmental management, but it faces two main challenges; ability to meet up the demands of the huge population and geographical area of the country, and the gap in funding.

AIDS is an acronym for acquired immune deficiency syndrome, a disease caused by the human immunodeficiency virus (HIV). When this virus attacks the immune system, there will be no more defenses against diseases and infections in the body (Oyebanji, 2013). About 3.1 million people are living with HIV in Nigeria. HIV occurrence among the general population is 3.6% while its prevalence among pregnant women is 4.1%. About 300,000 new infections occur yearly with people under the age 15 to 24 (UNAIDS, 2013). About 1.5 million people living with HIV require antiretroviral (ARVs) using the new WHO guidelines but only 30% of these people have access to it (UNAIDS, 2013). All these challenges in the health sector will need a new and compliment means of tackling it. Nanotechnology will be of great aid in the face of this particular lingering problem in the country.

APPLICATION OF NANOTECHNOLOGY IN MEDICINE

In medicine, nanotechnology helps predict the major diseases that are likely to develop by an individual. The goal would be to routinely and cheaply analyze several hundred substances in a patient's blood and estimate disease risks with a relatively high degree of accuracy (Schmidt, 2007). This would also provide a window on a person's overall state of health. Several research groups are in fact working on developing a "labon-a-chip" device, using nanotechnology to perform a comprehensive analysis of a drop of blood. This analysis would alert the doctor to early precursors of disease that reflect both genetic predispositions and environmental factors, such as diet, exercise, stress and exposure to air pollution. In pre-emptive medicine, it focuses on early intervention, but it also requires early diagnosis. It is to help detect treatable diseases earlier so that they can help patients preempt the full-blown development of illness or at least manage it effectively over a lifetime. Nanotechnology can enhance the development of sensitive diagnostic tests, as well as devices for health monitoring and disease management (Schavan, 2011).

Diabetes care is one important area that would stand to benefit, nanobased diagnostic tests could detect the earliest stages of insulin resistance, and similarly, preemptive medicine might be used to help a large portion of the population more effectively deal with cardiovascular disease and hypertension. This model could be expanded and used to manage many chronic diseases, e.g. lupus or arthritis. Likewise in personalized medicine, the vision is to make medicine more personalized comes from the notion that information about an individual can be used to monitor treatment. A doctor has a much greater chance of coming up with an effective medical strategy if he or she knows something about a patient's disease subtype, metabolism (particularly as it relates to drugs), liver status and risk for other diseases. Nanotechnology could provide new tools for gathering detailed information about variations in disease states and about unique parameters of treatment. More importantly, nanotechnology could spur the personalized medicine revolution by helping bring about real-time, sensitive monitoring of drug therapies. With more frequent feedback, a doctor could easily adjust drugs and dosages to personalize a patient's therapy. Indeed, treatments are expected to become more complex (Schmidt, 2007).

Nevertheless, in participatory (regenerative) medicine, the excitement about the potential for regenerative medicine has generally focused on stem cells, but nanotechnology could also lead to radically new treatments for spinal cord injury, macular degeneration, Type 1 diabetes and other dysfunctions. The goal, in all these cases, is to regenerate a part of the body that has been injured or has deteriorated as the result of disease, genetic defects or normal aging. Whether stem cells can be coaxed to rebuild tissues and restore function remains to be seen, but an equally promising approach is to employ nanostructured artificial tissues. It is still early, but many laboratories are experimenting with a wide variety of nanomaterial scaffolds that can be infused with cells to form artificial tissues, such as bone and liver. It appears possible to repair damaged nerves by injecting them with nanomaterials that form bridge-like lattices (Schavan, 2011). Other nanostructures show promise as foundations for growing three-dimensional networks of blood vessels. Regenerating damaged tissues is one approach, but lost function might also be restored using nanoenhanced replacement parts for the body devices

that hook right into the nervous system.

APPLICATION OF NANOTECHNOLOGY IN OTHER AREAS

Aside from the three major application of nanotechnology discussed above, the technology has been established to be useful and functional in many other areas. Nanotechnological developments are related in different ways to positive effects on the protection of environment and resources. For instance, in the chemical industry, new nanocatalysts are the basis for alternative reaction paths, it save more energy at lower temperatures and allow optimal material usage due to their selectivity (low amounts of by-products). As environmentally friendly materials, completely new raw material sources, as for example new bioplastics, have the potential to replace conventional polymers or even metals, e.g. in car manufacturing. They are made of renewables and are not only characterized by an almost neutral CO_2 balance, but also lead to increasing independence from petroleum-based raw materials. It has been reported also that Carbon Nanotubes (CNT) play an increasingly important role in the development of new materials (www.technologyreview.com). As for example, the substitution or the reduction of indium in indium tin oxide (ITO) for the production of transparent electrodes, e.g. in liquid crystal screens or organic light-emitting diodes, the use of conductive substances (e.g. conductive silver) or the utilization as catalyst (substitution of platinum or other catalyst metals) and the reinforcement of materials through CNT for lightweight-construction applications (reduction of material usage with same load capacity).

Literature also reveal that concept of nanotechnology can be applied in the development of low friction material, stab and bullet-proof nanoscale material, environmental protective material, nanomaterial for intelligent street and identification of counterfeiting products (www.inno-cnt.de). Other areas of application of nanotechnology include; nutrition and agriculture, communication, electronics, etc.

BENEFITS OF NANOTECHNOLOGY

The benefits of nanotechnology for sustainable development are enormous, but summarized below (Savage and Wentsel, 2008):

i. Cost effective use of renewable energy,
ii. Early environmental treatment and remediation,
iii. Low energy requirement and waste generations devices,
iv. Lighter and stronger nanomaterial,
v. Early disease detectors for preventive treatment,
vi. Smaller, accurate and sensitive sensing and monitoring devices.

Lack of natural and clean water threatens the security and economic growth of many communities in the world today, hence nanotechnology stand as a good substitute or supplement compared to other available water remediation technologies. The treatment of the unclean water and recycling of the purified water would bring significant reductions in cost, time, and labor to industry which later result into greater economic sustainability and overall system development (Savage and Mamadou, 2005). The design of nanotechnology enhanced greater benefits as regards renewable energy including an increased efficiency of lighting and heating, increased electrical storage capacity, a decrease in the amount of pollution from the use of energy (www.technologyreview.com). Nanotechnology provides an efficient energy conversion and energy storage (Baxter et al., 2009). This overall benefit deriving from nanotechnology will revive the economy of any nation because a balance in energy production will improve and sustain the economic growth through job creation.

Another area of benefit is nanomedicine. Nanotechnology stands a good chance of revolutionizing the practice of medicine. The control and synthesis of atoms and molecules into a nanoscale, offer a wide range of products for medical purposes that are yet to be harness. These novel nanostructures drugs act faster on target delivery for treating common conditions such as cancer, Parkinson's and cardiovascular disease compared to normal drugs (www.technologyreview.com). The engineering of nanomaterials as an artificial tissue would help replace diseased kidneys and livers, and even repair nerve damage (Schavan, 2011). Nanotechnology is also used in tissue engineering, to provide a better bioscaffold and a surface to grow tissues (Kingsley et al., 2013). Moreover, nanodevices could be integrated with the nervous system to create implants that restore vision and hearing and eventually build prosthetic limbs that better serve the disabled. It is clear that advances in nanomedicine could help vast numbers of people maintain their health, their independence and their participation in society (Schmidt, 2007). Other benefits are found in agriculture such as food security and soil analysis, cosmetics industry, communication industry, sanitation and environmental remediation e.t.c. There is no doubt that nanotechnology is a tool for sustainable development.

Conclusion

This review has clearly demonstrated that nanotechnology is not an industry nor will it produces new industries. However, it offers new competitive dimension to existing industries. The concept of nanotechnology therefore promised to deliver numerous benefits to the society and it will have tremendous potential if it can be developed. There is no doubts that nanotechnology is a promising tool of change in this our world today. In USA, Japan, Germany, South Africa,

nanotechnology has been invested on by their scientists, engineers, investors and even policy makers for sustainable development in different sector of their economy. Therefore, it will be of great importance if this tool of change; Nanotechnology is harness in this country, Nigeria.

Conflict of Interests

The author(s) have not declared any conflict of interests.

ACKNOWLEDGEMENTS

The authors wish to thank STEP B Program of Federal University of Technology, Minna, Niger State, Nigeria for their support towards the success of this review article.

REFERENCES

Abdollah E (2009). Applications of nanotechnology in oil and gas industry. Petrotech, New Dehli, India.

Adams WA, Impellitteri CA. (2009). The photocatalysis of n,n-diethyl-m-toluamide (DEET) using dispersions of degussa p-25 TiO2 particles. J. Photochem. Photobiol. A, 202:28-32. http://dx.doi.org/10.1016/j.jphotochem.2008.11.003

Adeola Y (2013). Nigeria and its energy challenges. www.dailyindependentnig.com

Alvarez PM, Jaramillo J, Lopez-Pinero F, Plucinski PK (2010). Preparation and characterization of magnetic TiO2 nanoparticles and their utilization for the degradation of emerging pollutants in water. Appl. Catal. B., 100:338-345. http://dx.doi.org/10.1016/j.apcatb.2010.08.010

Amalu C (2011). Nanotechnology Water Purification: How Efficient? Source: The Leadership Newspaper.

Amarjargal A, Tijing LD, Yu MH, Kim CH, Park CH, Kim DW, Kim CS (2012). Characterization and photocatalytic efficiency of TiO2/Ti beads fabricated by simple heat-treatment. J. Mater. Sci. Technol. 28:184-192. http://dx.doi.org/10.1016/S1005-0302(12)60040-1

An TC, Yang H, Li GY, Song WH, Cooper WJ, Nie XP (2010). Kinetics and mechanism of advanced oxidation processes (AOPs) in degradation of ciprofloxacin in water. Appl. Catal. B., 94:288294. http://dx.doi.org/10.1016/j.apcatb.2009.12.002

Antoniou MG, Shoemaker JA, de la Cruz AA, Dionysiou DD (2008). LC/MS/MS structure elucidation of reaction intermediates formed during the TiO2 photocatalysis of microcystin-LR. Toxicon. 51:1103-1118. http://dx.doi.org/10.1016/j.toxicon.2008.01.018

Baxter J, Bian Z, Chen G, Danielson D, Dresselhaus MS, Fedorov AG, Fisher TS, Jones CW, Maginn E, Kortshagen U, Manthiram A, Nozik A, Rolison DR, Sands T, Shi L, Sholl D, Wuo Y (2009). Nanoscale design to enable the revolution in renewable energy. Energy Environ. Sci.2:559-588. http://dx.doi.org/10.1039/b821698c

Belgiorno V, Rizzo L, Fatta D, Rocca CD, Lofrano G, Nikolaou A, Naddeo V, Meric S (2007). Review on endocrine disrupting-emerging compounds in urban wastewater: Occurrence and removal by photocatalysis and ultrasonic irradiation for wastewater reuse. Desalination 215:166-176. http://dx.doi.org/10.1016/j.desal.2006.10.035

Binks P (2007). Nanotechnology and water: opportunities and challenges. Victorian Water Sustainability Seminar. May 15, 2007.

Boroski M, Rodrigues AC, Garcia JC, Sampaio LC, Nozaki J, Hioka N (2009). Combined electrocoagulation and TiO2 photoassisted treatment applied to wastewater effluents from pharmaceutical and cosmetic industries. J. Hazard. Mater. 162:448-454. http://dx.doi.org/10.1016/j.jhazmat.2008.05.062

Choina J, Duwensee H, Flechsig GU, Kosslick H, Morawski AW, Tuan VA, Schulz A (2010). Removal of hazardous pharmaceutical from water by photocatalytic treatment. Cent. Eur. J. Chem. 8:1288-1297. http://dx.doi.org/10.2478/s11532-010-0109-9

Chong MN, Jin B, Chow CWK, Saint C (2010). "Recent developments in photocatalytic water treatment technology: A review." Water Res. 44(10):2997-3027. http://dx.doi.org/10.1016/j.watres.2010.02.039

Chung YC, Chen CY (2009). Degradation of azo dye reactive violet 5 by TiO2 photocatalysis. Environ. Chem. Lett. 7:347-352. http://dx.doi.org/10.1007/s10311-008-0178-6

Cloete ET, Michele K, Marelize B, Manue JL (2010). Nanotechnology in Water Treatment Applications. N.p.: Caister Academic Press.

Country Study Report (Nigeria Study Report) (2005). Enabling urban poor livelihood policy making: Understanding the role of energy.

Davies JC (2006). Managing the effects of Nanotechnology. Woodrow Wilson International Centre for Scholars, National Institutes of Health, Washington D.C., USA.

Dalrymple OK, Isaacs W, Stefanakos E, Trotz MA, Goswami DY (2011). Lipid vesicles as model membranes in photocatalytic disinfection studies. J. Photochem. Photobiol. A 221:64-70. http://dx.doi.org/10.1016/j.jphotochem.2011.04.025

Dias MG, Azevedo EB (2009). Photocatalytic decolorization of commercial acid dyes using solar irradiation. Water Air Soil Pollut. 204:79-87. http://dx.doi.org/10.1007/s11270-009-0028-6

Energy Commission of Nigeria and United Nations Development Programme (ECNUNDP) (2005). Renewable energy master plan. http://www.iceednigeria.org

Echavia GRM, Matzusawa F, Negishi N (2009). Photocatalytic degradation of organophosphate and phosphonoglycine pesticides using TiO2 immobilized on silica gel. Chemosphere 76:595-600. http://dx.doi.org/10.1016/j.chemosphere.2009.04.055

Emeline AV, Ryabchuk VK, Serpone N (2005). Dogmas and misconceptions in heterogeneous photocatalysis: Some enlightened reflections. J. Phys. Chem. B 109:18515-18521. http://dx.doi.org/10.1021/jp0523367

Esparza P, Borges ME, Diaz L, Alvarez-Galvan MC, Fierro JLG (2010) Photodegradation of dye pollutants using new nanostructured titania supported on volcanic ashes. Appl. Catal. A., 388:7-14. http://dx.doi.org/10.1016/j.apcata.2010.07.058

Fabbri D, Crime A, Davezza M, Medana C, Baiocchi C, Prevot AB (2009). Pramauro, E.Surfactant-assisted removal of swep residues from soil and photocatalytic treatment of the washing wastes. Appl. Catal. B., 92:318-325. http://dx.doi.org/10.1016/j.apcatb.2009.08.010

Fleischer T, Grunwald A (2008). Making nanotechnology developments sustainable: A role for technology assessment. J. Cleaner Prod. 16:889-898. http://dx.doi.org/10.1016/j.jclepro.2007.04.018

Gardner GE (2008). Alternative Energy and Nanotechnology. Public Communication of Science and Technology, USA.

Giraldo AL, Penuela GA, Torres-Palma RA, Pino NJ, Palominos RA, Mansilla HD (2010). Degradation of the antibiotic oxolinic acid by photocatalysis with TiO2 in suspension. Water Res. 44:5158-5167. http://dx.doi.org/10.1016/j.watres.2010.05.011

Graham D, Kisch H, Lawton LA, Robertson PKJ (2010). The degradation of microcystin-LR using doped visible light absorbing photocatalysts. Chemosphere 78:1182-1185. http://dx.doi.org/10.1016/j.chemosphere.2009.12.003

Gribbin J (1997). Richard Feymann: A Life in Science. Dutton, p. 170.

Hapeshi E, Achilleos A, Vasquez MI, Michael C, Xekoukoulotakis NP, Mantzavinos D, Kassinos D (2010). Drugs degrading photocatalytically: Kinetics and mechanisms of ofloxacin and atenolol removal on titania suspensions. Water Res. 44:1737-1746. http://dx.doi.org/10.1016/j.watres.2009.11.044

Innovation Alliance Carbon Nanotubes (2013). Innovation for Industry and Society. www.inno-cnt.de

Ioannou LA, Hapeshi E, Vasquez MI, Mantzavinos D, Fatta-Kassinos D (2011). Solar/TiO2 photocatalytic decomposition of beta-blockers atenolol and propranolol in water and wastewater. Sol. Energy 85:915-1926. http://dx.doi.org/10.1016/j.solener.2011.04.031

Jiuhui Q (2008). Research progress of novel adsorption processes in water purification: A review. J. Environ. Sci. 20:1-13. http://dx.doi.org/10.1016/S1001-0742(08)60001-7

Kiran G, Singh RP, Ashutosh P, Anjana P (2013). Photocatalytic

antibacterial performance of TiO2 and Ag-doped TiO2 against S. aureus. P. aeruginosa and E. coli. Beilstein J. Nanotechnol. 4:345-351. http://dx.doi.org/10.3762/bjnano.4.40
Kingsley JD, Dasgupta SRN, Saha P (2013). Nanotechnology for tissue engineering: Need, techniques and applications. J. Pharm. Res. 7(2):200-204. http://dx.doi.org/10.1016/j.jopr.2013.02.021
Klavarioti M, Mantzavinos D, Kassinos D (2009). Removal of residual pharmaceuticals from aqueous systems by advanced oxidation processes. Environ. Int. 35:402-417. http://dx.doi.org/10.1016/j.envint.2008.07.009
Krebs M (2010). Nigeria Reports Water Scarcity Across Numerous States. Digital Journal. http://www.digitaljournal.com/article/301656
Li W, Guo C, Su B, Xu J (2012). Photodegradation of four fluoroquinolone compounds by titanium dioxide under simulated solar light irradiation. J. Chem. Technol. Biotechnol. 87:643-650. http://dx.doi.org/10.1002/jctb.2759
Li GZ, Park S, Kang DW, Krajmalnik-Brown R, Rittmann BE (2011). 2,4,5-Trichlorophenol degradation using a novel TiO2-coated biofilm carrier: Roles of adsorption, photocatalysis, and biodegradation. Environ. Sci. Technol. 45:8359-8367. http://dx.doi.org/10.1021/es2016523
Lin YX, Ferronato C, Deng NS, Chovelon JM (2011). Study of benzylparaben photocatalytic degradation by TiO2. Appl. Catal. B., 104:353-360. http://dx.doi.org/10.1016/j.apcatb.2011.03.006
Liu H, Yang T (2003). Photocatalytic Inactivation of Escherichia coli and Lactobacillius helveticus by ZnO and TiO2 activated with ultra violet light. Process Biochem. 39:475-481. http://dx.doi.org/10.1016/S0032-9592(03)00084-0
Lopez L, Daoud WA, Dutta D (2010). Preparation of large scale photocatalytic TiO2 films by the sol-gel process. Surf. Coat. Technol. 205:251-257. http://dx.doi.org/10.1016/j.surfcoat.2010.06.028
Manoj AL, Shaji V, Santhosh SN (2012). Photocatalytic Water Treatment by Titanium Dioxide: Recent Updates. Catalysts 2:572-601. http://dx.doi.org/10.3390/catal2040572
Miranda-Garcia N, Maldonado MI, Coronado JM, Malato S (2010). Degradation study of 15 emerging contaminants at low concentration by immobilized TiO2 in a pilot plant. Catal. Today 151:107-113. http://dx.doi.org/10.1016/j.cattod.2010.02.044
Montoya JF, Velasquez JA, Salvador P (2009). The direct-indirect kinetic model in photocatalysis: A reanalysis of phenol and formic acid degradation rate dependence on photon flow and concentration in TiO2 aqueous dispersions. Appl. Catal. B. 88:50-58. http://dx.doi.org/10.1016/j.apcatb.2008.09.035
Oyebanji JO (2013). Health condition in Nigeria. http://www.onlinenigeria.com/health/
Pelentridou K, Stathatos E, Karasali H, Lianos P (2009). Photodegradation of the herbicide azimsulfuron using nanocrystalline titania films as photocatalyst and low intensity black light radiation or simulated solar radiation as excitation source. J. Hazard. Mater. 163:756-760. http://dx.doi.org/10.1016/j.jhazmat.2008.07.023
Pereira J, Vilar VJP, Borges MT, Gonzalez O, Esplugas S, Boaventura RAR (2011). Photocatalytic degradation of oxytetracycline using TiO2 under natural and simulated solar radiation. Sol. Energy 85:2732-2740. http://dx.doi.org/10.1016/j.solener.2011.08.012
Pradeep AT (2009). Noble metal nanoparticles for water purification: A critical review. Thin Solid Films 517(24):6441–6478. http://dx.doi.org/10.1016/j.tsf.2009.03.195
Pruss-Ustün A, Bos R, Gore F (2008). Safer water, better health: Costs, benefits and sustainability of interventions to protect and promote health. WHO, Geneva.
Qourzal S, Barka N, Tamimi M, Assabbane A, Nounah A, Ihlal A, Ait-Ichou Y (2009). Sol-gel synthesis of TiO2-SiO2 photocatalyst for beta-naphthol photodegradation. Mater. Sci. Eng. C, 29: 1616-1620. http://dx.doi.org/10.1016/j.msec.2008.12.024
Roco MC (1999). Nanotechnology, shaping the world atom by atom. National Science and Technology Council, Committee on Technology. The Interagency Working Group on Nanoscience, Engineering and Technology, September 1999, Washington D.C., USA.
Savage N, Wentsel R (2008). Draft nanomaterial research strategy (NRS). Environmental Protection Agency, United States, pp. 1-2.
Savage N, Mamadou SD (2005). Nanomaterials and water purification: Opportunities and challenges. N.p.: Springer, pp. 337-339.
Schavan A (2011). Acion Plan Nanotechnology 2015. Bundesministerium für Bildung und Forschung/Federal Ministry of Education and Research (BMBF) Division "Key Technologies; Strategy and Policy Issues"D-53170 Bonn.
Schmidt KF (2007). Nanofrontiers, vision for the future of nanotechnology. Project on Emerging Technologies. Woodrow Wilson International Centre for Scholars, National Institutes of Health, Washington D.C., USA.
Sharma VK, Triantis TM, Antoniou MG, He XX, Pelaez M, Han CS, Song WH, O'Shea KE, de la Cruz AA, Kaloudis T (2012). Destruction of microcystins by conventional and advanced oxidation processes: A review. Sep. Purif. Technol. 91:3-17. http://dx.doi.org/10.1016/j.seppur.2012.02.018
Smith AD (1997). Oxford Dictionary of Biochemistry and Molecular Biology. Oxford University Press, North Carolina, USA.
Tasseroul L, Pirard SL, Lambert SD, Paez CA, Poelman D, Pirard JP, Heinrichs B (2012). Kinetic study of p-nitrophenol photodegradation with modified TiO2 xerogels. Chem. Eng. J. 191:441-450. http://dx.doi.org/10.1016/j.cej.2012.02.050
Tiaji SB (2012a). Neglected Tropical Diseases: Background, Responses, and Issues for Congress, CRS Report R41607.
Tiaji SB (2012b). Global Access to Clean Drinking Water and Sanitation: U.S. and International Programs.
Tiwari DK, Behari J, Prasenjit S (2008). Application of Nanoparticles in Waste Water Treatment. World Appl. Sci. J. 3(3):417-419.
Theron J, Walker JA, Cloete TE (2008). Nanotechnology and Water Treatment: Applications and Emerging Opportunities. Crit. Rev. Microbiol. 34:43-69. http://dx.doi.org/10.1080/10408410701710442
Triantis TM, Fotiou T, Kaloudis T, Kontos AG, Falaras P, Dionysiou DD, Pelaez M, Hiskia A (2012). Photocatalytic degradation and mineralization of microcystin-LR under UV-A, solar and visible light using nanostructured nitrogen doped TiO2. J. Hazard. Mater. 211:196-202. http://dx.doi.org/10.1016/j.jhazmat.2011.11.042
MIT Technology Review. www.technologyreview.com
UNICEF, WHO (2012). Progress on Sanitation and Drinking Water, 2-4.
United Nations 2005 World Summit (2012). Available at http://www.globalissues.org/article/559/united-nations-world-summit-2005
UNESCO, UNIDO (2013). Joining Forces with UNESCO to Use Nanotechnology to Address Water Challenges. Conference on Emerging Ethical Issues in Science and Technology held in Bratislava.
United States Embassy in Nigeria (2012). Nigeria Tuberculosis facts sheets. Plot 1075, Diplomatic Drive Central Area Abuja, FCT, Nigeria. http://nigeria.usembassy.gov/
United States Embassy in Nigeria (2011). Nigeria Malaria facts sheets. Plot 1075, Diplomatic Drive Central Area Abuja, FCT, Nigeria. http://nigeria.usembassy.gov/
Nigeria MDG +10 Showcase No. 5 (2013). Roll Back Malaria in Nigeria. www.mdgs.gov.ng
UNAIDS (2013). Women, Girls and HIV in Nigeria. www.naca.gov.ng
Wang TC, Lu N, Li J, Wu Y (2011). Plasma-TiO2 catalytic method for high-efficiency remediation of p-nitrophenol contaminated soil in pulsed discharge. Environ. Sci. Technol. 45:9301-9307. http://dx.doi.org/10.1021/es2014314
Wang C, Zhang X, Liu H, Li X, Li W, Xu H (2009). Reaction kinetics of photocatalytic degradation of sulfosalicylic acid using TiO2 microspheres. J. Hazard. Mater.163:1101-1106. http://dx.doi.org/10.1016/j.jhazmat.2008.07.064
WHO (2013). AIDS, TB and Malaria.
Zhuang JD, Dai WX, Tian QF, Li ZH, Xie LY, Wang JX, Liu P, Shi XC, Wang DH (2010). Photocatalytic degradation of rhb over TiO2 bilayer films: Effect of defects and their location. Langmuir, 26:9686-9694. http://dx.doi.org/10.1021/la100302m
Zhang W, Li Y, Su Y, Mao K, Wang Q (2012). Effect of water composition on TiO2 photocatalytic removal of endocrine disrupting compounds (EDCs) and estrogenic activity from secondary effluent. J. Hazard. Mater. 215:252-258. http://dx.doi.org/10.1016/j.jhazmat.2012.02.060

academicJournals

Vol. 9(8), pp. 224-228, 30 April, 2014
DOI: 10.5897/SRE2014.5858
Article Number: 0ABD95944183
ISSN 1992-2248 © 2014

http://www.academicjournals.org/SRE

Scientific Research and Essays

Full Length Research Paper

Effect of routine pathological procedure on morphometric parameters of the heart in rat models

Ozgur Ozdemir*, Orhan Yavuz and Fatih Hatipoglu

Department of Pathology, Faculty of Veterinary Medicine, Selcuk University, Konya Campus 42079, TURKEY.

Received 2 March, 2014; Accepted 9 April, 2014

In this study, the aim was to investigate effects of routine protocols commonly used in pathology (formalin fixation, paraffin embedding, slicing and staining) on morphometrical parameters of hearts in rats. Six males and 6 females rats were used. All of the subjects were euthanized and then hearts were fixed in formalin solution. Hearts were cut at the level of musculus papillaris and cut surfaces area were photographed (Formalin group). Thereafter, cut surfaces of the hearts embedded in paraffin were also photographed (Paraffin group). Staining was done using H&E staining on 5 µm slices and their photographs were taken (Slide Group). Analyses of thickness, diameter and area on the photographs of heart were done by using image analysis software. Left ventricular mass (LVM), left ventricular mass index (LVMI) and cut surface area (CSA) were calculated. Significant differences were found in LVM and LVMI values between Paraffin and Formalin groups ($p<0.05$). Comparisons between males and females in accordance to their respective groups showed that there were no differences in Slide group ($p>0.05$) but there were significant differences in CSA values of Paraffin and Formalin group ($p<0.05$). In conclusion, in case reports, in which left ventricular hypertrophy is investigated by the help of LVM and LVMI, Formalin and Slide group method and results might be more useful. On the other hand, all the three methods might be used in experimental studies included in healthy control groups. Additionally, it was discussed that the gender has no effect on evaluation among groups in terms of LVM and LVMI.

Key words: Morphometry, heart, rat, routine pathology, left ventricular mass (LVM)

INTRODUCTION

It is prominent to utilize echocardiographical examinations in investigations of heart abnormalities on humans and especially in determination of heart hypertrophy, the data obtained from echocardiography is analysed by certain calculations (Casiglia et al., 2008; Devereux and Reichek, 1977; Gosse et al., 1999; Krauser and Devereux, 2006; Urhausen et al., 2004). The used method in investigation of left ventricular hypertrophy with echocardiography was developed by Devereux and Reichek (1977) and utilized in postmortal examinations by using ruler and caliper (Fineschi et al., 2001, 2007; Montisci et al., 2012; Ozdemir et al., 2013). Again, it has been echocardiographically seen that postmortal morphometrical examinations on hearth were carried out in experimental animals but in some cases the examinations were done immediately following deaths

*Corressponding author. E-mail: oozdemir@selcuk.edu.tr

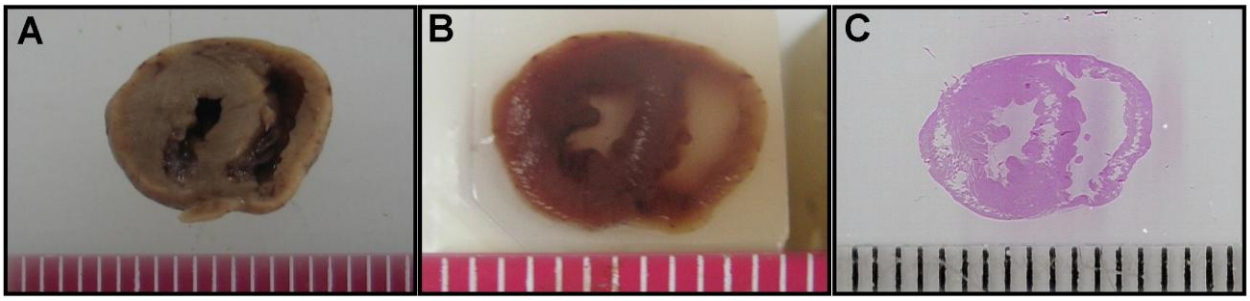

Figure 1. Sample of heart sections in routine histopathological procedure. (**A)** Formalin Group, (**B)** Paraffin Group, (**C)** Slide Group.

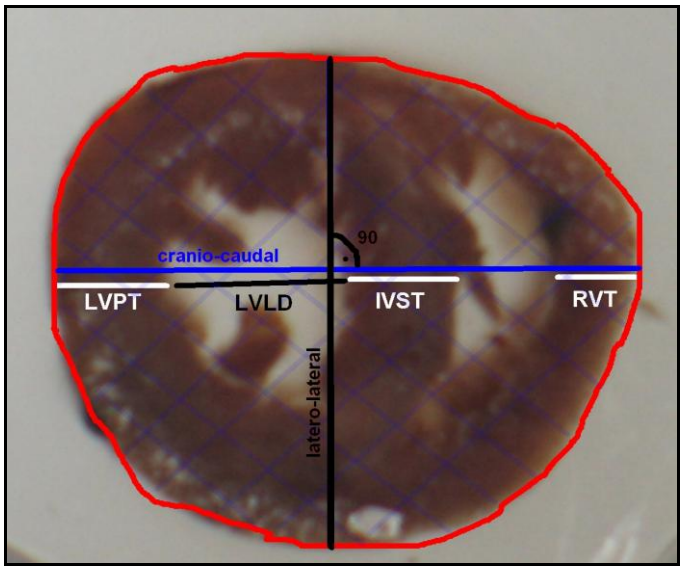

Figure 2. Measurement referance points on cut surface area of heart (Ozdemir et al., 2013). LVPT: Left ventricular posterior wall thickness; IVST: Interventricular septal thickness; LVLD: Left ventricular lumen diameter; RVT: Right ventricular thickness; CCD: Cranio-caudal diameter; LLD: Latero-lateral diameter; CSA: Cut surface area (scanned area).

and in some cases these examinations were done after section and staining are completed (Hinton et al., 2008; McAdamms et al., 2010; Noszczyk-Nowak et al., 2009; Woythaler et al., 1983). In retrospective studies, calculations were done in tissues usually after the formalin fixation (Chugh et al., 2000; Mannan et al., 2005).

Fixation, paraffin wax embedding and slicing are important processes of the routine pathology in postmortal investigations. Tissues usually somewhat shrink during formalin fixation and paraffin embedding. During the slicing process, the time spent between the sections wait in waterbath and transferring them on to lam, allows slices to expand and deteriorate (Luna, 1968; Unsaldi and Ciftci, 2010) and it could causes mistakes in morphometrical measurements.

In the present study, the aim was to investigate the effects of the routine fixation and tissue processing protocols commonly used in pathology (Formalin fixation, paraffin embedding, slicing and staining) on morphometrical parameters of the heart obtained from male and female rats.

MATERIALS AND METHODS

Six male and 6 female rats, 6 weeks of age, were used in the study. During the course of the study all rats were housed in polycarbonate cages (Techniplast, Italy) as 1 rat per 250 cm^2 and fed *adlibitum* with standart rat feed (Purina, Canada) and fresh water. All rats were euthanized under thiopental (40 mg/kg) anesthesia after body weight was measured. The hearts were wholly fixed in 10% formalin solution after heart weights was obtained. Then, they were transversally cut at the level of musculus papillaris and cross section surface were photographed (Formalin group) (Figure 1A). After routine tissue processing and parafin embedding, cut surfaces of paraffin wax tissues were photographed (Paraffin group) (Figure 1B). 5 µm thick sections were sliced at microtome and stained with Hematoxylin and Eosin (H&E). Also, stained preparations were photographed (Slide Group) (Figure 1C). Thickness, diameter and area of heart cut surfaces were analysed on photographs by using image analysis software (Digital Life Science Imaging, analySIS® LS Starter, 2.2, Build 1110, 23 An Olympus Company, Münster, Germany) in all groups. The values were measured as seen in Figure 2 (Ozdemir et al., 2013) in parameters of left ventriculus posterior thickness (LVPT), interventricular septum thickness (IVST), left ventriculus lumen diameter (LVLD), right ventriculus thickness (RVT), cut surface area (CSA), left ventricular area (LVA), right ventricular area (RVA), cut surface craniocaudal (CCD) and cut surface laterolateral (LLD) diameters (two measurement lines set right angle). Left ventricular mass (LVM) and left ventricular mass index (LVMI) were calculated according to Devereux and Reichek (1977), body surface area (BSA) was calculated according to Erer and Kiran (2005) after analyses.

$LVM\ (g) = 1.04\ ([LVPT + LVLD + IVST]^3 - [LVLD]^3) - 14\ g;$

$LVMI\ (g/m^2) = LVM / BSA$

$BSA(m^2) = [body\ weight\ (kg)]^{2/3} \times K/100$

The K value is a special factor to species and is accepted as 9 for

Table 1. Distribution of body weight, relative organ weight and body surface area values on groups of both male and female.

Analytical parameters	Male	Female
Body Weight (g)	271.00 ± 11.35[a]	221.50 ± 10.41[b]
Heart Weight (g)	1.06 ± 0.21[a]	0.87 ± 0.08[a]
Relative organ weight	0.39 ± 0.09[a]	0.39 ± 0.03[a]
Body surface area (m^2)	0.04± 0.00[a]	0.03 ± 0.00[b]

Different letters *(a, b, c)* in the same line indicate a statistically significant difference (p<0.05).

Table 2. Distrbution of length, area measurements and indexes of the heart on groups.

Analytical parameters	Male			Female		
	Formalin	Paraffin	Slide	Formalin	Paraffin	Slide
LVPT (mm)	3.51 ± 0.33[a]	2.56 ± 0.22[b]	3.05 ± 0.22[c]	3.37 ± 0.20[a]	2.52 ± 0.15[c]	2.93 ± 0.21[b]
IVST (mm)	2.67 ± 0.47[a]	2.05 ± 0.09[b]	2.24 ± 0.34[b]	2.67 ± 0.4334[a]	2.08 ± 0.40[b]	2.23 ± 0.27[b]
LVLD (mm)	2.54 ± 0.72[a]	2.74 ± 0.41[a]	2.28 ± 0.69[a]	2.19 ± 1.19[a]	2.65 ± 0.73[a]	2.49 ± 0.54[a]
RVT (mm)	1.49 ± 0.23[a]	1.07 ± 0.17[b]	1.20 ± 0.25[b]	1.64 ± 0.27[a]	1.10 ± 0.12[b]	1.34 ± 0.31[b]
CCD (mm)	11.37 ± 1.29[a]	9.59 ± 0.37[b]	10.50 ± 0.87[ab]	10.55 ± 0.31[a]	8.50 ± 0.46[b]	9.86 ± 0.65[a]
LLD (mm)	10.31 ± 1.16[a]	8.18 ± 0.62[b]	8.83 ± 0.60[b]	9.07 ± 0.16[a]	7.41 ± 0.22[c]	8.23 ± 0.41[b]
CSA (mm^2)	96.19 ± 14.65[a]	61.96 ± 5.55[c]	75.31 ± 8.07[b]	78.16 ± 3.98 [a]	50.60 ± 5.64 [c]	66.13 ± 8.27 [b]
LVA (mm^2)	3.69 ± 1.99[a]	3.45 ± 0.99[a]	3.24± 1.51[a]	1.97 ± 0.84 [a]	2.97 ± 1.16[a]	2.64 ± 0.78[a]
RVA (mm^2)	6.18 ± 3.93[a]	4.63 ± 2.67[a]	5.35 ± 4.12[a]	3.20 ± 0.23[a]	3.00 ± 1.33[a]	3.93 ± 1.78[a]
LVM (mg)	700.4 ± 314.1[a]	381.93 ± 61.48[b]	448.1 ± 98.6[ab]	563.0 ± 167.6[a]	364.93 ± 75.18[b]	442.5 ± 120.0[ab]
LVMI (g/m^2)	18.58 ± 8.44[a]	10.14 ± 1.70[b]	11.98 ± 5.49[ab]	17.07 ± 5.64[a]	11.11 ± 2.379[b]	13.5 ± 3.95 [ab]

Different letters (*a, b, c)* in the same line indicate a statistically significant difference (p<0.05). LVPT: Left ventricular posterior wall thickness, IVST: Interventricular septal thickness, LVLD: Left ventricular lumen diameter, RVT: Right ventricular thickness, CCD: Cranio-caudal diameter, LLD: Latero-lateral diameter, CSA: Cut surface area, LVA: left ventricular area, RVA: Right ventricular area, LVM: left ventriculus mass, LVMI: left ventriculus mass index, BSA: Body surface area.

mice and rats, 10 for cats, 10.1 for canines and 10.6 for a human of 70 kg body weight (Erer and Kiran, 2005).

Statistical analyses of the data were done using SPSS 13.0 pocket software (SPSS 13.0 for Windows/ SPSS® Inc, Chicago, USA). Comparison of the data between groups were done using ANOVA and Duncan tests, and between genders were done using independent t test. The values of p<0.05 was accepted as significant and results stated in Mean±SD.

RESULTS

Distribution of live body weight, relative organ weight and body surface area values on male and female groups were shown in Table 1, and measurements and calculations of the heart were shown in Table 2.

As an overall examination of the data, the highest values with exception of LVLD were seen in the Formalin group whereas the lowest values were in the Paraffin group both in males and females. As for LVLD value, the highest was seen in Paraffin group and the lowest in slide group among males whereas the highest value was in Paraffin group and the lowest was in Formalin group among females. While significant differences were seen in LVPT and CSA values both in males and females among the groups (p<0.05), the differences between groups are insignificant in LVLD, LVA and RVA values (p>0.05). In point of IVST, the Paraffin and Slide groups were similar but Formalin group showed significant differences (p<0.05). The LVM and LVMI values had significant differences between Paraffin and Formalin group (p<0.05), but Slide group values located between the Paraffin and the Formalin groups and had no stastical difference.

In comparisons of males and females according to the groups, there were no differences in Slide groups (p>0.05) whereas there were significcant differences in CSA (p<0.008), CCD (p<0.002) and LLD values (p<0.03) in Paraffin groups (Graphs 1 to 3) and there were differences in CSA values (p<0.05) (Graph 4) in Formalin groups.

DISCUSSION

Autopsy has been considered as the gold standart in studies regarding heart hypertrophy and it has been

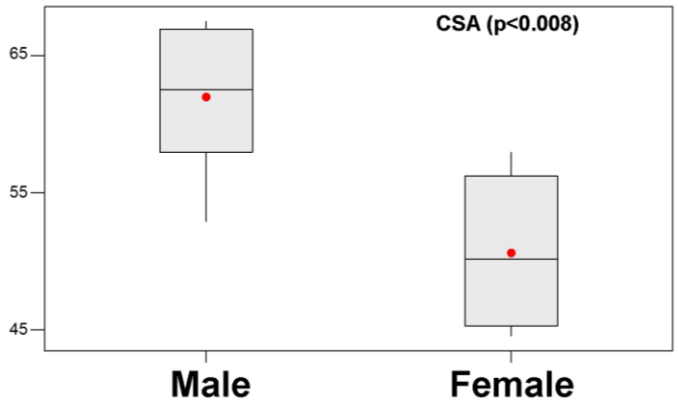

Graph 1. Cut surface area (CSA) (p<0.008) Paraffin groups.

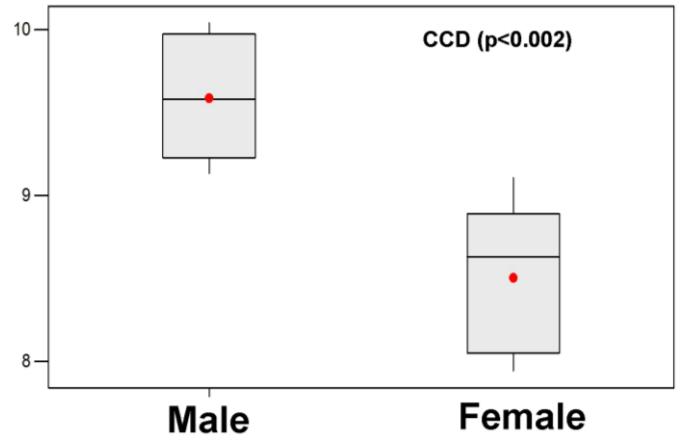

Graph 2. Cranio-caudal diameter (CCD) (p<0.002) Paraffin groups.

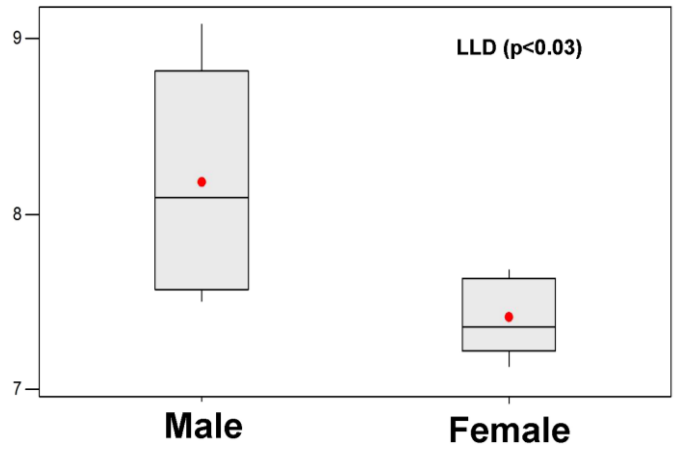

Graph 3. Latero-lateral diameter (LLD) (p<0.03) Paraffin groups.

stated that the most objective results of LVM are obtained by this way (Foppa et al., 2005). In studies regarding

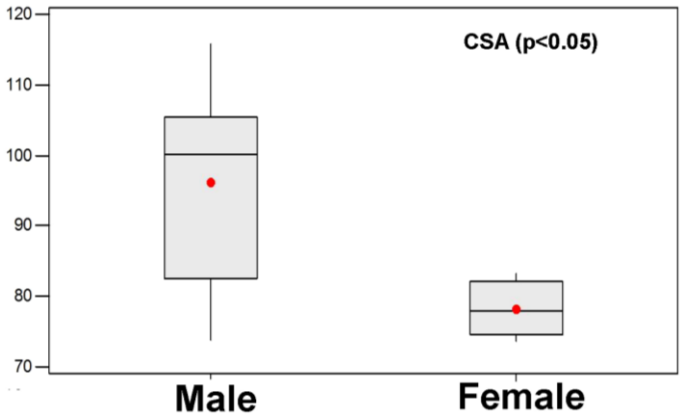

Graph 4. Cut surface area (CSA) (p<0.05) Formalin groups.

postmortal heart hypertrophy, the formulation based on Devereux and Reichek (1977) has been commonly used for the morphometrical measurement of the heart. This formulation has been applied on humans and experimental animals and the calculations have been done on LVM and LVMI (Casiglia et al., 2004; Fuster et al., 2005; Grandtner et al., 1974; Kasikcioglu et al., 2007; McAdamms et al., 2010; Noszczyk-Nowak et al., 2009; Ozdemir et al., 2013). In the present study, the evaluations were based on LVM and LVMI calculations too.

In experimental studies concerning the examination of the heart, postmortem measurements (prior to fixation) were not carried out due to certain reasons such as time differences between the time of death and measurements moment and due to the rigor mortis. In the study, the measurement were performed at the histopathological processing steps that consist of fixation, paraffin embedding and sectioning in microtome (Luna, 1968) in order to determine which step was more suitable.

In studies investigated, postmortal ventricular hypertrophy, the echocardiography, ruler and caliper usage and digital image analysis methods were used for heart measurements after formalin fixation (Cavalcanti and Duarte, 2008; Grandtner et al., 1974). In Ozdemir et al. (2013), where the effect of metenolone enanthate on morphometry of the heart were researched, the data were obtained by the method of digital image analysis on photographes taken from paraffin embedded tissues. Heart measurements in two different adult rat strains were done after staining the slides prepared from parafin blocks (McAdamms et al., 2010). In the present study, photos were taken firstly from formalin fixation tissue, later parafin embedded tissues and then from stained slides. LVM and LVMI values were calculated by the measurements obtained from these photos.

Tissues usually somewhat shrink during formalin fixation and paraffin embedding (Luna, 1968). In the present study the lowest values were seen in the Paraffin group and thus it was concluded that the paraffinization

has caused shrinkage more than formalin fixation in heart muscle. In another study conducted on rabbits, the histomorphometrical measurements of heart were lower than supravital measurements done by Electrocardiography (ECG) (Noszczyk-Nowak et al., 2009).

When LVM and LVMI values were considered, there were significant differences between Formalin and Paraffin groups whereas Slide group was similar to them and the values of it were between these two groups. It was commented that, in all groups LVM and LVMI values were higher than those reported by Ozdemir et al. (2013) and the values of LVPT, IVST and RVT were higher than those reported by McAdams et al. (2010).

Conclusion

It can be said that in case report investigation, left ventricular hypertrophy by the help of LVM and LVMI values, formalin fixed tissues and slide measurement findings were more useful, but in experimental study which includes healthy control groups, all three methods might be used. Additionally, it was discussed that the gender has no effect on evaluation among groups in terms of LVM and LVMI. Also the data can possibly contribute to studies that will be conducted on adolescent rats.

Conflict of Interests

The author(s) have not declared any conflict of interests.

REFERENCES

Casiglia E, Schiavon L, Tikhonoff V, Bascelli A, Martini B, Mazza A, Caffi S, Deste D, Bagato F, Bolzon M, Guidotti F, Nasto HH, Saug M, Guglielmi F, Pessina AC (2008). Electrocardiographic criteria of left ventricular hypertrophy in general population. Eur. J. Epidemiol. DOI 10.1007/s10654-008-9234-6. http://dx.doi.org/10.1007/s10654-008-9234-6

Cavalcanti JS, Duarte SM (2008). Morphometric study of the fetal hearth: A parameter for echocardiographic analysis. Radiol. Bras. 41:99-101.

Chugh SS, Kelly KL, Titus JL (2000). Sudden cardiac death with apparently normal heart. Circulation 102: 649-54. http://dx.doi.org/10.1161/01.CIR.102.6.649; PMid:10931805

Devereux RB, Reichek N (1977). Echocardiographicic determination of left ventricular mass in man: Anatomic validation of the method. Circulation 55:613-8. http://dx.doi.org/10.1161/01.CIR.55.4.613; PMid:138494

Erer H, Kıran MM (2005). Veterinary Oncology. 3th Edition, Damla Ofset Company, Konya, Turkey.

Fineschi V, Baroldi G, Monciotti F, Reattelli LP, Turillazzi E (2001). Anabolik steroid abuse and cardiac sudden death: A pathologic study. Arch. Pathol. Lab. Med. 125:253-255. PMid:11175645

Fineschi V, Riezzo I, Centini F, Silingardi E, Licata M, Beduschi G, Karch SB (2007). Sudden cardiac death during anabolicsteroid abuse: Morphologic and toxicologic findings in two fatal cases of bodybuilders. Int. J. Legal Med. 121:48-53. http://dx.doi.org/10.1007/s00414-005-0055-9; PMid:16292586

Foppa M, Duncan BB, Rohde LEP (2005). Echocardiography-based left ventricular mass estimation. How shoul we define hypertrophy? Cardiovasc. Ultrasound. 3:17. http://dx.doi.org/10.1186/1476-7120-3-17; PMCid:PMC1183230

Fuster RG, Argudo JAM, Albarova OG, Sos FH, Lopez SC, Codoner MB, Minano JAB, Albarran IR (2004). Left ventricular mass index as a prognostic factor in patients with severe aortic stenosis and ventricular dysfunction. Interact. Cardiovasc. Thorac. Surg. 4:260-266. http://dx.doi.org/10.1510/icvts.2004.098194; PMid:17670405

Gosse P, Jullien V, Lemetayer P, Clementy J (1999). Electrocardiographic definition of left ventricular hypertrophy in the hypertansive: Which method of indexation of left ventricular mass? J. Hum. Hypertens. 13: 505-509. http://dx.doi.org/10.1038/sj.jhh.1000885; PMid:10455470

Grandtner M, Turek Z, Kreuzer F (1974). Cardiac Hypertrophy in the first generation of rats native to simulated high altitue. Pflügers Arch. 350: 241-248. http://dx.doi.org/10.1007/BF00587803; PMid:4278725

Hinton RB, Alfieri CM, Witt SA, Glascock BJ, Khoury PR, Benson DW, Yutzey KE (2008). Mouse heart valve structure and function: ecocardiographic and morphometric analyses from the fetus through the aged adult. Am. J. Physol. Heart Circ. Phisiol. 294:H2480-H2488. http://dx.doi.org/10.1152/ajpheart.91431.2007; PMid:18390820

Kasikcioglu E, Oflaz H, Umman B, Bugra Z (2007). Androgenic anabolic steroids also impair right ventricular function. Int. J. Cardiol. http://dx.doi.org/10.1016/j.ijcard.2007.12.027

Krauser DG, Devereux RB (2006). Ventricular hypertrophy and hypertension. Herz 31: 305-316. http://dx.doi.org/10.1007/s00059-006-2819-5; PMid:16810470

Luna LG (1968) Manuals of Histologic Staining Methods of The Armed Forces Institute of Pathology, Third edition, McGraw-Hill Book Company, New York, USA.

Mannan S, Khalil M, Rahman H, Sultana SZ, Hossain MZ (2005). Morphometric study of atrioventricular orifices of postmortem heart of adult Bangladeshi people. Mymensingh Med. J. 14:182-184. PMid:16056207

McAdams RM, McPherson RJ, Dabestani NM, Gleason CA, Juul SE (2010). Left Ventricular Hypertrophy is Prevalent in Sprague–Dawley Rats. Comp. Med. 60:357–363. PMCid:PMC2958203

Montisci M, El Mazloum R, Cecchetto G, Terranova C, Ferrara SD, Thiene G, Basso C (2012). Anabolic androgenic steroids abuse and cardiac death in athletes: Morphological and toxicological findings in four fatal cases. Forens. Sci. Int. 217:e13-e18. http://dx.doi.org/10.1016/j.forsciint.2011.10.032; PMid:22047750

Noszczyk-Nowak A, Nicpon J, Nowak M, Slawuta P (2009). Preliminary reference values for electrocardiography, echocardiography and myocardial morphometry in the European Brown hare (Lepus europaeus). Acta Vet. Scand. 51:6. http://dx.doi.org/10.1186/1751-0147-51-6; PMCid:PMC2646734

Ozdemir O, Bozkurt I, Ozdemir M, Yavuz O (2013). Side Effect of Methenolone Enanthate on Rats heart in Puberty: Morphometrical study. Exp. Toxicol. Pathol. 65(6):745-750. http://dx.doi.org/10.1016/j.etp.2012.09.009

Unsaldi E, Ciftci MK (2010). Formaldehyde and its using areas, risk group, harmful effects and protective precautions against it. YYU. Vet. Fak. Derg. 21:71-75.

Urhausen A, Albers T, Kindermann W (2004). Are the cardiac effects of anabolic steroid abuse in strength athletes reversible? Heart 90:496-501. http://dx.doi.org/10.1136/hrt.2003.015719; PMCid:PMC1768225

Woythaler JN, Singer SL, Kwan OL, Meltzer RS, Reubner B, Bommer W, DeMaria A (1983). Accuracy of echocardiography versus electrocardiography in detecting left ventricular hypertrophy: Comparison with postmortem mass measurements. J. Am. Coll. Cardiol. 2:305-311. http://dx.doi.org/10.1016/S0735-1097(83)80167-3

academicJournals

Vol. 9(8), pp. 229-237, 30 April, 2014
DOI: 10.5897/SRE2014.5871
Article Number: F2A28FF44187
ISSN 1992-2248 © 2014

http://www.academicjournals.org/SRE

Scientific Research and Essays

Full Length Research Paper

The driving forces of fertilizer use intensity by crops in China: A complete decomposition model

Dan Pan

Institute of Poyang Lake Eco-Economics, Jiangxi University of Finance and Economics, Nanchang 330013, China.

Received 9 March, 2014; Accepted 9 April, 2014

Fertilizer plays an important role in raising agricultural production in China. However, the negative environmental consequences resulting from high fertilizer use intensity have posed serious challenges to agriculture sustainability in China. The goal of this study is to identify the underlying driving forces of fertilizer use intensity by crops that help to identify challenges and opportunities and provide advices for future policy measures. A complete decomposition method is employed to analyze the nature of the three factors that influence the changes in fertilizer use intensity by crops during the period of 2004 to 2011: fertilizer use efficiency effect, crop structure change effect and production efficiency effect. The results show that: (1) there were marked differences in the driving forces of fertilizer use intensity among different crops. The increase of fertilizer use intensity by grain crops was mostly affected by crop structure change and fertilizer use efficiency; the decline of fertilizer use intensity by economic crops was largely due to the crop structure change from high fertilizer use intensity type to low fertilizer use intensity type, while the increase of fertilizer use intensity by horticultural crops was mainly attributable to the crop structure change effect. The production efficiency had a positive effect on fertilizer use intensity decrease in all crops; (2) For the aggregate agricultural economy, the reduction of fertilizer use efficiency was the main factor in the growth of fertilizer use intensity, while the crop structure change and production efficiency change had minor effects on lowering fertilizer use intensity. We suggest that enhancing fertilizer use efficiency and changing crop structure should serve as essential approaches to reduce fertilizer use intensity in China.

Key words: Decomposition analysis, fertilizer use intensity, agriculture sustainability.

INTRODUCTION

The application of fertilizers is a major determinant in raising agricultural production and maintaining adequate food supplies in China (Wu, 2011). Despite a population of more than 1.3 billion which is about one-fifth of the world's total, China has been able to supply enough food for its growing population with about 7% of the world's arable land. A main contributor to such achievement is the increased use of chemical fertilizers (Zhong et al., 2007). According to the Food and Agriculture Organization (FAO), fertilizer globally contributes 40 to 60% of crop yield increase. In China, the figure was 57% during the period of 1978 to 2006 (Ma et al., 2014). Over the next two decades, due to the inadequate endowment and increased food security pressure, fertilizer will

E-mail:blesspanda@163.com; Tel: +86-18070062881; Fax: +86-791-8381-0892.

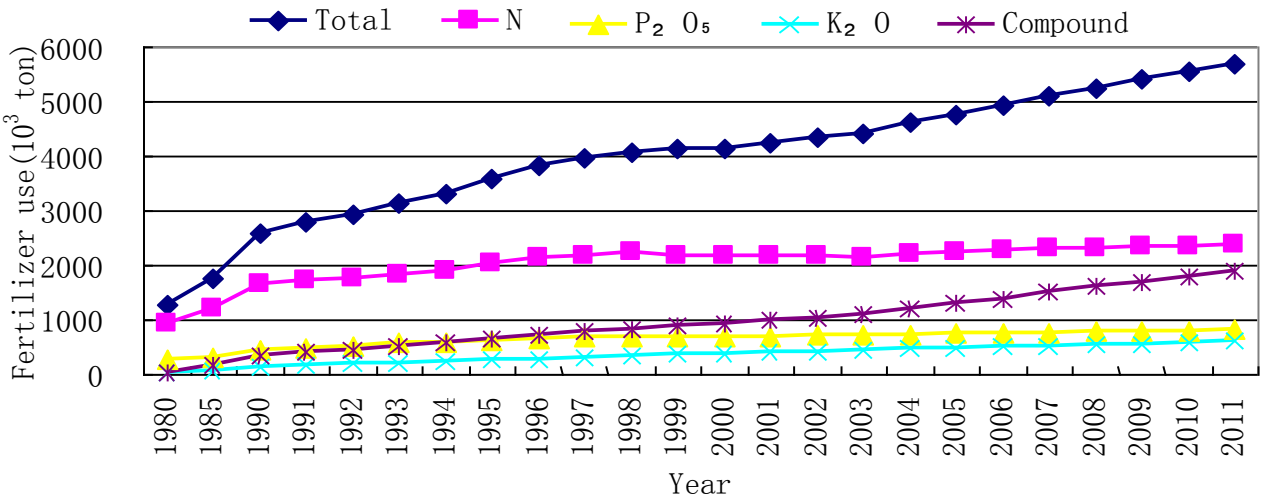

Figure 1. Fertilizer use amount in China from 1980 to 2011. Data Source: China Statistical Yearbook 2012.

Table 1. Fertilizer use rate during 1965-2009(unit: kg/ha).

Year / Country	1965	1970	1975	1980	1985	1990	1995	2000	2005	2006	2007	2008	2009
Netherlands	606	788	836	860	849	638	607	459	338	353	302	268	238
South Korea	156	262	420	390	417	490	549	455	643	470	511	480	362
Japan	338	376	364	373	419	386	354	325	348	333	350	278	291
China	25	44	70	158	143	221	287	279	408	434	479	463	504
Philippines	24	43	47	64	53	107	109	132	152	140	162	115	126
U.S.	64	82	101	114	95	100	113	105	119	126	123	106	109
India	5	14	21	34	53	74	86	103	128	136	143	153	167
World	37	53	70	88	94	100	94	100	115	120	127	119	122

Data Source: FAO, www.fao.org. Note: The fertilizer use here including nitrogenous fertilizer, phosphate fertilizer, potash fertilizer and compound fertilizer. These quantities are all measured in effective weight.

continue to make a key contribution to future agricultural development in China (Li et al., 2012).

The fertilizer use amount in China has grown rapidly in the late twentieth century, especially after the economic reform in the 1980s (Figure 1) (Gong et al., 2011). In addition, China's fertilizer use rate (kilograms per hectare, kg/ha hereafter) also has experienced a sustainable growth after 1960s and has surpassed the average level of the industrialized countries since 1980. From the late 1960s to 2009, fertilizer use rate in China has increased twenty times. By 2009, the fertilizer use rate in China has reached 504 kg/ha, which was 4 times greater than the global average (Table 1). Such high level of fertilizer use in China has raised concerns about its negative environmental consequences. For example, Zhu and Chen (2002), Ju et al. (2009) and Sun et al. (2012) showed that the high rate of fertilizer use has led to large N losses and has become the main source of water pollution and air pollution. A nation-wide pollution survey conducted by the Chinese Government identified that fertilizer was a major contributor to water-borne nitrogen, phosphorous pollution, and the increasing frequency of red tides (Zhang et al., 2013). Moreover, it is estimated that fertilizer production has accounted for 30% of agricultural greenhouse gas (GHG) emissions and was the source of about 8% of China's total GHG emissions (Liu and Zhang, 2011;Huang et al., 2012). Given the importance of fertilizer use with respect to GHG emissions and agriculture sustainability in China, a deeper understanding of the driving forces and their impacts on fertilizer use intensity is very important for the government to formulate fertilizer-reduction measures. Therefore, it is necessary to investigate the driving forces governing fertilizer use intensity.

Decomposition analysis is one of the widely employed tools for analysis of driving forces. In general, there are two kinds of decomposition techniques, one is the structural decomposition analysis (SDA) and the other is the index decomposition analysis (IDA) (Lei et al., 2012). SDA is based on input-output tables and is characterized

by capable of more refined decomposition of economic and technological effects. IDA uses index number concept in decomposition. The advantage of IDA is that it has various indicator forms, mathematical (additive and multiplicative) specifications and indices, and can be readily applied to various available data at different levels of aggregation (Hoekstra and Van den Bergh, 2003). Considering the fertilizer use data in China, IDA is more applicable for our study.

Nowadays, a range of different index methods are available in the IDA group, such as Divisia index and Laspeyres index (Mahony, 2013). How to decompose the residual term has crucial influence on the accuracy and reliability of these methods. Sun (1998) introduced a complete decomposition model where the residual term is distributed among the considered effects. Zhang and Ang (2001) referred to this model as the refined Laspeyres method, which has been widely adopted due to its simplification of both calculation and understanding. Nowadays, the complete decomposition method has become popular in carbon emission, energy conservation, pollutant reduction, and so on (Zhang et al., 2009; Lise, 2006). However, to the best of our knowledge, the application of this technique to the analysis of fertilizer use intensity is still scarce.

In addition, most of the previous studies on China's fertilizer use intensity were conducted at the national level or regional level which is likely to capture an aggregate trend of fertilizer use intensity in China. However, it is important to note that few studies have been conducted to examine China's fertilizer use intensity from the point of crops and thus may be neglecting the influence of a significant crop structural shift that from grain crops to economic and horticultural crops occurred in China beginning in the 1990s (Li et al., 2007; Ma et al., 2012). So with the rapid transition of China's agricultural production structure, crop perspectives are important to understand the trends of fertilizer use intensity in China.

Therefore, in this study, we attempt to extend further the complete decomposition technique to fertilizer use intensity, and aim to identify, quantify and explain major driving forces acting to the changes of fertilizer use intensity by crops in China. By utilizing decomposition analysis, we can improve the foundation for fertilizer reduction policies as it reveals the contributions of different factors to the evolution of fertilizer use intensity.

MATERIALS AND METHODS

Complete decomposition method

Fertilizer use intensity is the ratio of fertilizer input to agricultural output in the production process. It is usually taken as a typical index to evaluate the efficiency of fertilizer use. Given that the substantial difference of fertilizer use intensity among grain crops, economic crops, and horticultural crops, driving forces of fertilizer use intensity will be analyzed with decomposition method from the point of crops. The related symbol definitions in the complete decomposition model are listed in Table 2. Following an extended Kaya identity, the fertilizer use intensity can be expressed as follows:

$$e_t = \frac{F_t}{Y_t} = \frac{\sum_i F_{it}}{\sum_i Y_{it}} = \sum_i (\frac{F_{it}}{Y_{it}})(\frac{Y_{it}}{Y_t}) = \sum_i (\frac{F_{it}}{Y_{it}})(\frac{y_{it}a_{it}}{y_t a_t}) = \sum_i (\frac{F_{it}}{Y_{it}})(\frac{y_{it}}{y_t})(\frac{a_{it}}{a_t}) = \sum_i e_{it} \cdot p_{it} \cdot s_{it}, i = 1,2,3 \quad (1)$$

Let e_t denote the fertilizer use intensity of a target year t and e_0 denote the fertilizer use intensity of base year 0, then

$$e_t = \sum_i e_{it} p_{it} s_{it}; e_0 = \sum_i e_{i0} p_{i0} s_{i0} \quad (2)$$

So the variation of fertilizer use intensity between a base year 0 and a target year t can be decomposed to three effects: (1) the fertilizer use efficiency effect which is caused by the variation of fertilizer use efficiency (denoted by e_{eff}) (2) the crop structure effect which is induced by the adjustment of crop sown area (denoted by e_{str});(3) the production efficiency effect which is caused by the changes in the production efficiency (denoted by e_{pff}) in additive form, as follows:

$$\Delta e = e_t - e_0 = e_{eff} + e_{str} + e_{pff} \quad (3)$$

According to the complete decomposition model given by Sun (1998), each effect in the right hand side of Equation (3) can be computed as follows:

$$e_{eff} = \sum_i s_{i0} p_{i0} \Delta e_i + \frac{1}{2} \sum_i \Delta e_i (p_{i0} \Delta s_i + s_{i0} \Delta p_i) + \frac{1}{3} \sum_i \Delta e_i \Delta s_i \Delta p_i \quad (4)$$

$$e_{str} = \sum_i e_{i0} p_{i0} \Delta s_i + \frac{1}{2} \sum_i \Delta s_i (p_{i0} \Delta e_i + e_{i0} \Delta p_i) + \frac{1}{3} \sum_i \Delta e_i \Delta s_i \Delta p_i \quad (5)$$

$$e_{pff} = \sum_i e_{i0} s_{i0} \Delta p_i + \frac{1}{2} \sum_i \Delta p_i (s_{i0} \Delta e_i + e_{i0} \Delta s_i) + \frac{1}{3} \sum_i \Delta e_i \Delta s_i \Delta p_i \quad (6)$$

In the index number, we form

$$\frac{e_{eff}}{\Delta e} \times 100\% + \frac{e_{str}}{\Delta e} \times 100\% + \frac{e_{pff}}{\Delta e} \times 100\% = 100\% \quad (7)$$

Or

$$\frac{e_t}{e_0} = 1 + \frac{e_{eff}}{e_0} + \frac{e_{str}}{e_0} + \frac{e_{pff}}{e_0} \quad (8)$$

Data

According to the methodology listed above, the data used in this paper includes agricultural output, sown area and fertilizer use amount by crops. Data of agricultural output and sown area by different crops were collected from China Statistical yearbook

Table 2. Summary of notations and definitions in the complete decomposition model.

Variables	Definition
F_t	Fertilizer use amount in year t
F_{it}	Fertilizer use amount of crop i in year t
Y_t	Agricultural output in year t
Y_{it}	Agricultural output of crop i in year t
a_t	Total sown area in year t
a_{it}	Sown area of crop i in year t
f_t	Fertilizer use amount per unit area in year t
f_{it}	Fertilizer use amount per unit area of crop i in year t
e_t , e_0	Fertilizer use intensity in year t and year 0, respectively
e_{it} , e_{i0}	Fertilizer use intensity of crop i in year t and year 0, respectively
s_{it} , s_{i0}	Sown area share of crop i in year t and year 0, respectively
p_{it} , p_{i0}	Production efficiency of crop i in year t and year 0, respectively

issued by the State Statistics Bureau. Data of fertilizer use amount was gathered from the compiled materials of costs and profits of agricultural products of China issued by the National Development and Reform Commission. This dataset contains detail information on the costs of all inputs and yields of China's major crops for a sample of more than 60,000 households (Wang, 2010). Through this dataset, we can have a better understanding of fertilizer use intensity by crops in China.

To make data suitable for the complete decomposition analysis by crops, we divide the agricultural economy of China into three sectors: the grain crops sector, the economic crops sector, and the horticultural crops sector. The grain crops include wheat, rice, maize (corn), and soybean. The economic crops are comprised of peanut, rapeseed, cotton, sugarcane, sugar-beet, and tobacco. The horticultural crops are subdivided into vegetable crops and fruit crops (Xin et al., 2012). This study covers the period from 2004 to 2011 for several reasons. First, the fertilizer use amount of horticultural crops is available after 2004. Second, since 2004, the Chinese Government has issued a number of measures to promote fertilizer market reforms and the fertilizer price has fluctuated substantially. How fertilizer use intensity has been changed under these backgrounds deserves attention. Third, just as Ebenstein et al. (2011) pointed out that the fertilizer use has a "lock-in" effect, which implies that the next year's fertilizer use intensity can be significantly predicted by prior application. So, taking the recent years from 2004 to 2011 for analysis will give better advices on future fertilizer-reduction measures.

RESULTS AND DISCUSSION

Analysis of fertilizer use intensity in China

Table 3 shows the trend of fertilizer use intensity in the period of 2004 to 2011. It can be seen that the average fertilizer use intensity of the aggregate agricultural economy, grain crops, economic crops, and horticultural crops during 2004 to 2011 period were 3,854.8 kiloton/billion tons (Kt/Bt hereafter), 5,829.4, 4,455.7 and 2,538.6 Kt/Bt, respectively. This result indicated that the grain crops had the highest fertilizer use intensity, followed by the economic crops, while the fertilizer use intensity of horticultural crops was the lowest. As is well established in the previous literatures, fertilizer use intensity between 1,420 to 2,500 Kt/Bt is the internationally accepted level (Cui et al., 2010; Mcallister et al., 2012). Thus, it can be concluded that China's fertilizer use intensity was much higher than the internationally accepted level. Appropriate measures should be taken to reduce such high fertilizer use intensity.

Table 3 also presents the growth rates of fertilizer use intensity from 2004 to 2011. It showed that the fertilizer use intensity of aggregate agricultural economy rose from 3,815.8 Kt/Bt in 2004 to 4,027.7 Kt/Bt in 2011, with a growth rate of 5.55%, or 211.9 Kt/Bt. The fertilizer use intensity of grain crops and horticultural crops increased significantly from 5,443.8 and 2,691.1 Kt/Bt in 2004 to 5,939.4 and 2,816.6 Kt/Bt in 2011, with a growth rate of 9.10 and 4.66%, respectively. The fertilizer use intensity of economic crops recorded a slight decrease from 4,589.9 Kt/Bt in 2004 to 4,542.6 Kt/Bt in 2011.

Driving forces of fertilizer use intensity by grain crops

As shown in Table 4, the fertilizer use efficiency and crop

Table 3. The growth rates of fertilizer use intensity from 2004 to 2011.

Year	Aggregate	Grain crops	Economic crops	Horticultural crops
2004	3,815.8	5,443.8	4,589.9	2,691.1
2005	3,745.8	5,725.4	4,695.2	2,377.8
2006	3,865.5	5,780.6	4,569.3	2,499.9
2007	3,920.6	6,033.3	4,433.2	2,497
2008	3,610.2	5,643.9	3,909.4	2,273.1
2009	3,792.4	5,905.3	4,332.1	2,418.8
2010	4,060.9	6,163.7	4,573.7	2,734.5
2011	4,027.7	5,939.4	4,542.6	2,816.6
Average	3,854.8	5,829.4	4,455.7	2,538.6
2004-2011(Kt/Bt)	211.9	495.6	-47.3	125.5
2004-2011(%)	5.55	9.10	-1.03	4.66

Table 4. Decomposition of fertilizer use intensity in grain crops.

Period	Δe (Kt/Bt)	e_{eff} (Kt/Bt)	e_{str} (Kt/Bt)	e_{pff} (Kt/Bt)	$e_{eff} / \Delta e$	$e_{str} / \Delta e$	$e_{pff} / \Delta e$
2004-2005	281.65	278.78	15.21	-12.34	98.98	5.40	-4.38
2005-2006	55.16	43.23	8.72	3.21	78.37	15.81	5.82
2006-2007	252.66	276.42	-8.33	-15.43	109.40	-3.30	-6.11
2007-2008	-389.34	-409.54	12.52	7.68	105.19	-3.22	-1.97
2008-2009	261.39	291.16	-14.31	-15.46	111.39	-5.47	-5.91
2009-2010	258.38	255.57	12.13	-9.32	98.91	4.69	-3.61
2010-2011	-224.27	-221.91	-13.32	10.96	98.95	5.94	-4.89
Average	**495.63**	**471.87**	**41.65**	**-17.89**	**95.21**	**8.40**	**-3.61**

structure contribution rates were positive values in the growth of grain crops' fertilizer use intensity during 2004 to 2011. The accumulated fertilizer use efficiency effect was an increase of 471.87 Kt/Bt, which accounted for 95.21% of the total change in absolute value. The results indicated that the fertilizer use efficiency effect played the dominant role in increasing fertilizer use intensity of grain crops. This reflects that the advancement of fertilizer use efficiency is effective for reducing fertilizer use intensity in the grain crops. The crop structure effect was another factor that increased fertilizer use intensity over the study period, but its contribution was tiny. The accumulated crop structure effect was an increase of 41.65 Kt/Bt, which only accounted for 8.40% of the total fertilizer use intensity change in absolute value. The change in the production efficiency effect played a very minor role in decreasing fertilizer use intensity. This effect decreased fertilizer use intensity in most years except 2006 which resulted in an accumulated decrease of 17.89 Kt/Bt and accounted for 3.61% of the total fertilizer use intensity change in absolute value.

Driving forces of fertilizer use intensity by economic crops

Table 5 illustrates that the crop structure change was the most important factor in the reduction of fertilizer use intensity in the economic crops. The accumulated crop structure effect was a decrease of -435.65 Kt/Bt which accounted for 922.29% of the total change. This result indicated that the structure of China's economic crops has been optimized and has shown "fertilizer-saving" reorientation. The production efficiency change also had a positive effect on fertilizer use intensity decrease, but its contribution was trivial which only accounted for 9.65% of the total fertilizer use intensity change in absolute value. The fertilizer use efficiency change had a negative effect on fertilizer use intensity decrease. During 2004 to 2011, the fertilizer utilization efficiency lead to an increase of 831.94% of the total change in fertilizer use intensity, which reflected that the improvement of fertilizer use efficiency was necessary for fertilizer use intensity decrease in the economic crops.

Driving forces of fertilizer use intensity by horticultural crops

The decomposition results of horticultural crops were given in Table 6. For horticultural crops, the biggest contributor to the high increase of fertilizer use intensity was crop structure change effect. During the period of 2004 to 2011, 137.43 Kt/Bt fertilizer use intensity increase

Table 5. Decomposition of fertilizer use intensity in economic crops.

Period	Δe (Kt/Bt)	e_{eff} (Kt/Bt)	e_{str} (Kt/Bt)	e_{pff} (Kt/Bt)	e_{eff} / Δe	e_{str} / Δe	e_{pff} / Δe
2004-2005	105.37	160.87	-45.63	-9.87	152.67	-43.30	-9.37
2005-2006	-125.91	-12.89	-121.34	8.32	10.24	96.37	-6.61
2006-2007	-136.14	97.20	-222.36	-10.98	-71.39	163.33	8.07
2007-2008	-523.75	-459.73	-98.67	34.65	87.78	18.84	-6.62
2008-2009	422.59	344.46	123.56	-45.43	81.51	29.24	-10.75
2009-2010	241.62	285.19	-57.89	14.32	118.03	-23.96	5.93
2010-2011	-31.02	-73.79	34.56	8.21	237.90	-111.43	-26.47
Average	**-47.24**	**392.97**	**-435.65**	**-4.56**	**-831.94**	**922.29**	**9.65**

Table 6. Decomposition of fertilizer use intensity in horticultural crops.

Period	Δe (Kt/Bt)	e_{eff} (Kt/Bt)	e_{str} (Kt/Bt)	e_{pff} (Kt/Bt)	e_{eff} / Δe	e_{str} / Δe	e_{pff} / Δe
2004-2005	-313.27	20.31	-343.45	9.87	-6.48	109.63	-3.15
2005-2006	122.12	-2.49	133.56	-8.95	-2.04	109.37	-7.33
2006-2007	-2.87	-1.20	-2.65	0.98	41.86	92.26	-34.12
2007-2008	-223.97	16.61	-251.23	10.65	-7.42	112.17	-4.76
2008-2009	145.72	-6.30	159.87	-7.85	-4.32	109.71	-5.39
2009-2010	315.73	-7.74	343.23	-19.76	-2.45	108.71	-6.26
2010-2011	82.12	-10.60	111.26	-18.54	-12.91	135.49	-22.58
Average	**125.58**	**-7.88**	**137.43**	**-3.97**	**-6.27**	**109.44**	**-3.16**

was attributable to crop structure change, which accounted for 109.44% of the total change in absolute value. This indicated that it is necessary to adjust crop structure from high fertilizer use intensity type to low fertilizer use intensity type to strengthen low fertilizer utilization in the horticultural crops. The fertilizer use efficiency change had a negative effect on fertilizer use intensity increase. The accumulated fertilizer use efficiency effect was a decrease of -7.88 Kt/Bt, which accounted for -6.27% of the total fertilizer use intensity change. According to the China's 12th five-year plan of agriculture and rural economic development (2011 to 2015), with the rapid development of industrialization, urbanization, agricultural modernization process and the transformation of food consumption structure in China, the planting area of horticultural crops will maintain a sustained and rapid growth. Therefore, improving fertilizer use efficiency should serve as an essential approach to the reduction of fertilizer use intensity in China. The production efficiency change also had a negative effect on fertilizer use intensity increase, but its contribution was trivial which only accounted for 3.16% of the total fertilizer use intensity change in absolute value.

Driving forces of fertilizer use intensity by the aggregate agricultural economy

The changes of fertilizer use intensity in the aggregate agricultural economy of China were shown in Table 7. The fertilizer use efficiency effect played a dominant role in the growth of fertilizer use intensity in China. During 2004 to 2011, the fertilizer utilization efficiency accounted for 114.99% of the total change in fertilizer use intensity. As we all known, the maintenance of maximum crop yields to safeguard high levels of food security has been a central objective of the Chinese Government for many decades. Under the situation of high yield production, the Chinese Government encouraged farmers to use more fertilizer to attain higher yields and support China's domestic food security (Good and Beatty, 2011). China's food security success could not have been achieved without fertilizer use since 1980 (Figure 2). However, there is unequivocal evidence that fertilizer use is much higher than what is required for high crop yields and 95% food grain self-sufficiency. Approximately one-third of the cropland suffers from fertilizer overuse (Ju et al., 2009). Thus, the high level of fertilizer use tends to result in low fertilizer use efficiency.

The crop structure change and the production efficiency change were all negative values in the growth of fertilizer use intensity which indicated that these two factors were effective in reducing fertilizer use intensity in the aggregate agricultural economy. The accumulated crop structure change effect and production efficiency change were a decrease of -21.45 and -10.32 Kt/Bt respectively, which accounted for -10.12 and -4.87% of

Table 7. Decomposition of fertilizer use intensity for all crops.

Period	Δe (Kt/Bt)	e_{eff} (Kt/Bt)	e_{str} (Kt/Bt)	e_{pff} (Kt/Bt)	$e_{eff} / \Delta e$	$e_{str} / \Delta e$	$e_{pff} / \Delta e$
2004-2005	-70.01	-70.29	-2.06	2.34	100.40	2.94	-3.34
2005-2006	119.72	81.81	45.67	-7.76	68.33	38.15	-6.48
2006-2007	55.07	71.73	-13.45	-3.21	130.25	-24.42	-5.83
2007-2008	-310.36	-332.81	6.78	15.67	107.23	-2.18	-5.05
2008-2009	182.20	214.10	-21.58	-10.32	117.51	-11.84	-5.66
2009-2010	268.51	316.70	-31.45	-16.74	117.95	-11.71	-6.23
2010-2011	-33.24	-31.98	-3.24	1.98	96.21	9.75	-5.96
Average	**211.91**	**243.68**	**-21.45**	**-10.32**	**114.99**	**-10.12**	**-4.87**

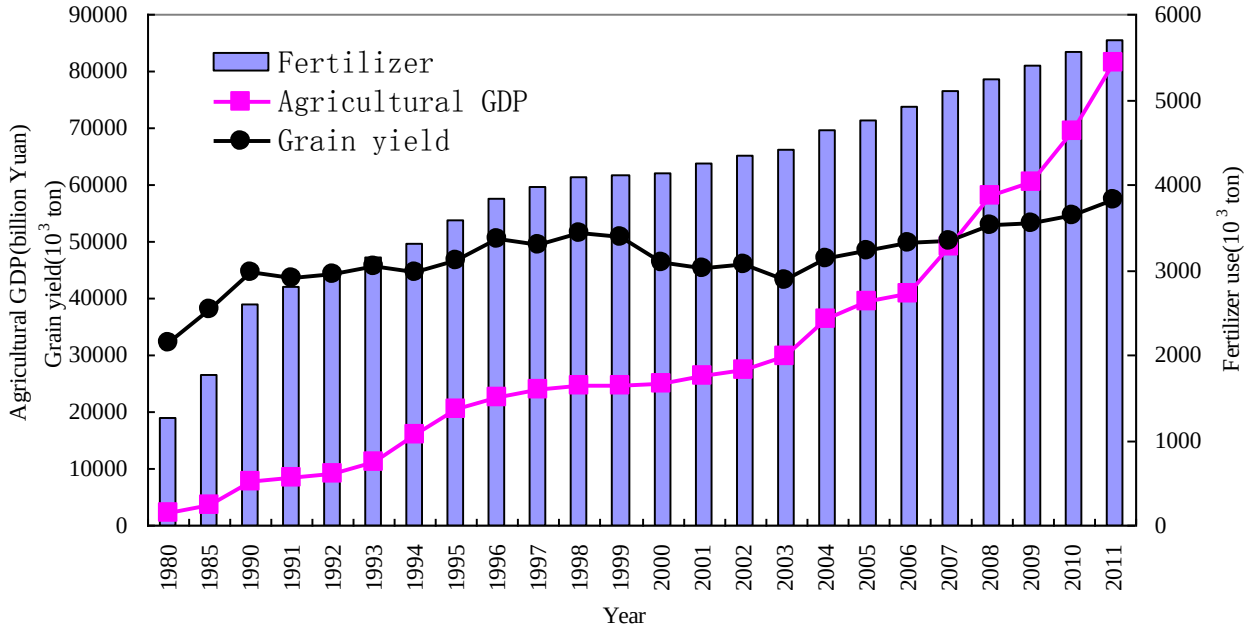

Figure 2. Agricultural GDP, grain yield and fertilizer use in China from 1980 to 2011.Data Source: China Statistical Yearbook 2012.

the total change, respectively.

Conclusion

In this paper, a complete decomposition method is used to study the underlying forces driving the fast-growing fertilizer use intensity in China during the period of 2004 to 2011. The factors that lead to changes in fertilizer use intensity are fertilizer use efficiency effect, crop structure change effect and production efficiency effect. We decompose the fertilizer use intensity from the crop level. This procedure sheds a better light on the driving forces influencing fertilizer use intensity and provides richer information that can be exploited for setting-up effective fertilizer use reduction countermeasures in each crop component. From this study, we may conclude: (1) Over the period of 2004 to 2011, the average fertilizer use intensity of the aggregate agricultural economy, grain crops, economic crops, and horticultural crops were all much higher than the internationally accepted level; (2) The fertilizer use intensity of grain crops increased 495.63 Kt/Bt during 2004 to 2011. The crop structure change and fertilizer use efficiency both had positive effects on the growth of fertilizer use intensity in grain crops, which increased 8.40 and 95.21% of the total fertilizer use intensity change, respectively. The production efficiency played a very minor role in decreasing fertilizer use intensity; (3) There was a slight decrease in the fertilizer use intensity of economic crops from 2004 to 2011, while this reduction was largely due to the crop structure change from high fertilizer use intensity

type to low fertilizer use intensity type. The fertilizer use efficiency change had a negative effect on fertilizer use intensity decrease of economic crops; (4) The fertilizer use intensity of horticultural crops increased 125.58 Kt/Bt from 2004 to 2011, while this increase was mainly induced by the crop structure change. The fertilizer use efficiency change and production efficiency change had negative effects on fertilizer use intensity increase of horticultural crops; (5) The change of fertilizer use intensity of aggregate agricultural economy was a 211.91 Kt/Bt increase during 2004 to 2011. The reduction of fertilizer use efficiency was the main factor in the growth of fertilizer use intensity of aggregate agricultural economy, while the crop structure change and production efficiency change had minor effects on lowering fertilizer use intensity of aggregate agricultural economy.

China's 12th five-year plan (2011 to 2015) has stated reducing fertilizer use intensity as one of the agricultural development priorities. In order to achieve harmonized development of both agricultural economic growth and environmental sustainability, China must make great efforts to reduce its fertilizer use intensity. Based on our results, the following strategies should be undertaken to fertilizer use intensity reduction.

(1) Enhancing fertilizer use efficiency. The effective approaches for fertilizer use efficiency advancement should include: using modified forms of N fertilizer, especially inclusion of inhibitors to slow the release of N into crop-available forms and decrease gaseous losses. This requires adjustment of subsidies to cover the additional cost of incorporating inhibitors and as an incentive for farmers to adopt new techniques, promoting production of organic fertilizers from animal manure, employing integrated water and nutrient management and so on. Subsidies for initial cost of equipment and policies to ensure that training is provided by equipment or fertilizer suppliers are also needed. These measures can greatly increase the efficiency of fertilizer use.

(2) Adopting more effective methods of delivering information, both technical and economic to farmers, including Farmer Field Schools and working with Farmer Associations. These must take account of the current situations in which many farmers are involved in off-farm activities that impose a constraint on labour and make "best practice" for farm operations impracticable. Working through Farmer Professional Associations and using Farmer Field Schools are obvious ways forward. In some situations, the development of technicians or service providers from the private sector (or public-private partnerships) for delivering advice would be a positive development. These innovations require new policies and practices by government agencies that enable multiple approaches.

(3) Changing crop structure. Crop structure will continue to exert an important influence on China's fertilizer use. The adjustment of crop structure from high fertilizer use intensity type to low fertilizer use intensity type will lower fertilizer use intensity. This adjustment needs to be addressed through the removal of perverse subsidies for fertilizer production. Fertilizer subsidies once played an important role in developing China's fertilizer industry but are now an unacceptable and unnecessary distortion. It is now time to reallocate these economic resources to more positive measures such as the introduction of payments to farmers for environmental services.

The conclusions drawn from this study have an important reference value for policy makers in assisting their design and implementation of appropriate fertilizer reduction measures and also have academic value in terms of enriching low carbon agricultural economy research systems in China. However, this study is still preliminary. Only three effect factors are considered in this paper. If a method can study more effect factors, it will be useful to find how these influence the changes in fertilizer use intensity. Then, generalizing the complete decomposition model which can consider more effect factors could be the subject of another future research.

Conflict of Interests

The author(s) have not declared any conflict of interests.

ACKNOWLEDGMENTS

We would like to thank the financial support from National Natural Science Foundation of China (No.71303099), Great National Social Science Fund Program (No.11&ZD155; No.12&ZD213), Technology Foundation of Jiangxi Education Department (No. GJJ13291), the MOE Layout Foundation of Humanities and Social Sciences (No. 11YJA790192), the Social Science Foundation of Jiangxi Province (No. 13YJ50), China Postdoctoral Science Foundation Funded Project (No. 2013T60646) and China Postdoctoral Science Foundation (No. 2012M521285).

REFERENCES

Cui Z, Chen X, Zhang F (2010). Current nitrogen management status and measures to improve the intensive wheat–maize system in China. Ambio. 39:376-384. http://dx.doi.org/10.1007/s13280-010-0076-6; PMid:21053721 PMCid:PMC3357710

Ebenstein A, Zhang J, McMillan MS, Chen K (2011). Chemical Fertilizer and Migration in China, National Bureau of Economic Research. http://dx.doi.org/10.3386/w17245; PMCid:PMC3116077

Gong P, Liang L, Zhang Q (2011). China must reduce fertilizer use too. Nature 473:284-285. http://dx.doi.org/10.1038/473284e; PMid:21593849

Good AG, Beatty PH (2011). Fertilizing nature: a tragedy of excess in the commons. PLoS Biol. 9:1-9. http://dx.doi.org/10.1371/journal.pbio.1001124; PMid:21857803 PMCid:PMC3156687

Hoekstra R, Van den Bergh JC (2003). Comparing structural decomposition analysis and index. Ecol. Econ. 25:39-64.

Huang J, Xiang C, Jia X, Hu R (2012). Impacts of training on farmers' nitrogen use in maize production in Shandong, China. J. Soil. Water

Conserv. 67:321-327. http://dx.doi.org/10.2489/jswc.67.4.321
Ju X, Xing G, Chen X, Zhang S, Zhang L, Liu X, Cui Z, Yin B, Christie P, Zhu Z (2009). Reducing environmental risk by improving N management in intensive Chinese agricultural systems. Proc. Natl. Acad. Sci. 106:3041-3046. http://dx.doi.org/10.1073/pnas.0813417106; PMid:19223587 PMCid:PMC2644255
Li X, Hu C, Delgado JA, Zhang Y, Ouyang Z (2007). Increased nitrogen use efficiencies as a key mitigation alternative to reduce nitrate leaching in north china plain. Agric. Water Manage. 89:137-147. http://dx.doi.org/10.1016/j.agwat.2006.12.012
Li YJ, Kahrl F, Pan JJ, Roland-Holst D, Su YF, Wilkes A, Xu JC (2012). Fertilizer use patterns in Yunnan Province, China: Implications for agricultural and environmental policy. Agr. Syst. 110:78-89. http://dx.doi.org/10.1016/j.agsy.2012.03.011
Lise W (2006). Decomposition of CO2 emissions over 1980–2003 in Turkey. Energy Pol. 34:1841-1852. http://dx.doi.org/10.1016/j.enpol.2004.12.021
Liu XJ, Zhang FS (2011). Nitrogen fertilizer induced greenhouse gas emissions in China. Curr. Opin. Environ. Sust. 3:407-413. http://dx.doi.org/10.1016/j.cosust.2011.08.006
Ma L, Feng S, Reidsma P, Qu F, Heerink N (2014). Identifying entry points to improve fertilizer use efficiency in Taihu Basin, China. Land Use Pol. 37:52-59. http://dx.doi.org/10.1016/j.landusepol.2013.01.008
Ma L, Velthof GL, Wang FH, Qin W, Zhang WF, Liu Z, Zhang Y, Wei J, Lesschen JP, Ma WQ (2012). Nitrogen and phosphorus use efficiencies and losses in the food chain in China at regional scales in 1980 and 2005. Sci. Total Environ. 434:51-61. http://dx.doi.org/10.1016/j.scitotenv.2012.03.028; PMid:22542299
Mahony TO (2013). Decomposition of Ireland's carbon emissions from 1990 to 2010: An extended Kaya identity. Energy Pol. 59:573-581. http://dx.doi.org/10.1016/j.enpol.2013.04.013
Mcallister CH, Beatty PH, Good AG (2012). Engineering nitrogen use efficient crop plants: the current status. Plant Biotechnol. J. 10:1011-1025. http://dx.doi.org/10.1111/j.1467-7652.2012.00700.x; PMid:22607381
Sun B, Zhang L, Yang L, Zhang F, Norse D, Zhu Z (2012). Agricultural Non-Point Source Pollution in China: Causes and Mitigation Measures. Ambio. 2:1-10.
Sun J (1998). Changes in energy consumption and energy intensity: A complete decomposition model. Ecol. Econ. 20:85-100.
Wang MY (2010). The rise of labor cost and the fall of labor input: Has China reached Lewis turning point? China Econ. J. 3:137-153. http://dx.doi.org/10.1080/17538963.2010.511905
Wu Y (2011). Chemical fertilizer use efficiency and its determinants in China's farming sector: Implications for environmental protection. China Agr. Econ. Rev. 3:117-130.
Xin L, Li X, Tan M (2012). Temporal and regional variations of China's fertilizer consumption by crops during 1998–2008. J. Geogr. Sci. 22:643-652. http://dx.doi.org/10.1007/s11442-012-0953-y
Zhang FQ, Ang BW (2001). Methodological issues in cross-country/region decomposition of energy and environment indicators. Ecol. Econ. 23:179-190.
Zhang M, Mu H, Ning Y (2009). Accounting for energy-related CO2 emission in China, 1991–2006. Energy Pol. 37:767-773. http://dx.doi.org/10.1016/j.enpol.2008.11.025
Zhang W, Dou Z, He P, Ju X, Powlson D, Chadwick D, Norse D, Lu Y, Zhang Y, Wu L (2013). New technologies reduce greenhouse gas emissions from nitrogenous fertilizer in China. Proc. Natl. Acad. Sci. 110:8375-8380. http://dx.doi.org/10.1073/pnas.1210447110; PMid:23671096 PMCid:PMC3666697
Zhong F, Ning M, Xing L (2007). Does crop insurance influence agrochemical uses under current Chinese situations? A case study in the Manasi watershed, Xinjiang. Agr. Econ. 36:103-112. http://dx.doi.org/10.1111/j.1574-0862.2007.00180.x
Zhu ZL, Chen DL (2002). Nitrogen fertilizer use in China–Contributions to food production, impacts on the environment and best management strategies. Nutr. Cycl. Agroecosyst. 63:117-127. http://dx.doi.org/10.1023/A:1021107026067

academicJournals

Vol. 9(8), pp. 238-248, 30 April, 2014
DOI: 10.5897/SRE2013.5772
Article Number: 1AF04F344192
ISSN 1992-2248 © 2014

http://www.academicjournals.org/SRE

Scientific Research and Essays

Full Length Research Paper

The improved generalized Riccati equation mapping method and its application for solving a nonlinear partial differential equation (PDE) describing the dynamics of ionic currents along microtubules

Elsayed M. E. Zayed*, Yasser A. Amer and Reham M. A. Shohib

Mathematics Department, Faculty of Sciences, Zagazig University, Zagazig, Egypt.

Received 10 December, 2013; Accepted 10 April, 2014

In this paper we apply the improved Riccati equation mapping method to construct many families of exact solutions of a nonlinear partial differential equation involving parameters of a special interest in nanobiosciences and biophysics which describe a model of microtubules as nonlinear RLC transmission lines. As results, we can successfully recover the previously known results that have been found using other methods. This method is straightforward and concise, and it can be applied to other nonlinear PDEs in mathematical physics. Comparison between our new results and the well-known results are given. Some comments on the well-known results are also presented at the end of this article.

Key words: Improved Riccati equation mapping method, exact traveling wave solutions, nonlinear partial differential equations (PDEs) of microtubules, Nonlinear RLC transmission lines.

PACS: 02.30.Jr, 05.45.Yv, 02.30.Ik

INTRODUCTION

In recent years, the exact traveling wave solutions for nonlinear partial differential equations (PDEs) has been investigated by many authors who are interested in non linear physical phenomena. Many powerful methods have been presented, such as the inverse scattering transform method (Ablowitz and Clarkson, 1991), the Hirota's bilinear method (Hirota, 1971), the Painleve expansion method (Weiss et al., 1983; Kudryashov, 1988, 1990, 1991), the Backlund truncated method (Miura, 1978; Rogers and Shadwick, 1982), the exp-function method (He and Wu, 2006; Yusufoglu, 2008; Zhang, 2008; Bekir, 2009, 2010; Aslan, 2011), the tanh-function method (Abdou, 2007; Fan, 2000; Zhang and Xia, 2008; Yusufoglu and Bekir, 2008), the Jacobi elliptic function

*Corresponding author. E-mail: e.m.e.zayed@hotmail.com

method (Chen and Wang, 2005; Liu et al., 2001; Lu, 2005), the (G'/G)-expansion method (Wang et al., 2008; Zhang et al., 2008; Zayed, 2009, 2010; Bekir, 2008; Ayhan and Bekir, 2012, Kudryashov, 2010a,b; Aslan, 2010, 2011, 2012a,b), the generalized Riccati equation mapping method (Zhu 2008; Zayed and Arnous, 2013, Zayed et al., 2013), and so on.

In the present paper, we shall use the improved Riccati equation mapping method to find the exact solutions of a nonlinear PDE of nanobiosciences. The main idea of this method is that the traveling wave solutions of nonlinear equations can be expressed by polynomials in Q, where $Q = Q(\xi)$ satisfies the generalized Riccati equation $Q' = r + pQ + qQ^2$ where $\xi = kx + \omega t$, where r, p, k, ω and q are constants. The degree of this polynomial can be determined by considering the homogeneous balance between the highest order derivatives and the nonlinear terms appearing in the given nonlinear equation, the coefficients of this polynomial can obtained by solving a set of algebraic equations resulted from the process of using the proposed method.

The objective of this paper is to apply the improved Riccati equation mapping method for finding many families of exact traveling wave solutions of the following nonlinear PDE of special interest in nanobiosciences, namely, the transmission line models for microtubules as nonlinear RLC transmission line (Sekulic et al., 2011a, Sataric et al., 2010):

$$R_2 C_0 L^2 u_{xxt} + L^2 u_{xx} + 2R_1 C_0 \delta u u_t - R_1 C_0 u_t = 0 \quad (1)$$

where $R_1 = 10^9 \Omega$ and $R_2 = 7 \times 10^6 \Omega$ stand for longitudinal and transversal component of resistance of an Elementary rings and parameter $\delta (\delta < 1)$ describes nonlinearity of ER capacitor in MT. Here $L = 8 \times 10^{-9} m$ while $C_0 = 1.8 \times 10^{-15} F$ is the total maximal capacitance of the ER. The physical details of the derivation of Equation (1) can be elaborated in Sataric et al. (2010). For further references about electrical models of microtubules, see for example Ilic et al. (2009), Sekulic et al. (2011b, 2012), Sataric et al. (2009); Freedman et al. (2010), and Sekulic and Sataric (2012). Recently, Equation (1) has been discussed in (Sekulic et al. 2011a) by using the modified extended tanh-function method, where its exact solutions have been found.

The rest of this paper can be organized as follows: First is description of the improved generalized Riccati equation method. Many families of exact traveling wave solutions for Equation (1) are next obtained. This is followed by illustrations on physical explanations for some obtained results. Thereafter, conclusions and comments on Sekulic et al. (2011a) as well as comparison between our new results and the well-known results obtained in Sekulic et al. (2011a) are investigated.

Description of the improved generalized Riccati equation mapping method

We suppose that a nonlinear PDE is in the following from:

$$P(u, u_x, u_t, u_{xx}, u_{tt}, ...) = o \quad (2)$$

where $u = u(x,t)$ is an unknown function , *P* is a polynomial in $u = u(x,t)$ and its partial derivatives in which the highest order derivatives and nonlinear terms are involved. Let us now give the main steps for solving Equation (2.1) using the improved Riccati equation mapping method (Zhu 2008; Zayed and Arnous, 2013; Zayed et al, 2013):

Step 1: We look for its traveling wave solution in the form

$$u(x,t) = u(\xi), \quad \xi = kx + \omega t \quad (3)$$

where k, ω are constants. Substituting (3) into Equation (2) gives the nonlinear ODE for $u(\xi)$ as follows:

$$H(u, u', u'', ...) = 0 \quad (4)$$

where H is a polynomial in $u(\xi)$ and its total derivatives $u', u'', u''', ...$ such that $u' = \frac{du}{d\xi}, u'' = \frac{d^2 u}{d\xi^2}, ...$

Step 2: We suppose that the solution of the ODE (4) can be expressed as follows:

$$u(\xi) = \sum_{i=-m}^{m} a_i Q^i(\xi) , \quad (5)$$

where $a_i (i = 0, \pm 1, \pm 2, ..., \pm m)$ are constants to be determined later such as $a_m \neq 0$ or $a_{-m} \neq 0$ and $Q = Q(\xi)$ is the solution of generalized Riccati equation

$$Q' = r + pQ + qQ^2 \quad (6)$$

where r, p and q are constants, such that $q \neq 0$.

Step 3: We determine the positive integer *m* in (5) by balancing the nonlinear terms and the highest order derivatives of $u(\xi)$ in Equation (4).

Step 4: Substituting (5) and along with Equation (6) into Equation (4) and then equating all the coefficients of $Q^i (i = 0, \pm 1, \pm 2, ..., \pm m)$ to zero yield a system of

algebraic equations which can be solved by using the Maple or Mathematica to find the values of the constants $a_i(-m,...,m)$ and k,ω.

Step 5: It is well-known (Zhu 2008; Zayed and Arnous, 2013; Zayed et al., 2013) that Equation (6) has many families of solutions as follows:

Type 1: When $\Delta = p^2 - 4qr > 0$ and $pq \neq 0$ or $qr \neq 0$ we have

$$\Phi_1(\xi) = -\frac{1}{2q}[p + \sqrt{\Delta}\tanh(\frac{\sqrt{\Delta}}{2}\xi)],$$

$$\Phi_2(\xi) = -\frac{1}{2q}[p + \sqrt{\Delta}\coth(\frac{\sqrt{\Delta}}{2}\xi)],$$

$$\Phi_3(\xi) = -\frac{1}{2q}[p + \sqrt{\Delta}(\tanh(\sqrt{\Delta}\xi) \pm i\,\mathrm{sech}(\sqrt{\Delta}\xi))], \quad i\sqrt{-1}$$

$$\Phi_4(\xi) = -\frac{1}{2q}[p + \sqrt{\Delta}(\coth(\sqrt{\Delta}\xi) \pm \mathrm{csch}(\sqrt{\Delta}\xi))],$$

$$\Phi_5(\xi) = -\frac{1}{4q}[2p + \sqrt{\Delta}(\tanh(\frac{\sqrt{\Delta}}{4}\xi) \pm \coth(\frac{\sqrt{\Delta}}{4}\xi))],$$

$$\Phi_6(\xi) = \frac{1}{2q}[-p + \frac{\sqrt{\Delta(A^2 + B^2)} - A\sqrt{\Delta}\cosh(\sqrt{\Delta}\xi)}{A\sinh(\sqrt{\Delta}\xi) + B}],$$

$$\Phi_7(\xi) = \frac{1}{2q}[-p - \frac{\sqrt{\Delta(B^2 - A^2)} + A\sqrt{\Delta}\cosh(\sqrt{\Delta}\xi)}{A\sinh(\sqrt{\Delta}\xi) + B}],$$

where *A* and *B* are two non-zero real constants satisfying B^2-A^2>0,

$$\Phi_8(\xi) = \frac{2r\cosh(\frac{\sqrt{\Delta}}{2}\xi)}{\sqrt{\Delta}\sinh(\frac{\sqrt{\Delta}}{2}\xi) - p\cos h(\frac{\sqrt{\Delta}}{2}\xi)},$$

$$\Phi_9(\xi) = \frac{-2r\sinh(\frac{\sqrt{\Delta}}{2}\xi)}{p\sinh(\frac{\sqrt{\Delta}}{2}\xi) - \sqrt{\Delta}\cosh(\frac{\sqrt{\Delta}}{2}\xi)},$$

$$\Phi_{10}(\xi) = \frac{2r\cosh(\frac{\sqrt{\Delta}}{2}\xi)}{\sqrt{\Delta}\sinh(\sqrt{\Delta}\xi) - p\cosh(\sqrt{\Delta}\xi) \pm i\sqrt{\Delta}}, \quad i = \sqrt{-1}$$

$$\Phi_{11}(\xi) = \frac{2r\sinh(\frac{\sqrt{\Delta}}{2}\xi)}{-p\sinh(\sqrt{\Delta}\xi) + \sqrt{\Delta}\cosh(\sqrt{\Delta}\xi) \pm \sqrt{\Delta}},$$

$$\Phi_{12}(\xi) = \frac{4r\sinh(\frac{\sqrt{\Delta}}{4}\xi)\cosh(\frac{\sqrt{\Delta}}{4}\xi)}{-2p\sinh(\frac{\sqrt{\Delta}}{4}\xi)\cosh(\frac{\sqrt{\Delta}}{4}\xi) + 2\sqrt{\Delta}\cosh^2(\frac{\sqrt{\Delta}}{2}\xi) - \sqrt{\Delta}},$$

Type 2: When $\Delta = p^2 - 4qr < 0$ and $pq \neq 0$ or $qr \neq 0$ we have

$$\Phi_{13}(\xi) = \frac{1}{2q}[-p + \sqrt{-\Delta}\tan(\frac{\sqrt{-\Delta}}{2}\xi)],$$

$$\Phi_{14}(\xi) = -\frac{1}{2q}[p + \sqrt{-\Delta}\cot(\frac{\sqrt{-\Delta}}{2}\xi)],$$

$$\Phi_{15}(\xi) = \frac{1}{2q}[-p + \sqrt{-\Delta}(\tan(\sqrt{-\Delta}\xi) \pm \sec(\sqrt{-\Delta}\xi))],$$

$$\Phi_{16}(\xi) = -\frac{1}{2q}[p + \sqrt{-\Delta}(\cot(\sqrt{-\Delta}\xi) \pm \csc(\sqrt{-\Delta}\xi))],$$

$$\Phi_{17}(\xi) = \frac{1}{4q}[-2p + \sqrt{-\Delta}(\tan(\frac{\sqrt{-\Delta}}{4}\xi) - \cot(\frac{\sqrt{-\Delta}}{4}\xi))],$$

$$\Phi_{18}(\xi) = \frac{1}{2q}[-p + \frac{\pm\sqrt{-\Delta(A^2 - B^2)} - A\sqrt{-\Delta}\cos(\sqrt{-\Delta}\xi)}{A\sin(\sqrt{-\Delta}\xi) + B}],$$

$$\Phi_{19}(\xi) = \frac{1}{2q}[-p - \frac{\pm\sqrt{-\Delta(A^2 - B^2)} - A\sqrt{-\Delta}\sin(\sqrt{-\Delta}\xi)}{A\sin(\sqrt{-\Delta}\xi) + B}],$$

where *A* and *B* are two non-zero real constants satisfying A^2-B^2>0,

$$\Phi_{20}(\xi) = -\frac{2r\cos(\frac{\sqrt{-\Delta}}{2}\xi)}{\sqrt{-\Delta}\sin(\frac{\sqrt{-\Delta}}{2}\xi) + p\cos(\frac{\sqrt{-\Delta}}{2}\xi)},$$

$$\Phi_{21}(\xi) = \frac{2r\sin(\frac{\sqrt{-\Delta}}{2}\xi)}{-p\sin(\frac{\sqrt{-\Delta}}{2}\xi) + \sqrt{-\Delta}\cos(\frac{\sqrt{-\Delta}}{2}\xi)},$$

$$\Phi_{22}(\xi) = -\frac{2r\cos(\frac{\sqrt{-\Delta}}{2}\xi)}{\sqrt{-\Delta}\sin(\sqrt{-\Delta}\xi) + p\cos(\sqrt{-\Delta}\xi) \pm \sqrt{-\Delta}},$$

$$\Phi_{23}(\xi) = \frac{2r\sin(\frac{\sqrt{-\Delta}}{2}\xi)}{-p\sin(\sqrt{-\Delta}\xi) + \sqrt{-\Delta}\cos(\sqrt{-\Delta}\xi) \pm \sqrt{-\Delta}},$$

$$\Phi_{24}(\xi) = \frac{4r\sin(\frac{\sqrt{-\Delta}}{4}\xi)\cos(\frac{\sqrt{-\Delta}}{4}\xi)}{-2p\sin(\frac{\sqrt{-\Delta}}{4}\xi)\cos(\frac{\sqrt{-\Delta}}{4}\xi) + 2\sqrt{-\Delta}\cos^2(\frac{\sqrt{-\Delta}}{2}\xi) - \sqrt{-\Delta}},$$

Type 3: When $r = 0 \, and \, pq \neq 0$ we have

$$\Phi_{25}(\xi) = \frac{-pd}{q[d + \cosh(p\xi) - \sinh(p\xi)]},$$

$$\Phi_{26}(\xi) = -\frac{p[\cosh(p\xi) + \sinh(p\xi)]}{q[d + \cosh(p\xi) + \sinh(p\xi)]},$$

where *d* is an arbitrary constant.

Type 4: When $r = p = 0 \, and \; q \neq 0$ we have

$$\Phi_{27}(\xi) = \frac{-1}{q\xi + c_1} \ ,$$

where c_1 is an arbitrary constant.

Step 6: Substituting the well known solutions of Equation (6) listed above in Step 5 into (5) we have many families of exact solutions of Equation (2).

MANY FAMILIES OF EXACT TRAVELING WAVE SOLUTIONS FOR EQUATION (1)

Here we apply the proposed improved generalized Riccati equation mapping method to find many families of exact traveling wave solutions of Equation (1). To the end we use the wave transformation

$$u(x,t) = u(\xi), \qquad \xi = \frac{1}{L}x - \frac{c}{\tau}t \, , \tag{7}$$

where $\tau = R_1 C_0 = 1.32 \times 10^{-6} s,$ and c is the dimensionless velocity of the wave, to reduce Equation (1) into the following ODE:

$$u'' - \frac{\alpha}{c}u' + \frac{\beta}{2}u^2 - \gamma u = 0 \tag{8}$$

where $\alpha = \frac{\tau}{R_2 C_0}, \ \beta = \frac{2R_1\delta}{R_2}, \gamma = \frac{R_1}{R_2}$.

By balancing $u''with \ u^2$, we have m=2. Hence the formal solution of Equation (8) takes the form:

$$u(\xi) = a_2 Q^2 + a_1 Q + a_0 \ + a_{-1}Q^{-1} + a_{-2}Q^{-2} \tag{9}$$

where $a_2, \ a_1, a_0, \ a_{-1}, a_{-2}$ are constants to be determined, such that $a_{-2} \neq 0$ or $a_2 \neq 0$.

Inserting (9) with the aid of Equation (6) into Equation (8) we get the following system of algebraic equations:

$$Q^4 : \qquad 6a_2 q^2 + \frac{\beta}{2}a_2^2 = 0,$$

$$Q^{-4} : \qquad 6a_{-2}r^2 + \frac{\beta}{2}a_{-2}^2 = 0,$$

$$Q^3 \ : \qquad 10a_2 pq + 2a_1 q^2 - \frac{2q\alpha}{c}a_2 + \beta a_1 a_2 = 0,$$

$$Q^{-3} \ : \qquad 10a_{-2}pr + 2a_{-1}r^2 + \frac{2r\alpha}{c}a_{-2} + \beta a_{-1}a_{-2} = 0,$$

$$Q^2 \ : \quad 8a_2 qr + 3a_1 pq + 4a_2 p^2 - \frac{\alpha}{c}(2a_2 p + a_1 q) + \frac{\beta}{2}(a_1^2 + 2a_0 a_2) - \gamma a_2 = 0,$$

$$Q^{-2} \ : \quad 8a_{-2}qr + 3a_{-1}pr + 4a_{-2}p^2 + \frac{\alpha}{c}(2a_{-2}p + a_{-1}r) + \frac{\beta}{2}(a_{-1}^2 + 2a_0 a_{-2}) - \gamma a_{-2} = 0,$$

$$Q \ : \quad 6a_2 pr + 2a_{-1}qr + a_1 p^2 - \frac{\alpha}{c}(2a_2 r + a_1 p) + \beta(a_{-1}a_2 + a_0 a_1) - \gamma a_1 = 0,$$

$$Q^{-1} \ : \quad 6a_{-2}pq + 2a_{-1}qr + a_{-1}p^2 + \frac{\alpha}{c}(2a_{-2}q + a_{-1}p) + \beta(a_1 a_{-2} + a_0 a_{-1}) - \gamma a_{-1} = 0,$$

$$Q^0 \ : \quad 2a_2 r^2 + a_1 pr + a_{-1}pq + 2a_{-2}q^2 - \frac{\alpha}{c}(a_1 r - a_{-1}q) + \frac{\beta}{2}(a_0^2 + 2a_{-1}a_1 + 2a_{-2}a_2) - \gamma a_o = 0.$$

By solving these algebraic equations with the aid of Maple or Mathematica we have the following cases:

Case 1

$$p = p, q = q, r = -\frac{1}{24q}(\gamma - 6p^2), a_0 = \frac{3}{2\beta}(-2p^2 + \frac{10}{3}\frac{p\gamma c}{\alpha} + \gamma), \ a_1 = \frac{12q(\frac{\alpha}{5c} - p)}{\beta},$$

$$a_2 = \frac{-12q^2}{\beta}, c = \frac{\alpha}{5}\sqrt{\frac{6}{\gamma}}, \ a_{-1} = a_{-2} = 0$$

Case 2

$$p = p, q = q, r = -\frac{1}{24q}(\gamma - 6p^2), a_0 = \frac{1}{2\beta}(-6p^2 - \frac{10p\gamma c}{\alpha} + 3\gamma), \ a_{-1} = \frac{(\frac{\alpha}{5c} + p)(\gamma - 6p^2)}{2q\beta},$$

$$a_{-2} = \frac{-(\gamma - 6p^2)^2}{48\beta q^2}, c = \frac{\alpha}{5}\sqrt{\frac{6}{\gamma}}, a_1 = a_2 = 0$$

Case 3

$$p = 0, q = q, \ r = -\frac{\gamma}{96q}, a_0 = \frac{5\gamma}{4\beta}, \ a_1 = \frac{12q\alpha}{5\beta c}, a_{-1} = \frac{\gamma\alpha}{40q\beta c}, a_2 = \frac{-12q^2}{\beta}$$

$$a_{-2} = \frac{-\gamma^2}{768\beta q^2}, c = \frac{\alpha}{5}\sqrt{\frac{6}{\gamma}}.$$

Exact traveling wave solutions of Equation (1) for Case 1

By using the case 1 and according to the values of solutions of type 1 in the proposed method, we obtain the following exact traveling wave solutions for Equation (1):

$$u_1(x,t) = \frac{3\gamma}{2\beta} + 2p[\frac{5\gamma c}{2\alpha} - \frac{3\alpha}{5\beta c}] - \frac{\alpha\sqrt{6\gamma}}{5\beta c}\tanh(\sqrt{\frac{\gamma}{24}}\xi) - \frac{\gamma}{2\beta}\tanh^2(\sqrt{\frac{\gamma}{24}}\xi),$$

$$u_2(x,t) = \frac{3\gamma}{2\beta} + 2p[\frac{5\gamma c}{2\alpha} - \frac{3\alpha}{5\beta c}] - \frac{\alpha\sqrt{6\gamma}}{5\beta c}\coth(\sqrt{\frac{\gamma}{24}}\xi) - \frac{\gamma}{2\beta}\coth^2(\sqrt{\frac{\gamma}{24}}\xi),$$

$$u_3(x,t)=\frac{3\gamma}{2\beta}+2p[\frac{5\gamma c}{2\alpha}-\frac{3\alpha}{5\beta c}]-\frac{\alpha\sqrt{6\gamma}}{5\beta c}\left[\tanh(\sqrt{\frac{\gamma}{6}}\xi)\pm i\ \sec h(\sqrt{\frac{\gamma}{6}}\xi)\right]$$
$$-\frac{\gamma}{2\beta}\left[\tanh(\sqrt{\frac{\gamma}{6}}\xi)\pm i\ \sec h(\sqrt{\frac{\gamma}{6}}\xi)\right]^2,$$

$$u_4(x,t)=\frac{3\gamma}{2\beta}+2p[\frac{5\gamma c}{2\alpha}-\frac{3\alpha}{5\beta c}]-\frac{\alpha\sqrt{6\gamma}}{5\beta c}\left[\coth(\sqrt{\frac{\gamma}{6}}\xi)\pm i\ \cos ch(\sqrt{\frac{\gamma}{6}}\xi)\right]$$
$$-\frac{\gamma}{2\beta}\left[\coth(\sqrt{\frac{\gamma}{6}}\xi)\pm i\ \cos ch(\sqrt{\frac{\gamma}{6}}\xi)\right]^2,$$

$$u_5(x,t)=\frac{3\gamma}{2\beta}+p[\frac{5\gamma c}{\alpha\beta}-\frac{6\alpha}{5\beta c}]-\frac{3\alpha}{5\beta c}\sqrt{\frac{\gamma}{6}}\left[\tanh(\sqrt{\frac{\gamma}{96}}\xi)\pm\coth(\sqrt{\frac{\gamma}{96}}\xi)\right]$$
$$-\frac{\gamma}{8\beta}\left[\tanh(\sqrt{\frac{\gamma}{96}}\xi)\pm\coth(\sqrt{\frac{\gamma}{96}}\xi)\right]^2,$$

$$u_6(x,t)=\frac{3\gamma}{2\beta}+\frac{p}{\beta}[\frac{5\gamma c}{\alpha}-\frac{6\alpha}{5c}]+\frac{\alpha\sqrt{6\gamma}}{5\beta c}\left[\frac{(\sqrt{A^2+B^2}-A\cosh(\sqrt{\frac{\gamma}{6}}\xi)}{(A\sinh(\sqrt{\frac{\gamma}{6}}\xi)+B)}\right]-\frac{\gamma}{2\beta}\left[\frac{(\sqrt{A^2+B^2}-A\cosh(\sqrt{\frac{\gamma}{6}}\xi)}{(A\sinh(\sqrt{\frac{\gamma}{6}}\xi)+B)}\right]^2,$$

$$u_7(x,t)=\frac{3\gamma}{2\beta}+\frac{p}{\beta}[\frac{5\gamma c}{\alpha}-\frac{6\alpha}{5c}]+\frac{\alpha\sqrt{6\gamma}}{5\beta c}\left[\frac{(\sqrt{B^2-A^2}+A\cosh(\sqrt{\frac{\gamma}{6}}\xi)}{(A\sinh(\sqrt{\frac{\gamma}{6}}\xi)+B)}\right]-\frac{\gamma}{2\beta}\left[\frac{(\sqrt{B^2-A^2}+A\cosh(\sqrt{\frac{\gamma}{6}}\xi)}{(A\sinh(\sqrt{\frac{\gamma}{6}}\xi)+B)}\right]^2,$$

where A and B are two non-zero real constants satisfying $B^2-A^2>0$,

$$u_8(x,t)=\frac{3}{2\beta}[-2p^2+\frac{10p\gamma c}{3\alpha}+\gamma]+\frac{24qr}{\beta}\left(\frac{(-p+\frac{\alpha}{5c})\cosh(\sqrt{\frac{\gamma}{24}}\xi)}{(\sqrt{\frac{\gamma}{6}}\sinh(\sqrt{\frac{\gamma}{24}}\xi)-\sqrt{\frac{\gamma}{6}}\cosh(\sqrt{\frac{\gamma}{24}}\xi))}\right)$$
$$-\frac{48q^2r^2\cosh^2(\sqrt{\frac{\gamma}{24}}\xi)}{\beta\left(\sqrt{\frac{\gamma}{6}}\sinh(\sqrt{\frac{\gamma}{24}}\xi)-\sqrt{\frac{\gamma}{6}}\cosh(\sqrt{\frac{\gamma}{24}}\xi)\right)^2},$$

$$u_9(x,t)=\frac{3}{2\beta}[-2p^2+\frac{10p\gamma c}{3\alpha}+\gamma]-\frac{24qr}{\beta}\left(\frac{(-p+\frac{\alpha}{5c})\sinh(\sqrt{\frac{\gamma}{24}}\xi)}{(p\sinh(\sqrt{\frac{\gamma}{24}}\xi)-\sqrt{\frac{\gamma}{6}}\cosh(\sqrt{\frac{\gamma}{24}}\xi))}\right)$$
$$-\frac{48q^2r^2\sinh^2(\sqrt{\frac{\gamma}{24}}\xi)}{\beta\left(p\sinh(\sqrt{\frac{\gamma}{24}}\xi)-\sqrt{\frac{\gamma}{6}}\cosh(\sqrt{\frac{\gamma}{24}}\xi)\right)^2},$$

$$u_{10}(x,t)=\frac{3}{2\beta}[-2p^2+\frac{10p\gamma c}{3\alpha}+\gamma]+\frac{24qr}{\beta}\left(\frac{(-p+\frac{\alpha}{5c})\cosh(\sqrt{\frac{\gamma}{24}}\xi)}{(\sqrt{\frac{\gamma}{6}}\sinh(\sqrt{\frac{\gamma}{6}}\xi)-p\cosh(\sqrt{\frac{\gamma}{6}}\xi)\pm i\sqrt{\frac{\gamma}{6}})}\right)$$
$$-\frac{48q^2r^2\cosh^2(\sqrt{\frac{\gamma}{24}}\xi)}{\beta\left(\sqrt{\frac{\gamma}{6}}\sinh(\sqrt{\frac{\gamma}{6}}\xi)-p\cosh(\sqrt{\frac{\gamma}{6}}\xi)\pm i\sqrt{\frac{\gamma}{6}}\right)^2},$$

$$u_{11}(x,t)=\frac{3}{2\beta}[-2p^2+\frac{10p\gamma c}{3\alpha}+\gamma]+\frac{24qr}{\beta}\left(\frac{(-p+\frac{\alpha}{5c})\sinh(\sqrt{\frac{\gamma}{24}}\xi)}{(-p\sinh(\sqrt{\frac{\gamma}{6}}\xi)-\sqrt{\frac{\gamma}{6}}\cosh(\sqrt{\frac{\gamma}{6}}\xi)\pm\sqrt{\frac{\gamma}{6}})}\right)$$
$$-\frac{48q^2r^2\sinh^2(\sqrt{\frac{\gamma}{24}}\xi)}{\beta\left(-p\sinh(\sqrt{\frac{\gamma}{6}}\xi)-\sqrt{\frac{\gamma}{6}}\cosh(\sqrt{\frac{\gamma}{6}}\xi)\pm\sqrt{\frac{\gamma}{6}}\right)^2},$$

$$u_{12}(x,t)=\frac{3}{2\beta}[-2p^2+\frac{10p\gamma c}{3\alpha}+\gamma]+\frac{24qr}{\beta}\left(\frac{(-p+\frac{\alpha}{5c})\sinh(\sqrt{\frac{\gamma}{24}}\xi)}{(-p\sinh(\sqrt{\frac{\gamma}{24}}\xi)+\sqrt{\frac{\gamma}{6}}\cosh(\sqrt{\frac{\gamma}{24}}\xi))}\right)$$
$$-\frac{48q^2r^2\sinh^2(\frac{\sqrt{\gamma}}{2\sqrt{6}}\xi)}{\beta\left(-p\sinh(\sqrt{\frac{\gamma}{24}}\xi)+\sqrt{\frac{\gamma}{6}}\cosh(\sqrt{\frac{\gamma}{24}}\xi)\right)^2},$$

where $\xi=\frac{1}{L}x-\frac{\alpha}{5}\sqrt{\frac{6}{\gamma}}\frac{t}{\tau}$.

Remark 1. If $\gamma=6p^2$, then $r=0$ and $\Delta=p^2$. Consequently we have

$$a_0=\frac{12P^2}{\beta},\quad ,\ a_2=\frac{-12q^2}{\beta},c=\frac{\alpha}{5p},\ a_{-1}=a_1=a_{-2}=0\cdot$$

According to the values of the solutions of type 3 in Sec.2, we obtain the following exact traveling wave solutions for Equation (1):

$$u_{13}(x,t)=\frac{12p^2}{\beta}-\frac{12q^2}{\beta}\left(\frac{pd}{q[d+\cosh(p\xi)-sinh(p\xi)]}\right)^2,$$

$$u_{14}(x,t)=\frac{12p^2}{\beta}-\frac{12q^2}{\beta}\left(\frac{p[\cosh(p\xi)+sinh(p\xi)]}{q[d+\cosh(p\xi)-sinh(p\xi)]}\right)^2,$$

where $\xi=\frac{1}{L}x-\frac{\alpha}{5p}\frac{t}{\tau}$.

Exact traveling wave solutions of Equation (1) for case 2.

By using the case 2 and according to the values of solutions of type 1 in the proposed method, we obtain the following exact traveling wave solutions for Equation (1):

$$u_1(x,t)=\frac{1}{2\beta}[-6p^2-\frac{10p\gamma c}{\alpha}+3\gamma]-\frac{(\gamma-6p^2)(p+\frac{\alpha}{5c})}{\beta}\left[p+\sqrt{\frac{\gamma}{6}}\tanh(\sqrt{\frac{\gamma}{24}}\xi)\right]^{-1}$$
$$-\frac{(\gamma-6p^2)^2}{12\beta}\left[p+\sqrt{\frac{\gamma}{6}}\tanh(\sqrt{\frac{\gamma}{24}}\xi)\right]^{-2}$$

$$u_2(x,t)=\frac{1}{2\beta}[-6p^2-\frac{10p\gamma c}{\alpha}+3\gamma]-\frac{(\gamma-6p^2)(p+\frac{\alpha}{5c})}{\beta}\left[p+\sqrt{\frac{\gamma}{6}}\coth(\sqrt{\frac{\gamma}{24}}\xi)\right]^{-1}$$
$$-\frac{(\gamma-6p^2)^2}{12\beta}\left[p+\sqrt{\frac{\gamma}{6}}\coth(\sqrt{\frac{\gamma}{24}}\xi)\right]^{-2}$$

$$u_3(x,t)=\frac{1}{2\beta}[-6p^2-\frac{10p\gamma c}{\alpha}+3\gamma]-\frac{(\gamma-6p^2)(p+\frac{\alpha}{5c})}{\beta}\left[p+\sqrt{\frac{\gamma}{6}}[\tanh(\sqrt{\frac{\gamma}{6}}\xi)\pm i\,\mathrm{sech}(\sqrt{\frac{\gamma}{6}}\xi)\right]^{-1}$$
$$-\frac{(\gamma-6p^2)^2}{12\beta}\left[p+\sqrt{\frac{\gamma}{6}}[\tanh(\sqrt{\frac{\gamma}{6}}\xi)\pm i\,\mathrm{sech}(\sqrt{\frac{\gamma}{6}}\xi)\right]^{-2}$$

$$u_4(x,t)=\frac{1}{2\beta}[-6p^2-\frac{10p\gamma c}{\alpha}+3\gamma]-\frac{(\gamma-6p^2)(p+\frac{\alpha}{5c})}{\beta}\left[p+\sqrt{\frac{\gamma}{6}}[\coth(\sqrt{\frac{\gamma}{6}}\xi)\pm\mathrm{csch}(\sqrt{\frac{\gamma}{6}}\xi)\right]^{-1}$$
$$-\frac{(\gamma-6p^2)^2}{12\beta}\left[p+\sqrt{\frac{\gamma}{6}}[\coth(\sqrt{\frac{\gamma}{6}}\xi)\pm\mathrm{csch}(\sqrt{\frac{\gamma}{6}}\xi)\right]^{-2}$$

$$u_5(x,t)=\frac{1}{2\beta}[-6p^2-\frac{10p\gamma c}{\alpha}+3\gamma]-\frac{2(\gamma-6p^2)(p+\frac{\alpha}{5c})}{\beta}\left[2p+\sqrt{\frac{\gamma}{96}}\xi[\tanh(\sqrt{\frac{\gamma}{96}}\xi)\pm\coth(\sqrt{\frac{\gamma}{96}}\xi)\right]^{-1}$$
$$-\frac{(\gamma-6p^2)^2}{3\beta}\left[2p+\sqrt{\frac{\gamma}{6}}\xi[\tanh(\sqrt{\frac{\gamma}{96}}\xi)\pm\coth(\sqrt{\frac{\gamma}{96}}\xi)\right]^{-2}$$

$$u_6(x,t)=\frac{1}{2\beta}[-6p^2-\frac{10p\gamma c}{\alpha}+3\gamma]+\frac{(\gamma-6p^2)(p+\frac{\alpha}{5c})}{\beta}\left[-p+\frac{\sqrt{\frac{\gamma}{6}}[\sqrt{A^2+B^2}-A\cosh(\sqrt{\frac{\gamma}{6}}\xi)]}{A\sinh(\sqrt{\frac{\gamma}{6}}\xi)+B}\right]^{-1}$$
$$-\frac{(\gamma-6p^2)^2}{12\beta}\left[-p+\frac{\sqrt{\frac{\gamma}{6}}[\sqrt{A^2+B^2}-A\cosh(\sqrt{\frac{\gamma}{6}}\xi)]}{A\sinh(\sqrt{\frac{\gamma}{6}}\xi)+B}\right]^{-2}$$

$$u_7(x,t)=\frac{1}{2\beta}[-6p^2-\frac{10p\gamma c}{\alpha}+3\gamma]+\frac{(\gamma-6p^2)(p+\frac{\alpha}{5c})}{\beta}\left[-p-\frac{\sqrt{\frac{\gamma}{6}}[\sqrt{B^2-A^2}-A\cosh(\sqrt{\frac{\gamma}{6}}\xi)]}{A\sinh(\sqrt{\frac{\gamma}{6}}\xi)+B}\right]^{-1}$$
$$-\frac{(\gamma-6p^2)^2}{12\beta}\left[-p-\frac{\sqrt{\frac{\gamma}{6}}[\sqrt{B^2-A^2}-A\cosh(\sqrt{\frac{\gamma}{6}}\xi)]}{A\sinh(\sqrt{\frac{\gamma}{6}}\xi)+B}\right]^{-2}$$

where A and B are two non-zero real constants satisfying $B^2-A^2>0$,

$$u_8(x,t)=\frac{1}{2\beta}[-6p^2-\frac{10p\gamma c}{\alpha}+3\gamma]-\frac{(\gamma-6p^2)(p+\frac{\alpha}{5c})}{4qr\beta}\left[\frac{\cosh(\sqrt{\frac{\gamma}{24}}\xi)}{\sqrt{\frac{\gamma}{6}}\sinh(\sqrt{\frac{\gamma}{24}}\xi)-p\cosh(\sqrt{\frac{\gamma}{24}}\xi)}\right]^{-1}$$
$$-\frac{(\gamma-6p^2)^2}{192\beta q^2r^2}\left[\frac{\cosh(\sqrt{\frac{\gamma}{24}}\xi)}{\sqrt{\frac{\gamma}{6}}\sinh(\sqrt{\frac{\gamma}{24}}\xi)-p\cosh(\sqrt{\frac{\gamma}{24}}\xi)}\right]^{-2}$$

$$u_9(x,t)=\frac{1}{2\beta}[-6p^2-\frac{10p\gamma c}{\alpha}+3\gamma]-\frac{(\gamma-6p^2)(p+\frac{\alpha}{5c})}{4qr\beta}\left[\frac{\sinh(\sqrt{\frac{\gamma}{24}}\xi)}{p\sinh(\sqrt{\frac{\gamma}{24}}\xi)-\sqrt{\frac{\gamma}{6}}\cosh(\sqrt{\frac{\gamma}{24}}\xi)}\right]^{-1}$$
$$-\frac{(\gamma-6p^2)^2}{192\beta q^2r^2}\left[\frac{\sinh(\sqrt{\frac{\gamma}{24}}\xi)}{p\sinh(\sqrt{\frac{\gamma}{24}}\xi)-\sqrt{\frac{\gamma}{6}}\cosh(\sqrt{\frac{\gamma}{24}}\xi)}\right]^{-2}$$

$$u_{10}(x,t)=\frac{1}{2\beta}[-6p^2-\frac{10p\gamma c}{\alpha}+3\gamma]+\frac{(\gamma-6p^2)(p+\frac{\alpha}{5c})}{4qr\beta}\left[\frac{\cosh(\sqrt{\frac{\gamma}{24}}\xi)}{\sqrt{\frac{\gamma}{6}}\sinh(\sqrt{\frac{\gamma}{6}}\xi)-p\cosh(\sqrt{\frac{\gamma}{6}}\xi)\pm i\sqrt{\frac{\gamma}{6}}}\right]^{-1}$$
$$-\frac{(\gamma-6p^2)^2}{192\beta q^2r^2}\left[\frac{\cosh(\sqrt{\frac{\gamma}{24}}\xi)}{\sqrt{\frac{\gamma}{6}}\sinh(\sqrt{\frac{\gamma}{6}}\xi)-p\cosh(\sqrt{\frac{\gamma}{6}}\xi)\pm i\sqrt{\frac{\gamma}{6}}}\right]^{-2}$$

$$u_{11}(x,t)=\frac{1}{2\beta}[-6p^2-\frac{10p\gamma c}{\alpha}+3\gamma]+\frac{(\gamma-6p^2)(p+\frac{\alpha}{5c})}{4qr\beta}\left[\frac{\sinh(\sqrt{\frac{\gamma}{24}}\xi)}{-p\sinh(\sqrt{\frac{\gamma}{6}}\xi)+\sqrt{\frac{\gamma}{6}}\cosh(\sqrt{\frac{\gamma}{6}}\xi)\pm\sqrt{\frac{\gamma}{6}}}\right]^{-1}$$
$$-\frac{(\gamma-6p^2)^2}{192\beta q^2r^2}\left[\frac{\sinh(\sqrt{\frac{\gamma}{24}}\xi)}{-p\sinh(\sqrt{\frac{\gamma}{6}}\xi)+\sqrt{\frac{\gamma}{6}}\cosh(\sqrt{\frac{\gamma}{6}}\xi)\pm\sqrt{\frac{\gamma}{6}}}\right]^{-2}$$

$$u_{12}(x,t)=\frac{1}{2\beta}[-6p^2-\frac{10p\gamma c}{\alpha}+3\gamma]+\frac{(\gamma-6p^2)(p+\frac{\alpha}{5c})}{4qr\beta}\left[\frac{\sinh(\sqrt{\frac{\gamma}{24}}\xi)}{-p\sinh(\sqrt{\frac{\gamma}{24}}\xi)+\sqrt{\frac{\gamma}{6}}\cosh(\sqrt{\frac{\gamma}{24}}\xi)}\right]^{-1}$$
$$-\frac{(\gamma-6p^2)^2}{192\beta q^2r^2}\left[\frac{\sinh(\sqrt{\frac{\gamma}{24}}\xi)}{-p\sinh(\sqrt{\frac{\gamma}{24}}\xi)+\sqrt{\frac{\gamma}{6}}\cosh(\sqrt{\frac{\gamma}{24}}\xi)}\right]^{-2}$$

where $\xi=\frac{1}{L}x-\frac{\alpha}{5}\sqrt{\frac{\gamma}{6}}\frac{t}{\tau}$.

Exact traveling wave solutions of Equation (1) for Case 3

By using the case 3 and according to the values of solutions of type 1 in the proposed method, we obtain the following exact traveling wave solutions for Equation (1):

$$u_1(x,t)=\frac{5\gamma}{4\beta}-\frac{\alpha\sqrt{6\gamma}}{5\beta c}\tanh(\sqrt{\frac{\gamma}{24}}\xi)+\frac{12qr}{\beta}\tanh^2(\sqrt{\frac{\gamma}{24}}\xi)+\frac{\alpha\sqrt{6\gamma}}{20\beta c}\coth(\sqrt{\frac{\gamma}{24}}\xi)-\frac{\gamma}{32\beta}\coth^2(\sqrt{\frac{\gamma}{24}}\xi)$$

$$u_2(x,t)=\frac{5\gamma}{4\beta}-\frac{\alpha\sqrt{6\gamma}}{5\beta c}\coth(\sqrt{\frac{\gamma}{24}}\xi)+\frac{12qr}{\beta}\coth^2(\sqrt{\frac{\gamma}{24}}\xi)+\frac{\alpha\sqrt{6\gamma}}{20\beta c}\tanh(\sqrt{\frac{\gamma}{24}}\xi)-\frac{\gamma}{32\beta}\tanh^2(\sqrt{\frac{\gamma}{24}}\xi)$$

$$u_3(x,t)=\frac{5\gamma}{4\beta}-\frac{\alpha\sqrt{6\gamma}}{5\beta c}\left(\tanh(\sqrt{\frac{\gamma}{6}}\xi)\pm i\,\mathrm{sech}(\sqrt{\frac{\gamma}{6}}\xi)\right)+\frac{12qr}{\beta}\left(\tanh(\sqrt{\frac{\gamma}{6}}\xi)\pm i\,\mathrm{sech}(\sqrt{\frac{\gamma}{6}}\xi)\right)^2$$
$$+\frac{\alpha\sqrt{6\gamma}}{20\beta c}\left(\tanh(\sqrt{\frac{\gamma}{6}}\xi)\pm i\,\mathrm{sech}(\sqrt{\frac{\gamma}{6}}\xi)\right)^{-1}-\frac{\gamma}{32\beta}\left(\tanh(\sqrt{\frac{\gamma}{6}}\xi)\pm i\,\mathrm{sech}(\sqrt{\frac{\gamma}{6}}\xi)\right)^{-2}$$

$$u_4(x,t)=\frac{5\gamma}{4\beta}-\frac{\alpha\sqrt{6\gamma}}{5\beta c}\left(\coth(\sqrt{\frac{\gamma}{6}}\xi)\pm\mathrm{csch}(\sqrt{\frac{\gamma}{6}}\xi)\right)+\frac{12qr}{\beta}\left(\coth(\sqrt{\frac{\gamma}{6}}\xi)\pm\mathrm{csch}(\sqrt{\frac{\gamma}{6}}\xi)\right)^2$$
$$+\frac{\alpha\sqrt{6\gamma}}{20\beta c}\left(\coth(\sqrt{\frac{\gamma}{6}}\xi)\pm\mathrm{csch}(\sqrt{\frac{\gamma}{6}}\xi)\right)^{-1}+\frac{\gamma}{32\beta}\left(\coth(\sqrt{\frac{\gamma}{6}}\xi)\pm\mathrm{csch}(\sqrt{\frac{\gamma}{6}}\xi)\right)^{-2}$$

$$u_5(x,t)=\frac{5\gamma}{4\beta}-\frac{\alpha}{5\beta c}\sqrt{\frac{3\gamma}{2}}\left(\tanh(\sqrt{\frac{\gamma}{96}}\xi)\pm\coth(\sqrt{\frac{\gamma}{96}}\xi)\right)+\frac{3qr}{\beta}\left(\tanh(\sqrt{\frac{\gamma}{96}}\xi)\pm\coth(\sqrt{\frac{\gamma}{96}}\xi)\right)^2$$
$$-\frac{\alpha\sqrt{6\gamma}}{10\beta c}\left(\tanh(\sqrt{\frac{\gamma}{96}}\xi)\pm\coth(\sqrt{\frac{\gamma}{96}}\xi)\right)^{-1}-\frac{\gamma}{8\beta}\left(\tanh(\sqrt{\frac{\gamma}{96}}\xi)\pm\coth(\sqrt{\frac{\gamma}{96}}\xi)\right)^{-2}$$

$$u_6(x,t)=\frac{5\gamma}{4\beta}+\frac{\alpha\sqrt{6\gamma}}{5\beta c}\left(\frac{\sqrt{A^2+B^2}-A\cosh(\sqrt{\frac{\gamma}{6}}\xi)}{A\sinh(2\sqrt{-qr}\xi)+B}\right)+\frac{12qr}{\beta}\left(\frac{\sqrt{A^2+B^2}-A\cosh(\sqrt{\frac{\gamma}{6}}\xi)}{A\sinh(\sqrt{\frac{\gamma}{6}}\xi)+B}\right)^2$$
$$+\frac{\alpha\sqrt{6\gamma}}{20\beta c}\left(\frac{\sqrt{A^2+B^2}-A\cosh(\sqrt{\frac{\gamma}{6}}\xi)}{A\sinh(\sqrt{\frac{\gamma}{6}}\xi)+B}\right)^{-1}-\frac{\gamma}{32\beta}\left(\frac{\sqrt{A^2+B^2}-A\cosh(\sqrt{\frac{\gamma}{6}}\xi)}{A\sinh(\sqrt{\frac{\gamma}{6}}\xi)+B}\right)^{-2}$$

$$u_7(x,t)=\frac{5\gamma}{4\beta}-\frac{\alpha\sqrt{6\gamma}}{5\beta c}\left(\frac{\sqrt{B^2-A^2}+A\cosh(\sqrt{\frac{\gamma}{6}}\xi)}{A\sinh(\sqrt{\frac{\gamma}{6}}\xi)+B}\right)+\frac{12qr}{\beta}\left(\frac{\sqrt{B^2-A^2}+A\cosh(\sqrt{\frac{\gamma}{6}}\xi)}{A\sinh(\sqrt{\frac{\gamma}{6}}\xi)+B}\right)^2$$
$$-\frac{\alpha\sqrt{6\gamma}}{20\beta c}\left(\frac{\sqrt{B^2-A^2}+A\cosh(\sqrt{\frac{\gamma}{6}}\xi)}{A\sinh(\sqrt{\frac{\gamma}{6}}\xi)+B}\right)^{-1}-\frac{\gamma}{32\beta}\left(\frac{\sqrt{B^2-A^2}+A\cosh(\sqrt{\frac{\gamma}{6}}\xi)}{A\sinh(\sqrt{\frac{\gamma}{6}}\xi)+B}\right)^{-2}$$

where *A* and *B* are two non-zero real constants satisfying B^2-A^2>0,

$$u_8(x,t)=\frac{5\gamma}{4\beta}-\frac{\alpha\sqrt{6\gamma}}{5\beta c}\coth(\sqrt{\frac{\gamma}{24}}\xi)+\frac{3q}{\beta r}\coth^2(\sqrt{\frac{\gamma}{24}}\xi)+\frac{\alpha\gamma}{20q\beta c}\sqrt{\frac{\gamma}{24}}\tanh(\sqrt{\frac{\gamma}{24}}\xi)+\frac{\gamma^2 r}{192\beta q}\tanh^2(\sqrt{\frac{\gamma}{24}}\xi)$$

$$u_9(x,t)=\frac{5\gamma}{4\beta}-\frac{\alpha\sqrt{6\gamma}}{5\beta c}\tanh(\sqrt{\frac{\gamma}{24}}\xi)+\frac{3q}{\beta r}\tanh^2(\sqrt{\frac{\gamma}{24}}\xi)+\frac{\alpha\gamma}{20q\beta c}\sqrt{\frac{\gamma}{24}}\coth(\sqrt{\frac{\gamma}{24}}\xi)+\frac{\gamma^2 r}{192\beta q}\coth^2(\sqrt{\frac{\gamma}{24}}\xi)$$

$$u_{10}(x,t)=\frac{5\gamma}{4\beta}-\frac{\alpha\sqrt{6\gamma}}{5\beta c}\left(\frac{\cosh(\sqrt{\frac{\gamma}{24}}\xi)}{\sinh(\sqrt{\frac{\gamma}{6}}\xi)\pm i}\right)+\frac{12qr}{\beta}\left(\frac{\cosh(\sqrt{\frac{\gamma}{24}}\xi)}{\sinh(\sqrt{\frac{\gamma}{6}}\xi)\pm i}\right)^2-\frac{\alpha\sqrt{6\gamma}}{20\beta c}\left(\frac{\coth(\sqrt{\frac{\gamma}{24}}\xi)}{\sinh(\sqrt{\frac{\gamma}{6}}\xi)\pm i}\right)^{-1}$$
$$-\frac{\gamma}{32\beta}\left(\frac{\cosh(\sqrt{\frac{\gamma}{24}}\xi)}{\sinh(\sqrt{\frac{\gamma}{6}}\xi)\pm i}\right)^{-2}$$

$$u_{11}(x,t)=\frac{5\gamma}{4\beta}-\frac{\alpha\sqrt{6\gamma}}{5\beta c}\left(\frac{\sinh(\sqrt{\frac{\gamma}{24}}\xi)}{coh(\sqrt{\frac{\gamma}{6}}\xi)\pm i}\right)+\frac{12qr}{\beta}\left(\frac{\sinh(\sqrt{\frac{\gamma}{24}}\xi)}{\cosh(\sqrt{\frac{\gamma}{6}}\xi)\pm i}\right)^2-\frac{\alpha\sqrt{6\gamma}}{20\beta c}\left(\frac{\sinh(\sqrt{\frac{\gamma}{24}}\xi)}{\cosh(\sqrt{\frac{\gamma}{6}}\xi)\pm i}\right)^{-1}$$
$$-\frac{\gamma}{32\beta}\left(\frac{\sinh(\sqrt{\frac{\gamma}{24}}\xi)}{\cosh(\sqrt{\frac{\gamma}{6}}\xi)\pm i}\right)^{-2}$$

$$u_{12}(x,t)=\frac{5\gamma}{4\beta}-\frac{\alpha\sqrt{6\gamma}}{5\beta c}\left(\frac{\sinh(\sqrt{\frac{\gamma}{24}}\xi)}{\cosh(\sqrt{\frac{\gamma}{24}}\xi)-1}\right)+\frac{12qr}{\beta}\left(\frac{\sinh(\sqrt{\frac{\gamma}{24}}\xi)}{\cosh(\sqrt{\frac{\gamma}{24}}\xi)-1}\right)^2-\frac{\alpha\sqrt{6\gamma}}{20\beta c}\left(\frac{\sinh(\sqrt{\frac{\gamma}{24}}\xi)}{\cosh(\sqrt{\frac{\gamma}{24}}\xi)-1}\right)^{-1}$$
$$-\frac{\gamma}{31\beta}\left(\frac{\sinh(\sqrt{\frac{\gamma}{24}}\xi)}{\cosh(\sqrt{\frac{\gamma}{24}}\xi)-1}\right)^{-2}$$

where, $\xi=\frac{1}{L}x-\frac{\alpha}{5}\sqrt{\frac{\gamma}{6}}\frac{t}{\tau}$.

Remark 2

We have noted in the two cases 1, 2 that $\Delta=\frac{\gamma}{6}>0$ while in case 3 we have $\Delta=\frac{\gamma}{24}>0$. This yields that all the solutions of type 2 in the proposed method cannot be considered in this paper. Therefore, Equation (1) has no trigonometric function solutions.

PHYSICAL EXPLANATIONS FOR SOME OBTAINED RESULTS

Here, we will present some graphs for the obtained solutions of Equation (1) by selecting some special values of the parameters in the exact solutions using the mathematical software Maple, which can be shown below in Figures 1 to 6. From these explicit solutions, we see that $u_1(x,t)$ in both cases 1, 2 are kink shaped soliton solutions while $u_2(x,t)$ in these two cases are singular kink shaped soliton solutions. The two solutions $u_1(x,t)$ and $u_2(x,t)$ in case 3 are kink-singular shaped soliton solutions. The graphical representations of these solutions are shown in the following figures:

CONCLUSIONS AND COMMENTS

Here we give some comments on the solutions (22) to (27) of the second model of microtubules (16) in Sekulic et al. (2011a). We have found that some of these solutions are incorrect. Thus, we will correct these solutions and then compare between some of our results in the present article and the corrected solutions as follows:

1) There is a minor error in Equation (18) of Sekulic et al. (2011a). The correction is to replace β by $\frac{\beta}{2}$ in Equation (18).

2) The results of Case I in Sekulic et al. (2011a) do not satisfy the algebraic Equation (21). After a careful revision, we have shown that the correction of this case should be in the form:

$$b=-\frac{\gamma}{24},\ a_0=\frac{3\gamma}{4\beta},\ \ a_1=\frac{6\alpha}{5\beta c},a_2=\frac{-6}{\beta},c=\frac{\alpha}{5}\sqrt{\frac{6}{\gamma}},\ b_1=b_2=0 \quad (10)$$

It is easy to see that the corrected values (10) satisfy the algebraic Equation (21) of Sekulic et al. (2011a).

Hence with replacing β by $\frac{\beta}{2}$ in (10), the result (22) of Sekulic et al. (2011a) should be rewritten in the corrected form:

$$u(x,t)=\frac{3\gamma}{2\beta}-\frac{12\alpha}{5\beta c}\sqrt{\frac{\gamma}{24}}\tanh\left(\sqrt{\frac{\gamma}{24}}\left(\frac{1}{L}x-\frac{\alpha}{5}\sqrt{\frac{\gamma}{6}}\frac{t}{\tau}\right)\right)-\frac{\gamma}{2\beta}\tanh^2\left(\sqrt{\frac{\gamma}{24}}\left(\frac{1}{L}x-\frac{\alpha}{5}\sqrt{\frac{\gamma}{6}}\frac{t}{\tau}\right)\right) \quad (11)$$

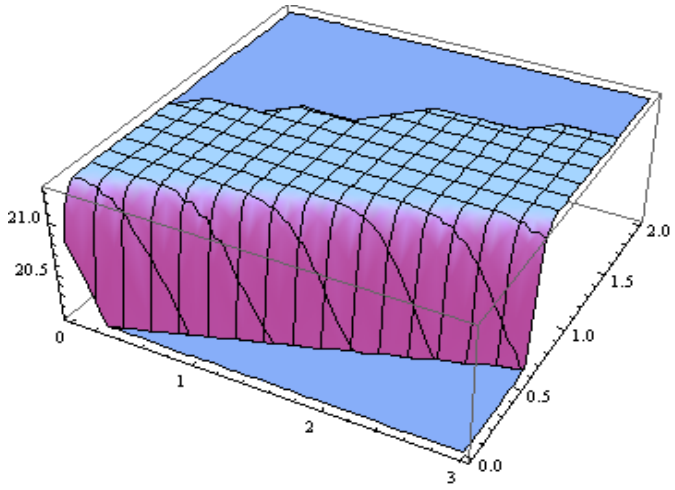

Figure 1. The plot of $u_1(x,t)$ of case 1, where $p=1, q=1, \alpha=104.76, \beta=142.86, \gamma=142.86.$

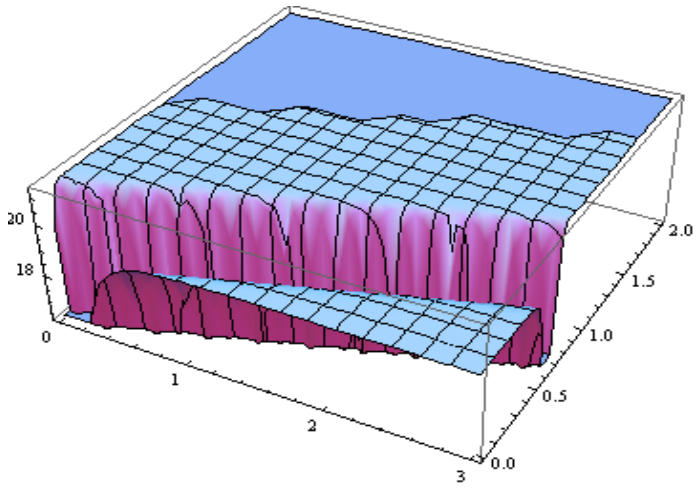

Figure 2. The plot of $u_2(x,t)$ of case 1, where $p=1, q=1, \alpha=104.76, \beta=142.86, \gamma=142.86.$

On comparing the corrected result (11) with our result $u_1(x,t)$ of "Exact traveling wave solutions of Equation (1) for case 1", we conclude that they are equivalent if $p=0$ and $q=1$.

3) The results of Case II in Sekulic et al. (2011a) do not satisfy the algebraic Equation (21) too. After a careful revision, we have shown that the correction of this case should be in the form:

$$b=\frac{\gamma}{24}, a_0=\frac{\gamma}{4\beta}, \ a_1=\frac{6\alpha}{5\beta c}, a_2=\frac{-6}{\beta}, c=\frac{\alpha}{5}\sqrt{\frac{-6}{\gamma}}, \ b_1=b_2=0 \quad (12)$$

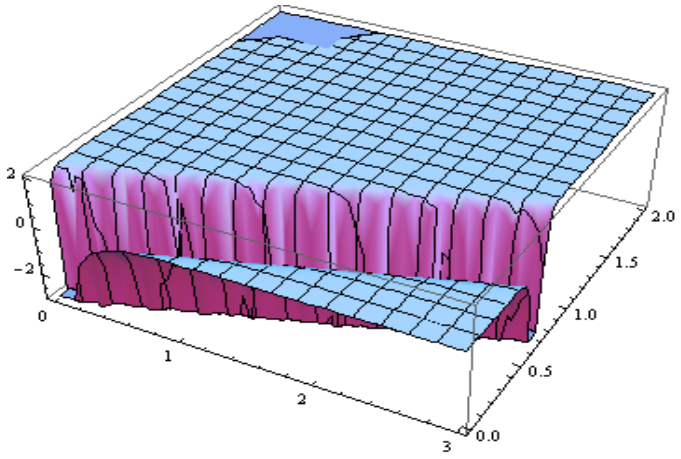

Figure 3. The plot of $u_1(x,t)$ of case 2, where $p=1, q=1, \alpha=104.76, \beta=142.86, \gamma=142.86.$

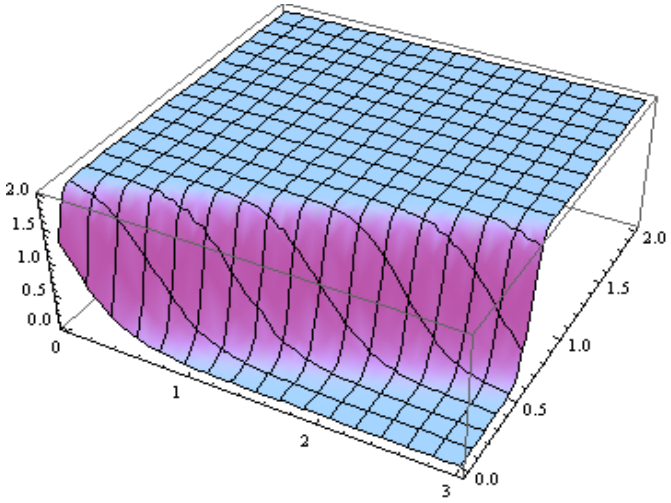

Figure 4. The plot of $u_2(x,t)$ of case 2, where $p=1, q=1, \alpha=104.76, \beta=142.86, \gamma=142.86.$

It is easy to see that the values of (12) satisfy the algebraic Equation (21) of Sekulic et al. (2011a). From the values of (12) we deduce that $\gamma=\frac{-6\alpha^2}{25c^2}$ which is negative. This contradicts that $\gamma=\frac{R_1}{R_2}>0$. Therefore, Case 2 in Sekulic et al. (2011a) should be rejected.

4) The results of Case III in Sekulic et al. (2011a) do not satisfy the algebraic Equation (21) too. After a careful revision, we have shown that the correction of this case should be in the form:

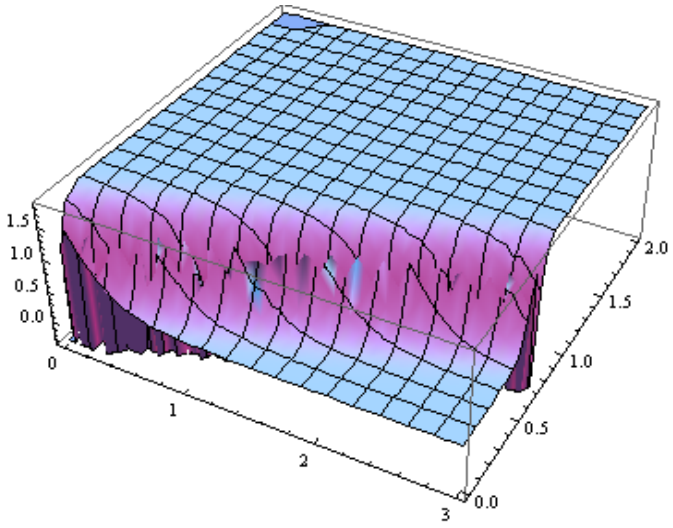

Figure 5. The plot of $u_1(x,t)$ of case 3, where $p=0, q=1, \alpha=104.76, \beta=142.86, \gamma=142.86.$

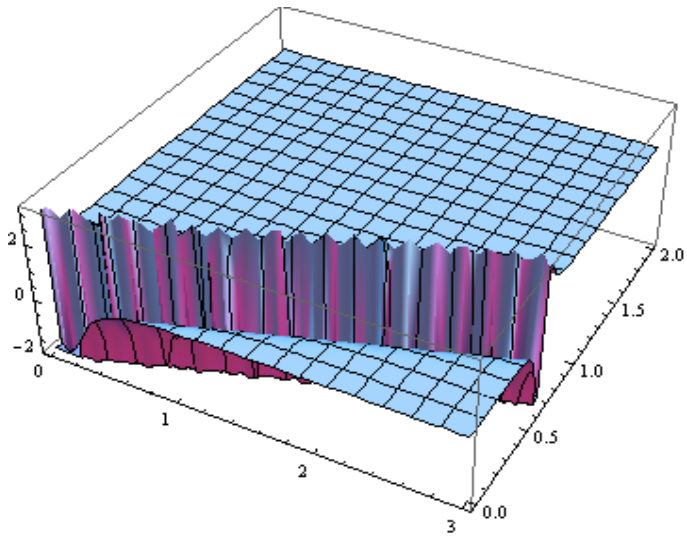

Figure 6. The plot of $u_2(x,t)$ of case 3, where $p=0, q=1, \alpha=104.76, \beta=142.86, \gamma=142.86.$

$$b=-\frac{\gamma}{24},\ a_0=\frac{3\gamma}{4\beta},\ b_1=\frac{\alpha\gamma}{20\beta c},b_2=\frac{-\gamma^2}{96\beta},c=\frac{\alpha}{5}\sqrt{\frac{6}{\gamma}},\ a_1=a_2=0 \quad (13)$$

It is easy to see that the corrected values of (13) satisfy the algebraic Equation (21) of Sekulic et al. (2011a).

Hence with replacing β by $\frac{\beta}{2}$ in (13), the result (24) of (Sekulic et al, 2011a) should be rewritten in the corrected form:

$$u(x,t)=\frac{3\gamma}{2\beta}-\frac{\alpha\gamma}{10\beta c}\sqrt{\frac{24}{\gamma}}\coth\left(\sqrt{\frac{\gamma}{24}}\left(\frac{1}{L}x-\frac{\alpha}{5}\sqrt{\frac{6}{\gamma}}\frac{t}{\tau}\right)\right)-\frac{\gamma}{2\beta}\coth^2\left(\sqrt{\frac{\gamma}{24}}\left(\frac{1}{L}x-\frac{\alpha}{5}\sqrt{\frac{6}{\gamma}}\frac{t}{\tau}\right)\right) \quad (14)$$

On comparing the corrected result (14) with our result $u_1(x,t)$ of 'Exact traveling wave solutions of Equation (1) for case 2', we conclude that they are equivalent if $p=0$ and $q=1$.

5) The results of Case IV of Sekulic et al. (2011a) still do not satisfy the algebraic Equation (21). After a careful revision, we have shown that the correction of this case should be in the form:

$$b=\frac{\gamma}{24},\ c=\frac{\alpha}{5}\sqrt{\frac{-6}{\gamma}},\ a_1=a_2=0, b_2=\frac{-\gamma^2}{96\beta},\ b_1=-\frac{\alpha\gamma}{20\beta c},a_0=\frac{\gamma}{4\beta} \quad (15)$$

It is easy to see that the corrected values of (15) satisfy the algebraic Equation (21) of Sekulic et al. (2011a). From the values of Equation (15) we deduce that $\gamma=\frac{-6\alpha^2}{25c^2}$ which is negative. This contradicts that $\gamma=\frac{R_1}{R_2}>0$. Therefore, the case IV in Sekulic et al. (2011a) should be rejected.

6) The results of Case V in Sekulic et al. (2011a) also do not satisfy the algebraic Equation (21). After a careful revision, we have shown that the correction of this case should be

$$b=-\frac{\gamma}{96},a_0=\frac{5\gamma}{8\beta},\ b_1=\frac{\alpha\gamma}{80\beta c},b_2=\frac{-\gamma^2}{1536\beta},c=\frac{\alpha}{5}\sqrt{\frac{6}{\gamma}},\ a_1=\frac{6\alpha}{5\beta c},\ a_2=-\frac{6}{\beta} \quad 16)$$

It is easy to see that the corrected values of (16) satisfy the algebraic Equation (21) of Sekulic et al. (2011a).

Hence with replacing β by $\frac{\beta}{2}$ in Equation (13), the result (26) of Sekulic et al. (2011a) should be rewritten in the corrected form:

$$u(x,t)=\frac{5\gamma}{4\beta}-\frac{12\alpha}{5\beta c}\sqrt{\frac{\gamma}{96}}\tanh\left(\sqrt{\frac{\gamma}{96}}\left(\frac{1}{L}x-\frac{\alpha}{5}\sqrt{\frac{6}{\gamma}}\frac{t}{\tau}\right)\right)-\frac{\gamma}{8\beta}\tanh^2\left(\sqrt{\frac{\gamma}{96}}\left(\frac{1}{L}x-\frac{\alpha}{5}\sqrt{\frac{6}{\gamma}}\frac{t}{\tau}\right)\right)$$
$$+\frac{\alpha\gamma}{40\beta c}\sqrt{\frac{96}{\gamma}}\coth\left(\sqrt{\frac{\gamma}{96}}\left(\frac{1}{L}x-\frac{\alpha}{5}\sqrt{\frac{6}{\gamma}}\frac{t}{\tau}\right)\right)-\frac{\gamma}{8\beta}\coth^2\left(\sqrt{\frac{\gamma}{96}}\left(\frac{1}{L}x-\frac{\alpha}{5}\sqrt{\frac{6}{\gamma}}\frac{t}{\tau}\right)\right) \quad (17)$$

On comparing the corrected result (17) with our result $u_1(x,t)$ of 'Exact traveling wave solutions of Equation (1) for Case 3', we conclude that they are equivalent if $p=0$ and $q=1$.

7) The results of case VI in Sekulic et al. (2011a) do not

also satisfy Equation (21). After a careful revision, we have shown that the correction of this case should be in the form:

$$b=\frac{\gamma}{96},\ c=\frac{\alpha}{5}\sqrt{\frac{-6}{\gamma}},\ b_2=-\frac{\gamma^2}{1536\beta},\ b_1=-\frac{\alpha\gamma}{80\beta c},\ a_2=\frac{-6}{\beta},\ a_1=\frac{6\alpha}{5\beta c},\ a_0=\frac{3\gamma}{8\beta} \quad (18)$$

It is easy to see that the corrected values of (18) satisfy the algebraic Equation (21) of Sekulic et al. (2011a). From the values of Equation (18) we deduce that $\gamma=\frac{-6\alpha^2}{25c^2}$ which is negative. This contradicts that $\gamma=\frac{R_1}{R_2}>0$.

Therefore, the case VI in Sekulic et al. (2011) should be rejected.

From these discussions we deduce that our results in the present article are new and recover the well-known results obtained in Sekulic et al. (2011a) after its corrections obtained above.

Conflict of Interests

The author(s) have not declared any conflict of interests.

ACKNOWLEDGEMENTS

The authors wish to thank the referees for their comments on this paper.

REFERENCES

Abdou MA (2007).The extended tanh method and its applications for solving nonlinear physical models. Appl. Math. Comput.190(1):988-996. http://dx.doi.org/10.1016/j.amc.2007.01.070

Ablowitz MJ, Clarkson PA (1991). Solitons, nonlinear evolution equations and inverse scattering transform. Cambridge University Press, New York. http://dx.doi.org/10.1017/CBO9780511623998; PMid:9905818

Aslan I (2010). A note on the (G'/G) -expansion method again. Appl. Math. Comput. 217(2):937-938. http://dx.doi.org/10.1016/j.amc.2010.05.097

Aslan I (2011). Exact and explicit solutions to the discrete nonlinear Schrödinger equation with a saturable nonlinearity. Phys. Lett. A. 375(47):4214-4217. http://dx.doi.org/10.1016/j.physleta.2011.10.009

Aslan I (2012a). Some exact solutions for Toda type lattice differential equations using the improved (G'/G)– expansion method. Math. Methods Appl. Sci. 35(4):474-481. http://dx.doi.org/10.1002/mma.1579

Aslan I (2012b). The discrete (G'/G) -expansion method applied to the differential-difference Burgers equation and the relativistic Toda lattice system. Numer. Methods Par. Diff. Eqs. 28(1):127-137. http://dx.doi.org/10.1002/num.20611

Aslan I (2011). Comment on application of exp-function method (3+1)dimensional nonlinear evolution equation.[Comput Math. Appl. 56(2008):1451-1456], Comput. Math. Appl. 61(6):1700-1703. http://dx.doi.org/10.1016/j.camwa.2011.01.043

Ayhan B, Bekir A (2012). The (G'/G) -expansion method for the nonlinear lattice equations. Commun. Nonlin. Sci. Numer. Simul. 17(9):3490-3498. http://dx.doi.org/10.1016/j.cnsns.2012.01.009

Bekir A (2008). Application of the (G'/G) -expansion method for nonlinear evolution equations. Phys. Lett. A. 372(19):3400-3406. http://dx.doi.org/10.1016/j.physleta.2008.01.057

Bekir A (2009). The exp-function for Ostrovsky equation. Int. J. Nonlin. Sci. Numer. Simul. 10:735-739. http://dx.doi.org/10.1515/IJNSNS.2009.10.6.735

Bekir A (2010). Application of exp-function method for nonlinear differential-difference equations. Appl. Math. Comput. 215(11):4049-4053. http://dx.doi.org/10.1016/j.amc.2009.12.003

Chen Y, Wang Q (2005). Extended Jacobi elliptic function rational expansion method and abundant families of Jacobi elliptic function solutions to (1+1)-dimensional dispersive long wave equation. Chaos Solit. Fract. 24(3):745-757. http://dx.doi.org/10.1016/j.chaos.2004.09.014

Fan E (2000). Extended tanh-function method and its applications to nonlinear equations. Phys. Lett. A. 277:212-218. http://dx.doi.org/10.1016/S0375-9601(00)00725-8

Freedman H, Rezania V, Priel A, Carpenter E, Noskov SY, Tuszynski JA (2010). Model of Ionic Currents through Microtubule Nanopores and the Lumen. Phys. Rev. E. 81(5):051912. http://dx.doi.org/10.1103/PhysRevE.81.051912; PMid:20866266

He JH, Wu XH.(2006). Exp-function method for nonlinear wave equations. Chaos Solit. Fract. 30(3):700-708. http://dx.doi.org/10.1016/j.chaos.2006.03.020

Hirota R (1971). Exact solutions of the KdV equation for multiple collisions of solutions. Phys. Rev. Lett. 27:1192-1194. http://dx.doi.org/10.1103/PhysRevLett.27.1192

Ilic DI, Sataric MV, Ralevic N (2009), Atomic and molecular physics: Microtubule as a transmission line for ionic currents, Chin. Phys. Lett. 26:073101-073103. http://dx.doi.org/10.1088/0256-307X/26/7/073101

Kudryashov NA (1988). Exact solutions of a generalized evolution of wave dynamics. J. Appl. Math. Mech. 52:361-365. http://dx.doi.org/10.1016/0021-8928(88)90090-1

Kudryashov NA (1990). Exact solutions of a generalized Kuramoto-Sivashinsky equation. Phys. Lett. A. 147(5-6):287-291. http://dx.doi.org/10.1016/0375-9601(90)90449-X

Kudryashov NA (1991).On types of nonlinear non integrable equations with exact solutions. Phys. Lett. A. 155(4-5):269-275. http://dx.doi.org/10.1016/0375-9601(91)90481-M

Liu S, Z. Fu Z, Zhao Q (2001). Jacobi elliptic function expansion method and periodic wave solutions of nonlinear wave equations. Phys. Lett. A. 289(1-2):69-74. http://dx.doi.org/10.1016/S0375-9601(01)00580-1

Lu D (2005). Jacobi elliptic function solutions for two variant Boussinesq equations, Chaos Solit. Fract. 24(5): 1373. http://dx.doi.org/10.1016/j.chaos.2004.09.085

Miura MR (1978). Backlund transformation, Springer, Berlin, Germany.

Rogers C, Shadwick WF (1982). Baclund Transformation and Their Applications. Academic Press, New York. p. 161.

Sataric MV, Ilic DI, Ralevic NM and Tuszynski JA (2009). A nonlinear model of ionic wave propagation along microtubules. Eur. Biophys. J. Biophys. Lett. 38:637-647. http://dx.doi.org/10.1007/s00249-009-0421-5; PMid:19259657

Sataric MV, Sekulic DL, Zivanov MB (2010). Solitonic ionic currents along microtubules. J. Comput. Theor. Nanosci. 7:2281-2290. http://dx.doi.org/10.1166/jctn.2010.1609

Sekulic DL, Sataric MV, Zivanov MB (2011a). Symbolic computation of some new nonlinear partial differential equations of nanobiosciences using modified extended tanh-function method. Appl. Math. Comput. 218:3499-3506. http://dx.doi.org/10.1016/j.amc.2011.08.096

Sekulic DL, Sataric BM, Tuszynski JA, Sataric MV (2011b). Nonlinear ionic pulses along microtubules. Eur. Phys. J. E. Soft Matter 34(5):1-11. http://dx.doi.org/10.1140/epje/i2011-11049-0; PMid:21604102

Sekulić DL, Satarić MV (2012). Microtubule as nanobioelectronic nonlinear circuit, Serbian J. Elect. Eng. 9:107-119. http://dx.doi.org/10.2298/SJEE1201107S

Sekulic DL, Sataric MV,Zivanov MB, Bajic JS (2012). Soliton-like pulses along electrical nonlinear transmission line, Electr. Elect. Eng.121:53-58.

Wang M, Li X, Zhang J (2008). The (G'/G)-expansion method and traveling wave solutions of nonlinear evolution equations in mathematical physics. Phys. Lett. A. 372:417-423. http://dx.doi.org/10.1016/j.physleta.2007.07.051

Weiss J, Tabor T, Carnevale G (1983). The Painlevé property for partial

differential equations. J. Math. Phys. 24(3):552-526. http://dx.doi.org/10.1063/1.525721
Yusufoglu E (2008).New solitary for the MBBM equations using exp-function method. Phys. Lett. A. 372:442-446. http://dx.doi.org/10.1016/j.physleta.2007.07.062
Yusufoglu E, Bekir A (2008). Exact solutions of coupled nonlinear Klein-Gordon equations. Math. Comput. Model. 48:1694-1700. http://dx.doi.org/10.1016/j.mcm.2008.02.007
Zayed EME (2009). The (G'/G) -expansion method and its applications to some nonlinear evolution equations in the mathematical physics. J. Appl. Math. Comput. 30:89-103. http://dx.doi.org/10.1007/s12190-008-0159-8
Zayed EME (2010). Traveling wave solutions for higher dimensional nonlinear evolution equations using the (G'/G)-expansion method. J. Appl. Math. Inf. 28:383-395.
Zayed EME, Arnous AH (2013). Many exact solutions for nonlinear dynamics of DNA model using the generalized Riccati equation mapping method. Sci. Res. Essays 8:340-346.
Zayed EME, Amer YA, Shohib RMA (2013). The improved Riccati equation mapping method for constructing many families of exact solutions for nonlinear partial differential equation on nanobioscience. Int. J. Phys. Sci. 8(22):1246-1255.
Zhang S (2008). Application of exp-function method to high–dimensional nonlinear evolution equation. Chaos Solit. Fract.38:270-276. http://dx.doi.org/10.1016/j.chaos.2006.11.014
Zhang S, Xia T (2008). A further improved tanh function method exactly solving the (2+1)- dimensional dispersive long wave equations. Appl. Math. E-Notes 8:58-66.
Zhang S, Tong JL, Wang W (2008). A generalized (G'/G)-Expansion method for the mKdV equation with variable coefficients. Phys. Lett. A. 372:2254-2257. http://dx.doi.org/10.1016/j.physleta.2007.11.026
Zhu SD (2008). The generalized Riccati equation mapping method in nonlinear evolution equation: application to (2+1)-dimensional Boiti-lion-Pempinelle equation. Chaos Solit. Fract. 37:1335-1342. http://dx.doi.org/10.1016/j.chaos.2006.10.015

academicJournals

Vol. 9(8), pp. 249-256, 30 April, 2014
DOI: 10.5897/SRE2014.5817
Article Number: C543F4644199
ISSN 1992-2248 © 2014

http://www.academicjournals.org/SRE

Scientific Research and Essays

Full Length Research Paper

Genetic diversity of *Quercus liaotungensis* Koidz populations at different altitudes

J. Wang, Q. Y. Wei, S. J. Lu, Y. F. Chen and Y. L. Wang*

College of Life Science, Shanxi Normal University, 041000 Linfen, China.

Received 23 January, 2014; Accepted 27 March, 2014

To estimate genetic diversity and genetic structures of *Q. liaotungensis* at different altitudes in Xingtangsi, eight natural populations were surveyed by sequence-related amplified polymorphism (SRAP) markers. A total of 179 bands were amplified by 12 pairs of SRAP primer combinations. The average number of amplification band for each pair primers was 14.9. The percentage polymorphic band (*PPB*) of *Q. liaotungensis* was 100%, Nei's gene diversity (*H*) and Shannon information index (*I*) was 0.3482 and 0.5264 respectively, which indicated the high genetic diversity occurred in *Q. liaotungensis* populations. The highest genetic diversity harbored in population 6, while the lowest in population 4. The genetic diversity of all eight studied populations showed a low-high-low variation pattern along elevation gradients. Analysis of molecular variance (AMOVA) explored that the genetic variation mainly existed within populations (80%) and only 20% of genetic variation between populations of *Q. liaotungensis* (*p*<0.001). STRUCTURE and Principal coordinate analysis (PCoA) further confirmed the AMOVA analysis. Based on the genetic distance between populations, eight populations were mainly clustered into two groups. *Q. liaotungensis'* intrinsic biological characteristics, effective gene flow and microenvironmental heteroplasmy resulted in the genetic distribution of *Q. liaotungensis* populations in Xingtangsi.

Key words: Genetic diversity, gene flow, *Q. liaotungensis*, sequence-related amplified polymorphism (SRAP), Xingtangsi.

INTRODUCTION

Genetic diversity is the product of long-term evolution of a species (Xiao, 2003). It plays an important role in biological diversity, and lays a foundation for the ecological system's diversity and species diversity. The high or low genetic diversity of a species reflects its ability to adapt to the environment changes, and the level of the diversity directly affects the survival and potential evolution of species (Ohsawa and Ide, 2008; Kurt et al., 2011). Genetic diversity can significantly change with the variation of altitudes that regulate ecological conditions in a particular habitat of the plant (Erich and Johann, 2002; Semang et al., 2003; Feng et al., 2004; Ohsawa et al., 2008; Kurt et al., 2011). Consequently, a change pattern of genetic diversity in plant populations along an altitude

*Corresponding author. E-mail: ylwangbj@hotmail.com. Tel: +86 03572051630.

for theoretical interests, utilization and conservation altitude can cause a drastic change in environmental gradient becomes an increasingly attractive subject both Williams, 1979; Baur and Raboud, 1988; Agar et practices because sometimes a relatively small change in al.,2012).Now, some studies have shown that the level of conditions, such as temperature and moisture (Heath and genetic diversity of plant populations decreases or increases along altitudinal gradients (Premoli, 2003).However, there are also researches indicating opposite results, the genetic differentiation within populations fluctuate to a large extent (Li et al., 1998) or do not correlate (Saenz-Romero and Tapia-Olivares, 2003) with an increase in altitude.

Sequence-related amplified polymorphism (SRAP) is a novel, simple and reliable PCR-based marker system (Abedian et al., 2012; Amar et al., 2011; Liu et al., 2008) that amplifies open reading frames (ORFs) (Li and Quiros, 2001) using specific primer pairs. The forward primers preferentially amplify exonic regions, while the reverse primers preferentially amplify intronic regions and regions with promoters. Compared with other molecular markers, SRAP is simple, reproducible, has a reasonable throughput rate, and can be used for different materials, according to its unique primer design (Dong et al., 2010; Cai et al., 2011). In recent years, SRAP markers have been used in many areas, such as plant genetic diversity analysis (Zuo et al., 2009; Zhang et al., 2011; Qu et al., 2008; Fan et al., 2008), identification of varieties (Gai et al., 2011; Li et al., 2006; Zheng et al., 2009), genetic mapping and gene localization (Wang et al., 2007a).

Q. liaotungensis, being a deciduous broad-leaved tree, belongs to *Quercus* of Fagaceae*,* and widely distributes in the northeast and north of China and Inner Mongolia provinces (regions) (Jia et al., 2009). It is wind-pollinated plant, has widely ecological amplitude, can grow on drought, infertility, warm and humid surroundings. Its reproduction is strong, contains more seeding and young seedling understory. The nuts of *Q. liaotungensis* are eaten by some animals because of rich nutrition, high content of nitrogen-free extract, and little crude fiber (Li, 2005). By SSR markers, the genetic diversity of natural *Q. liaotungensis* populations was at a higher level in Shanxi Province, and the majority of genetic variation occurred within populations (Qin et al., 2012). *Q. liaotungensis* populations at Dongling Mountain region also have very high genetic variability, the diversity in the central population was higher than that of the marginal one (Yun et al., 1998). Within its habitats in Xingtangsi, *Q. liaotungensis* plays a very important role in preventing soil erosion and water loss, in regulating microclimate, and also in maintaining ecological stability in general. However, the pattern of genetic variation present in the natural populations of *Q. liaotungensis* along altitudinal gradients is little known. In this study, using SRAP markers to analyze the genetic diversity of *Q. liaotungensis* populations at different altitudes, explore the change pattern of genetic diversity along elevation gradients, and further reveal the factors affected the genetic diversity and structure of *Q. liaotungensis* in Xingtangsi.

MATERIALS AND METHODS

Plant sampling

A total of eight wild populations of *Q. liaotungensis* were sampled along an altitude gradient – 1300, 1400, 1500, 1600, 1700, 1800, 1900, and 2000 m above sea level in Xingtangsi of Huozhou, Shanxi province. Those studied populations marked as population 1 (1300 m), 2 (1400 m), 3 (1500 m), 4 (1600), 5 m (1700 m), 6 (1800 m), 7 (1900 m), 8 (2000 m) respectively. Within each population, 10 to 20 individuals were randomly collected. To avoid collecting the same clone, each sampled individual from the same population was collected from different locations about 30 to 50 m apart. Fresh leaves were collected and immediately stored in liquid nitrogen for genomic DNA extraction.

DNA extraction and PCR amplification

Genomic DNA was extracted using the modified 2×CTAB method (Li et al., 2009). The quality and concentration of the extracted DNA was determined using a UV visible spectrophotometer (Biomate, Thermo Spectronic, Cambridge, UK) and by electrophoresis in 0.8% agarose gels. The DNA samples were diluted to a concentration of 30 ng·μL^{-1} for PCR amplification. DNA samples were stored at -20°C prior to SRAP analysis.

SRAP primers were synthesized by Xi'an Kehao Bioengineering Limited Liability Company. An individual was randomly selected from each population of *Q. liaotungensis* to screen the suitable primer combinations from 88 primer combinations of SRAP. Of these 88 SRAP primer pairs, 12 primer combinations (Table 1) with clear amplification bands and good repeatability were selected to amplify all individuals of eight populations.

The reaction system PCR amplification was optimized in 10 μl, the annealing temperature and PCR amplification cycles of different pair primers were optimized. Within 10 μl reaction system contained: 0.4 μl primers (0.2 μl Me + 0.2 μl Em), 1 μl genomic DNA, 5 μl Mix, and 3.6 μl ddH_2O.

All PCR reactions were performed in a PTC-100 PCR programmable Thermal Controller in the following steps: Pre-denaturation at 94°C for 5 min, denaturation at 94°C for 1 min, annealing at 35°C for 1 min, extension at 72°C for 90 s, 10 cycles of denaturation at 94°C for 1 min, annealing at 60°C for 1 min, and extension at 72°C for 1 min, 35 cycles of denaturation at 94°C for 1 min, and finally extension at 72°C for 10 min.

The amplification product was detected by 12%(W/V) denatured polyacrylamide gel electrophoresis running at 200 V constant voltage for 200 min and then silver stained according to previously reported procedures (Liu et al., 2008).

Data analysis

As the SRAP marker is dominant, we assumed that each band represented the phenotype at a single biallelic locus. All clearly detectable amplified fragments were scored as either present (1) or absent (0), and a matrix of SRAP data was assembled.

The parameters of genetic diversity: observed number of alleles per locus (*N*a), effective number of alleles for per locus (*N*e), the percentage of polymorphic bands (*PPB*), Shannon information index (*I*), and Nei's gene diversity(*H*) were estimated by using POPGENE (version 1.31) (Yeh et al., 1997) software. The coefficient of gene differentiation (*G*st) and the level of gene flow (*N*m) were also

Table 1. SRAP primers sequences in this study.

Forward	Sequence(5'-3')	Reverse	Sequence(3'-5')
Me1	TGAGTCCAAACCGGATA	Em2	GACTGCGTACGAATTTGC
Me3	TGAGTCCAAACCGGAAT	Em6	GACTGCGTACGAATTGCA
Me5	TGAGTCCAAACCGGAAG	Em8	GACTGCGTACGAATTCTG
Me6	TGAGTCCAAACCGGTAA	Em9	GACTGCGTACGAATTCGA
Me7	TGAGTCCAAACCGGTCC	Em10	GACTGCGTACGAATTCAG
		Em11	GACTGCGTACGAATTCCA

Table 2. Genetic diversity of *Q. liaotungensis* populations at different altitudes.

Population	*Na*	*Ne*	*H*	*I*	*PPB*（%）	H_T	*Hs*	G_{ST}	*Nm*
1	1.9162	1.4798	0.2896	0.4428	91.62				
2	1.8771	1.4536	0.2802	0.4297	87.71				
3	1.8324	1.5049	0.2917	0.4353	83.24				
4	1.7542	1.4579	0.2632	0.3927	75.42				
5	1.8045	1.4705	0.2736	0.4103	80.45				
6	1.9050	1.5748	0.3312	0.4917	90.50				
7	1.8883	1.4454	0.2735	0.4217	88.83				
8	1.8939	1.4350	0.2689	0.4159	89.39				
Average	1.8590	1.4778	0.2840	0.4300	85.90				
Species level	2.0000	1.5738	0.3482	0.5264	100.00	0.3482	0.2840	0.1844	2.2108

Na=observed number of alleles; *Ne*=effective number of alleles; *H*=Nei's gene diversity; *I*=Shannon information index; *PPB*=The percentage of polymorphic band; *N*m=estimate of gene flow from *G*st; *H*s=gene diversity within populations; H_T=total gene diversity; *G*st=coefficient of gene differentiation.

measured by using POPGENE. Based on the genetic distance among populations, the dendrogram of populations were made using MEAG (version 5.0) software.

The analysis of molecular variance (AMOVA) was employed to estimate within- and among-population diversity using GenAlEx version 6.0 (Peakall et al., 2006). To further examine the genetic relationships among the populations, the principal coordinate analysis (PCoA) was also used by GenAlEx.

Population structure was analyzed using the software package STRUCTURE version 2.2 (Pritchard et al., 2000; Falush et al., 2003, 2007). The calculation was carried out under an admixture ancestry model and correlated allele frequency model. A burn-in period of 10,000 generations, followed by 50,000 iterations, was used to cluster the population. The assumed number of populations (*K*) was set from 2 to 8. The Δ*K* statistic, based on the rate of change of log likelihood of data [*l* (*K*)] between successive *K* values, was used to select the optimal *K*, following Evanno et al. (2005).

RESULTS

Genetic diversity of *Q. liaotungensis* populations

A total of 179 clear and highly polymorphic bands were detected by 12 SRAP primer combinations. The length of amplified bands was from 125 to 2000 bp. The number of polymorphic bands for per primer combination ranged from 8 to 21, with an average of 14.9.

High genetic diversity in populations of *Q. liaotungensis* was detected by SRAP (Table 2). At the species level, the percentage of polymorphic bands (*PPB)* was 100%, observed number of alleles (*Na*) was 2.0000, effective number of alleles (*Ne*) was 1.5738, Shannon diversity index (*I*) was 0.5264 and Nei's gene diversity index (*H*) was 0.3482 (Table 2). Within each population, the percentage of polymorphic band (*PPB*) ranged from 75.42 to 91.62%, with an average of 85.90%. Shannon information index (*I*) ranged from 0.3927 to 0.4917; Nei's gene diversity (*H*) showed the similar trends, ranging from 0.2632 to 0.3312. Observed number of alleles (*N*a) ranged from 1.7542 to 1.9050. Effective number of alleles ranged from 1.4579 to 1.5748.

At the population level, the average genetic diversity of *Q. liaotungensis* populations was: *PPB*=85.90%, *Na*=1.8590, *Ne*=1.4778, *I*=0.2840, *H*=0.4300 (Table 2). The genetic diversity of population 6 was the highest among all the populations involved in this study (*PPB*: 90.50%, *Na*: 1.9050, *Ne*: 1.5748, *H*: 0.3312, *I*: 0.4917), while the genetic diversity of population 4 was the lowest (*PPB*: 75.42%, *Na*: 1.7542, *Ne*: 1.4579, *H*: 0.2632, *I*: 0.3927). The genetic diversity of all studied *Q. liaotungensis* populations was different along an altitude gradient. As can be seen from Table 2, the genetic

Table 3. Analysis of molecular variance (AMOVA) within/among *Q. liaotungensis* populations.

Source of variance	d.f	SSD	MSD	Ratio of variance (%)
Among populations	7	767.150	109.593	20
Within populations	72	2300.000	31.944	80
Total	79	3 067.150		100

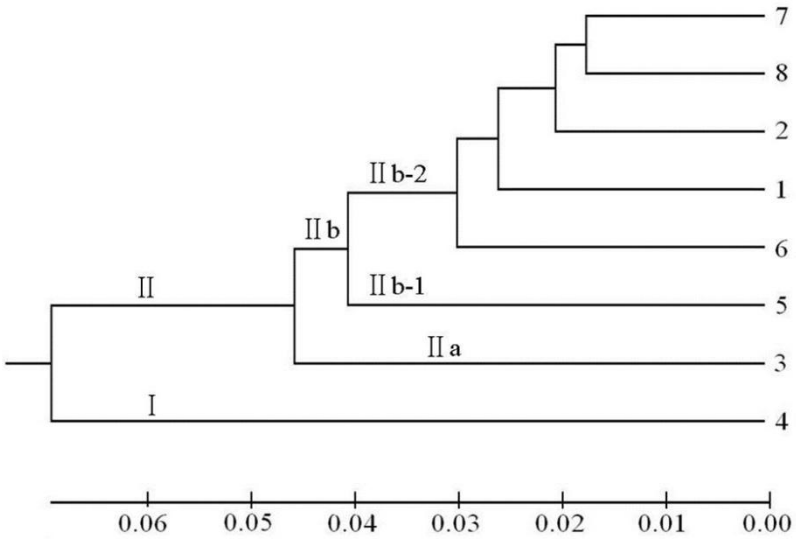

Figure 1. Dendrogram of *Q. liaotungensis* populations based on genetic distance.

diversity of *Q. liaotungensis* populations showed the low-high-low variation pattern with elevation increase. The highest level of genetic diversity was present at an altitude of 1800 m, and following the altitude of 1500 m.

Genetic structure of *Q. liaotungensis* populations

The Nei's gene diversity index always was regarded as one parameter to estimate the genetic differentiation of plant populations (Qin et al., 2010). The average gene diversity (H_S) was 0.2840 within populations of *Q. liaotungensis*. And the coefficient of genetic differentiation among populations (*G*st) was 0.1844 (Table 2). Those indexes revealed that the genetic variance mainly occurred among individuals within populations for *Q. liaotungensis*.

AMOVA (Table 3) showed that there was a significant (p<0.001) genetic difference within eight populations of *Q. liaotungensis*. Of the total genetic diversity, there were 31.978 variance components among populations and 7.265 within populations. The 80% of total variation was contributed by individuals within populations, and 20% occurred among populations. AMOVA result was consistent with the coefficient of genetic differentiation *G*st.

In addition, the effective gene flow per generation for *Q. liaotungensis* was *N*m=2.2108, which was higher than that of the widespread species (*N*m=1.881, Hamrick, 1987).

Genetic distances among populations ranged from 0.0354 to 0.1535 (data not shown), with an average of 0.0873. The genetic identities among populations varied from 0.8577 to 0.9652, with an average of 0.9170. The longest distance occurred between population 7 and population 8, while the shortest was between population 1 and population 4.

The Unweighted Pair Group Method with Arithmetic Mean (UPGMA) cluster analysis based on the genetic distance among populations revealed that all eight populations of *Q. liaotungensis* were separated into two groups (I-II) (Figure 1). Group I included only population 4, while the other populations clustered around Group II. Within Group II, the population 3 clustered around the subgroup IIa, the population 5 clustered around the subgroup IIb-1; other populations gathered around the subgroup IIb-2.

Principal coordinate analysis (PCoA) plot revealed a similar grouping of populations with the UPGMA dendrogram (Figure 2). The first three eigen vectors accounted for 80.10% of the variation observed. In the two-dimensional PCoA, the first two coordinates explained 62.26% (42.08% for axis 1 and 20.18% for axis 2,

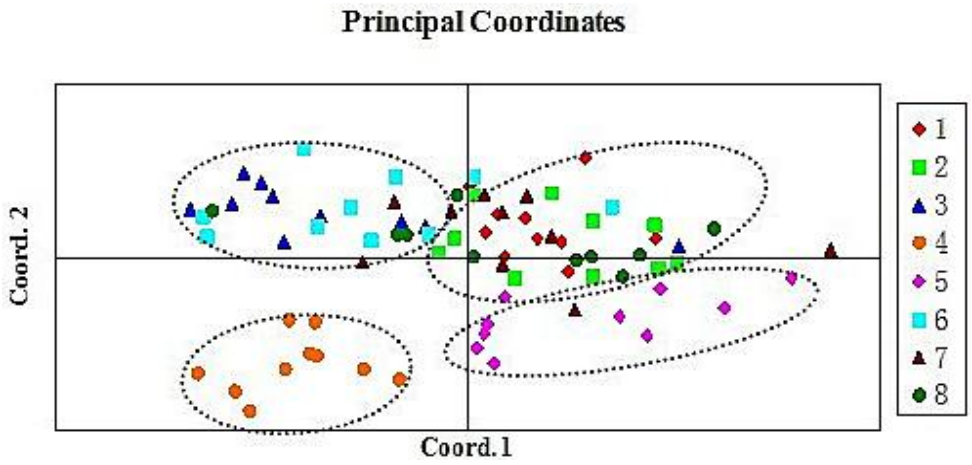

Figure 2. Principal coordinates analysis (PCoA) for *Q. liaotungensis* individuals.

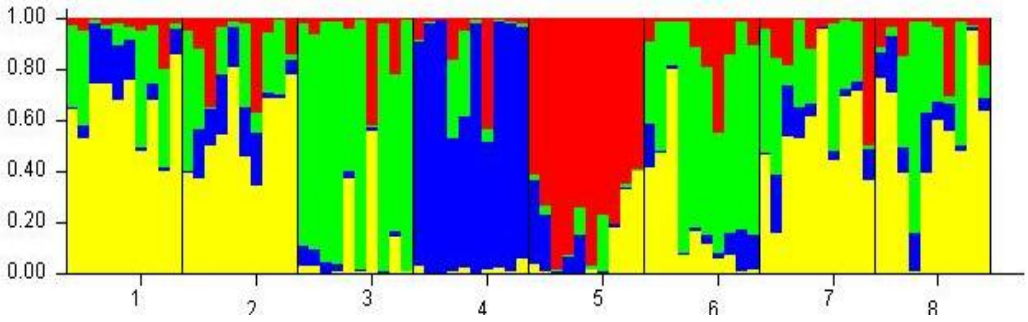

Figure 3. Estimated genetic structure for *K*=4 obtained with the STRUCTURE program for 8 populations of *Q. liaotungensis.*

respectively) of the total variance. The studied eight populations of *Q. liaotungensis* were generally divided into 4 groups. The population 4 alone gathered a group, population 5 gathered a group, population 3 and 6 gathered together, population 1, 2, 7 and 8 gathered together (Figure 2).

The pattern of genetic diversity and structure was further analyzed with a Bayesian-based approach implemented in the program STRUCTURE. The obvious optimum for the ad hoc quantity based on the second order rate of change of the likelihood function with respect to Δ*K* was observed for *K*=4. As a result, the entire populations were successfully assigned to four subgroups (Figure 3). This result was consistent with the PCoA analysis.

DISCUSSION

The genetic diversity of a species can be affected by various factors (Xie et al., 2010; Wang et al., 2007b; Jiang et al., 2009), such as life patterns, breeding system, geographical distribution, mechanism of seed dispersal (Xie et al., 2007, He et al., 2007).

In this study, there existed high genetic diversity in *Q. liaotungensis* populations at Xingtangsi (*PPB*=100%) (Table 2). Compared with other species of Fagaceae, the level of genetic diversity of *Q. liaotungensis* populations at Xingtangsi was higher than that of *Q. mongolica* populations located at Daqinggou (*PPB*=71.7%) and *Q. liaotungensis* populations at Donglingshan (*PPB*=67.6%) (Yun et al., 1998), similar to that of *Q. mongolica* populations (*PPB*=96.8%) (Li et al., 2003).

High genetic diversity of *Q. liaotungensis* populations may have a correlation with the biological characteristics and evolutionary history of this species. *Q. liaotungensis* is an old monoecism plant with unisexual and wind pollination, whose ancestor might have a rich genetic basis that is widely preserved in the long-time evolution. Meanwhile, *Q. liaotungensis*, as a kind of perennial species, can conserve its genetic diversity in quite a long time. Field investigations had found that the survival rate of seedlings of *Q. liaotungensis* in the natural forest was high at Xingtangsi. There were more seedlings and saplings for *Q. liaotungensis,* whose age structure was an ascending pattern. Based on those findings, we can infer

that there existed a high genetic diversity basis for *Q. liaotungensis* in natural forest. In addition, *Q. liaotungensis* can grow in different habitats dying to its intrinsic biological properties, such as strong adaptability, wide ecological amplitude, drought and barren resistance. The heterogeneous environment could promote local adaptation and fixation of different alleles in *Q. liaotungensis*, which also make a contribution to its high genetic diversity.

Among eight populations, the genetic diversity of population 4 was the lowest (*PPB*=75.42%, *I*=0.3927, *H*=0.2632, Table 2), followed by the population 5 (*PPB*=80.45%, *I*=0.4103, *H*=0.2736) and population 3 (*PPB*=83.24%, *I*=0.4353, *H*=0.2917). Those populations located at the medium altitudes in Xingtangsi. With the development of tourism in Xingtangsi, human activity with an elevation between 1500 and 1700 m was very frequent. Subsequently, the large areas of vegetation destroyed by the people and the ecological environment were relatively serious. Those irreversible changes caused the decrease in genetic diversity of intermediate altitude populations. High-altitude populations 6, 7 and 8, located on the edge of the *Q. liaotungensis* distribution in Xingtangsi, had relatively high genetic diversity (above 1800 m). Generally, the temperature drop is about 0.55 with the elevation increasing to l00 m. The rainfall is increased with the rise of altitude; so, the surrounding of those populations was relatively poor, and the environment selection pressure for those populations was relatively bigger; as a result, these populations' genetic diversity was relatively higher. Under the influence of human activity and livestock grazing, it easily led to genetic drift and made the loss of genetic diversity of the populations at low altitude. However, interestingly, populations 1 and 2 at low altitudes had relatively high genetic diversity. The reasons are as follows: *Q. liaotungensis* is still a kind of wild natural population in Xingtangsi, the community structure that had less human destruction is relatively complete, and that the tree age at all levels saved certain individuals of *Q. liaotungensis*, thus avoiding some adverse effect on genetic diversity of *Q. liaotungensis* populations. Based on field investigation, the rich seedling, good recruitment, and different microhabitat resulted in the high genetic diversity in the population 1 and 2.

If the inhabited elevation of the population was divided into three levels - high, medium and low, there should have four kinds of relationship between the genetic diversity and altitudes: i) The genetic diversity of medium elevation is higher than low and high altitude populations; ii) In the high altitude population, genetic diversity is lower than low altitude populations; iii) In the high altitude population, genetic diversity is higher than low altitude populations; iv) The genetic diversity of populations has no relationship with altitude (Ohsawa and Ide, 2008; Ohsawa et al., 2008). In this paper, the population 6 has the highest genetic diversity at altitude of 1800 m. With the rise of altitude, the level of genetic diversity of *Q. liaotungensis* populations gradually decreased. When the altitude dropped to 1300 m, the level of genetic diversity of *Q. liaotungensis* has a certain degree of increase. Therefore, a close relationship had existed between the elevation and genetic diversities of *Q. liaotungensis* populations. The genetic diversity of *Q. liaotungensis* presents a low-high-low pattern along altitude gradient. Those results supported the viewpoint that the genetic diversity of medium elevation is higher than low and high altitude populations.

AMOVA analysis showed that 80% of total genetic variation of *Q. liaotungensis* was contributed within populations and 20% among populations (p<0.001).

The genetic structure of populations not only depended on breeding system, origin and evolution process, but also affected by natural selection, gene flow and other factors (Peng et al., 2007; Ishihama et al., 2005). High level of gene flow could prevent the genetic differentiation among population, while low level of gene flow might make the population better adapt to the local environment, and increase the genetic isolation among populations. Wright (1931) pointed out that if the gene flow among populations was less than 1, the gene drift would play an important role in influencing genetic variation and genetic structure (Hey et al., 2012). *Q. liaotungensis'* pollen, being small and light, can distribute from high altitude to low altitude. *Q. liaotungensis'* nuts, large volume, can fall to low altitude area because of the gravity. And the nuts' nutrition was rich, which was important food for small mammals and birds. Thus, the seeds flow among different population could occur. Effective flow of pollen and seed made the high level of gene flow among populations of *Q. liaotungensis* (N_m=2.2108). Although the genetic variation mainly existed in *Q. liaotungensis* populations, a significant genetic differentiation still occurred among populations (Table 3, Figures 2 and 3). In a small area, the genetic drift was a main factor that caused the genetic differentiation among populations (Li et al., 2011; Zhang et al., 2010). The microhabitat heterogeneity in the relatively small geographical area also resulted in the genetic differentiation among populations (Li et al., 2004; Zhang et al., 2005; Zhao et al., 2001). With increasing elevation, climate, vegetation and soil showed obvious vertical variation; the temperature, water, light, and other ecological factors were also significantly different in different altitudes for different population of *Q. liaotungensis*, which eventually led to the genetic differentiation that occurs among populations.

Conclusion

Q. liaotungensis populations had high genetic diversity, and the genetic variation mainly existed within populations. There a significant genetic differentiation occurred among populations. The genetic diversity of all studied eight *Q. liaotungensis* presents a low-high-low pattern along

altitude gradient. *Q. liaotungensis'* biology characteristics, effective gene flow and environmental heteroplasmy resulted in the genetic distribution pattern of *Q. liaotungensis* populations in Xingtangsi.

Conflict of Interests

The author(s) have not declared any conflict of interests.

ACKNOWLEDGEMENTS

This research was supported by the funding of the undergraduate innovative experiment project of Shanxi Normal University (SD2010XCSY-19), the Natural Science Foundation of Shanxi Normal University (ZR1106) and the Natural Science Foundation of Shanxi Province (2011011031-2).

REFERENCES

Abedian M, Talebi M, Golmohammdi HR, Sayed-Tabatabaei BE (2012). Genetic diversity and population structure of mahaleb cherry (Prunus mahaleb L.) and sweet cherry (Prunus avium L.) using SRAP markers. Biochem. Syst. Ecol. 40:112-117. http://dx.doi.org/10.1016/j.bse.2011.10.005

Agar G, Yildirim N, Ercisli S (2012). Genetic and biochemical differentiation in Vitis vinifera (Kabarcik) populations grown at different altitudes in Coruh Valley. Genet. Mol. Res. 11 (1):211-220. http://dx.doi.org/10.4238/2012.February.3.1; PMid:22370888

Amar M, Biswas M, Zhang Z, Guo W (2011). Exploitation of SSR, SRAP and CAPS-SNP markers for genetic diversity of Citrus germplasm collection. Sci. Hortic. 128:220-227. http://dx.doi.org/10.1016/j.scienta.2011.01.021

Baur B, Raboud C (1988). Life history of the snail Arianta arbustorum along an altitudinal gradient. J. Anim. Ecol.57: 71-87. http://dx.doi.org/10.2307/4764

Cai XY, Feng ZY, Zhang XX, Xu W, Hou BW, Ding XY (2011). Genetic diversity and population structure of an endangered Orchid (Dendrobium loddigesii Rolfe) from China revealed by SRAP markers. Sci. Hortic. 129:877-881. http://dx.doi.org/10.1016/j.scienta.2011.06.001

Dong P, Wei YM, Chen GY, Li W, Wang JR, Nevo E, Zheng YL (2010). Sequence-related amplified polymorphism (SRAP) of wild emmer wheat (Triticum dicoccoides) in Israel and its ecological association. Biochem. Syst. Ecol. 38:1-11. http://dx.doi.org/10.1016/j.bse.2009.12.015

Erich G, Johann JS (2002). Phenotypic and isozyme variation in Cystopteris fragilis (Pteridophyta) along an altitudinal gradient in Switzerland. Flora 197:203-213. http://dx.doi.org/10.1078/0367-2530-00031

Evanno G, Regnaut S, Goudet J (2005). Detecting the number of cluster of individuals using the software STRUCTURE: A simulation study. Mol. Ecol. 14:2611-2620. http://dx.doi.org/10.1111/j.1365-294X.2005.02553.x; PMid:15969739

Falush D, Stephens M, Pritchard JK (2003). Inference of population structure: extensions to linked loci and correlated allele frequencies. Genetics 164:1567-1587. PMid:12930761 PMCid:PMC1462648

Falush D, Stephens M, Pritchard JK (2007). Inference of population structure using multilocus genotype data: Dominant markers and null alleles. Mol. Ecol. Notes 7:574-578. http://dx.doi.org/10.1111/j.1471-8286.2007.01758.x; PMid:18784791 PMCid:PMC1974779

Fan ZH, Li TC, Qiu J, Li ZP, Lin Y, Cai YP (2008.) Studies on genetic diversity of medicinal Dendrobium by SRAP. China J. Chin. Mater. Med. 1:6-10.

Feng FJ, Wang FY, Li CS (2004). Genetic differentiation of Pinus koraiensis under different altitude conditions in Changbai Mountains. J. Northeast Univ. 32:1-3.

Gai SP, Gai WL, Huang JY (2011). Comparison of SSR and SRAP marker for varieties identification in Maize (Zea mays L.). J. Plant Genet. Res. 3:468-472.

Hamrick JL (1987). Gene flow and distribution of genetic variation in plant populations. Academes Press, New York, pp.53-67.

He J, Yang BY, Chen SF, Gao LM, Wang H (2007). Assessment of genetic diversity of Paris polyphylla (Trilliaceae) by ISSR markers. Acta Bot. Yunnanica 4:388-392.

Heath D, Williams DR (1979). Life at High Altitude. Edward Arnold, London.

Hey J, Pinho C (2012). Population genetics and objectivity in species diagnosis. Evolution 66(5):1413-1429. http://dx.doi.org/10.1111/j.1558-5646.2011.01542.x; PMid:22519781

Ishihama F, Ueno S, Tsumura Y, Washitani L (2005). Gene flow and inbreeding depression inferred from fine-scale genetic structure in an endangered heterostylous perennial Primula sieboldii. Mol. Ecol. 14(4):983-990. http://dx.doi.org/10.1111/j.1365-294X.2005.02483.x; PMid:15773930

Jia P, Yan M, Shi X, Lu P, He YH, Shi L, Zhou JC (2009). The study on the tree layer of Quercus liaotungensis community in MT. Huoshan of Shanxi province-interspecific relationship and population age structure. J. Mountain Agri. Bio. 3:208-213.

Jiang XM, Wen Q, Ye JS, Xiao FM, Jiang M (2009). RAPD analysis on genetic diversity in eight natural populations of Phoebe bournei from Fujian and Jiangxi province, China. Acta Ecol. Sin. 1:438-444.

Kurt Y, Bilgen BB, Kaya N, Isik K (2011). Genetic comparison of Pinus brutia ten populations from different elevations by RAPD markers. Not. Bot. Horti Agrobo. Cluj-Napoca 39(2):299-304.

Li G, Quiros CF (2001). Sequence-related amplified polymorphism (SRAP), a new marker system based on a simple PCR reaction: Its application to mapping and gene tagging in Brassica. Theor. Appl. Genet. 103:455-461. http://dx.doi.org/10.1007/s001220100570

Li JC, Ke Y, Li BS (1998). The variation of genetic diversity of Quercus aquifolioides in different elevations. Acta Bot. Sin. 40:761-767.

Li JH, Li XS, Tian CY, Zou LP, Wang DP (2011). Genetic diversity of wild populations in Daduisi National Forest Park. Ecol. Environ. Sci. 20(12):1799-1804.

Li JM, Jin ZX, Zhong ZC (2004). RAPD analysis of genetic diversity of Sargentodoxa cuneata at different altitude and the influence of environmental factors. Acta Ecol. Sin. 3:567-573.

Li L, Zheng XY, Liu LW (2006). Analysis of genetic diversity and identification of Cucumber varieties by SRAP. Mol. Plant Breed. 5:702-708.

Li M (2005). Study on Phenotypic Diversity of Natural Populations in Quercus liaotungensis. Master dissertation, Beijing Forestry University, Beijing.

Li RH, Xia YS, Liu XZ, Sun LL, Guo PG, Miao KY, Chen JH (2009). CTAB-improved method of DNA extraction in plant. Res. Explor. Lab. 9:14-16.

Li WY, Gu WC, Zhou SL (2003). AFLP analysis on genetic diversity of Quercus mongolica populations. Sci. Silv. Sin. 5:29-36.

Liu LW, Zhao LP, Gong YQ, Wang MX, Chen LM, Yang JL, Wang Y, Yu FM, Wang LZ (2008). DNA fingerprinting and genetic diversity analysis of ate-bolting radish cultivars with RAPD, ISSR and SRAP markers. Sci. Hortic. 116:240-247. http://dx.doi.org/10.1016/j.scienta.2007.12.011

Ohsawa T, Ide Y (2008). Global patterns of genetic variation in plant species along vertical and horizontal gradients on mountains. Global Ecol. Biogeogr. 17:152-163. http://dx.doi.org/10.1111/j.1466-8238.2007.00357.x

Ohsawa T, Saito Y, Sawada H, Ide Y (2008). Impact of altitude and topography on the genetic diversity of Quercus serrata populations in the Chichibu Mountains, central Japan. Flora-Morph, Distrib. Func. Ecol. Plants 203(3):187-196. http://dx.doi.org/10.1016/j.flora.2007.02.007

Peakall R, Smouse PE (2006). GenALEx6: Genetic analysis in Excel population genetic software for teaching and research. Mol. Ecol. Notes 6(1):288-295.

http://dx.doi.org/10.1111/j.1471-8286.2005.01155.x
Peng YQ, Shao JW, Zhang XP, Zhang ZX, Zhu GP (2007). Genetic diversity of the endangered and endemic species, Primula merrilliana (Primulaceae), revealed by RAPD analysis. Acta Bot. Yunnanica 5:549-553.
Premoli AC (2003).Isozyme polymorphisms provide evidence of clinal variation with elevation in Nothofagus pumilio. J. Hered. 94:218-226. http://dx.doi.org/10.1093/jhered/esg052; PMid:12816962
Pritchard JK, Stephens M, Donnelly P (2000). Inference of population structure using multilocus genotype data. Genetics 155:945-959. PMid:10835412 PMCid:PMC1461096
Qin YY, Han HR, Kang FF, Zhao Q (2012). Genetic diversity in natural populations of Quercus liaotungensis in Shanxi Province based on nuclear SSR markers. J. Beijing For. Univ. 34(2):61-65.
Qin YY, Wang YL, Zhang QD, Bi RC, Yan GQ (2010). Analysis on the population genetic diversity of an endangered plant (Elaeagnus mollis) by SSR Markers. J. Wuhan Bot. Res. 4:466-472.
Qu Z, Wei YH, Li DW, Xiao LZ, Xu HX, Xie KQ, Zhou MQ, Hu ZL (2008). Genetic diversity analysis of Nelumbo nucifera based on SRAP markers. Amino Acids Bio. Res. 3:21-25.
Saenz-Romero C, Tapia-Olivares BL (2003). Pinus oocarpa isoenzymatic variation along an altitudinal gradient in Michoacaán, México. Silv. Genet. 52:237-240.
Semang K, Bjornstad A, Stedje B (2003). Genetic diversity and differentiation in Ethiopian populations of Phytolacca dodecandra as revealed by AFLP and RAPD analyses. Genet. Res. Crop Evol. 50:649-661. http://dx.doi.org/10.1023/A:1024447404492
Wang JF, Kuroda C, Gong X (2007b). Assessment of genetic variation and differentiation of Ligularia tongolensis (Compositae) detected by ISSRs. Acta Bot. Yunnanica 5:537-542.
Wang JS, Yao JC, Liu L, Wang YJ, Li W (2007a). Construction of a molecular genetic map for Melon (Cucumis melo L.) based on SRAP. Acta Hortic. Sin. 1:135-140.
Wright S (1931). Evolution in Mendelian population. Genetics 16:97-159. PMid:17246615 PMCid:PMC1201091
Xiao LS, Ge XJ, Gong X, Zheng SX (2003). Genetic diversity of Cycas guizhouensis. Acta Bot. Yunnanica 25:648-652.
Xie GW, Peng XY, Zheng YL, Zhang JX (2007). Genetic diversity of endangered plant Monimopetalum chinense in China detected by ISSR analysis. Sci. Silv. Sin. 8:48-53.
Xie WG, Zhang XQ, Chen YX (2010). Identification and genetic variation analysis of Orchardgrass hybrids (Dactylis glomerata) by SSR molecular markers. Acta Pratacul. Sin. 2:212-217.
Yeh FC, Yang RC, Boyle T (1997). POPGENG, the user friendly shareware for population genetic analysis. Molecular Biology and Biotechnology Center. University of Alberta, Edmonton, Canada.
Yun R, Zhong M, Wang HX, Wei W, Hu ZA, Qian YQ (1998). Study on DNA diversity of Liaodong oak population at Dongling Mountain region, Beijing. Acta. Bota. Sin. 40(2):169-175.
Zhang XY, Chen FD, Zhang F, Chen SM, Fang WM (2011). Analysis of genetic diversity among different geographical populations of wild species of Dendranthema. J. Nanjing Agric. Univ. 1:29-34.
Zhang YH, Hou Y, Lou AR (2010). Population genetic diversity of Rhodiola dumulosa in Northern China inferred from AFLP markers. Chin. J. Plant Ecol. 34(9):1084-1094.
Zhang ZH, Tang T, Zhou RC, Wang YG, Jian SG, Zhong CR, Shi SH (2005). Effects of divergent habitat on genetic structure of population of Excoecaria agallocha, a mangrove associate. Acta Genet. Sin. 12:1286-1292.
Zhao LF, Li S, Pan Y, Yan GQ, Zhao GF (2001). Population differentiation of Psathyrostachys huashanina along an altitudinal gradient detected by random amplified polymorphic DNA. Acta Bot. Boreali-Occidentalia Sin. 3:391-400.
Zheng YQ, Zong JQ, Xue DD, Chen X, Liu JX (2009). Application of SRAP markers to the identification of Eremochloa ophiuroides (Munro) hack hybrids. Acta Agre. Sin. 2:135-140.
Zuo DD, Zhao HT, Liu C, Mu D, Wang XW, Ming J (2009). Wenetic diversity in natural populations of Chimonanthus praecox (L.) link revealed by SRAP markers. Acta Hortic. Sin. 8:1197-1202.

academicJournals

Vol. 9(8), pp. 257-263, 30 April, 2014
DOI: 10.5897/SRE2014.5846
Article Number: 91C18ED44201
ISSN 1992-2248 © 2014

http://www.academicjournals.org/SRE

Scientific Research and Essays

Full Length Research Paper

Synthesis of Chebyshev-I filter using folding and retiming

Nongmaithem Lalleima Chanu[1]* and Vimal Kant Pandey[2]

Department of ECE, M-Tech Digital Electronics, DIT Dehradun, India – 248009.

Received 25 February 2014; Accepted 9 April, 2014

In synthesizing Digital signal processing (DSP) architecture, maintaining low silicon area and high performance becomes an important factor which can be achieved by various optimization techniques. To achieve this, we employ two design optimization techniques: folding and retiming, which are applied to 3rd order Chebyshev I high pass digital filter to minimize the functional units (adders, multipliers) and to reduce the number of registers. Folding transformation is used to determine the control circuits in DSP architecture by executing multiple algorithm operation on a single functional unit. Retiming using register minimization is applied after folding, thereby reducing the numbers of multipliers and adders from 7 to 1 and 6 to 1, respectively, without affecting the input and output characteristics of the filter.

Key words: Data flow graph (DFG), Chebyshev filter, folding, retiming, lifetime analysis.

INTRODUCTION

Tremendous growth of digital signal processing (DSP) and its importance promotes advances in certain fields of applications such as telecommunication, military, instrumentation and control, image processing, seismology, speech processing and biomedical signal processing. DSP programs are executed repetitively for an infinite number of times and they are assumed to be non-terminating (Jackson et al., 2003; Salivahanan et al., 2010). This can be exploited by designing more efficient DSP system in terms of speed, area and power. The strategy of designing an efficient filter also needs to concentrate on reducing the number of functional units.

Advancement in technology and emerging trends required DSP architecture with less space and power consumption where the signal processing algorithm are modified to accommodate the circuit. To achieve the goals such as less area, high speed and low power different algorithms are proposed such as pipelining, folding, retiming etc. The transformation in which multiple algorithm operations are time multiplexed to a single functional unit is known as folding. This algorithm provides a technique for designing control circuits for hardware and helps to synthesize DSP architecture that can be operated using single or multiple clocks. Folding reduces the number of functional units; it may also lead to the usage of large number of registers (Keshab, 2012; Rajalakshmi et al., 2013). To avoid this, retiming technique is used to compute the minimum number of registers require to implement a folded DSP architecture and to allocate data to these registers to provide

*Corresponding author. E-mail: lallei.chanu98@gmail.com

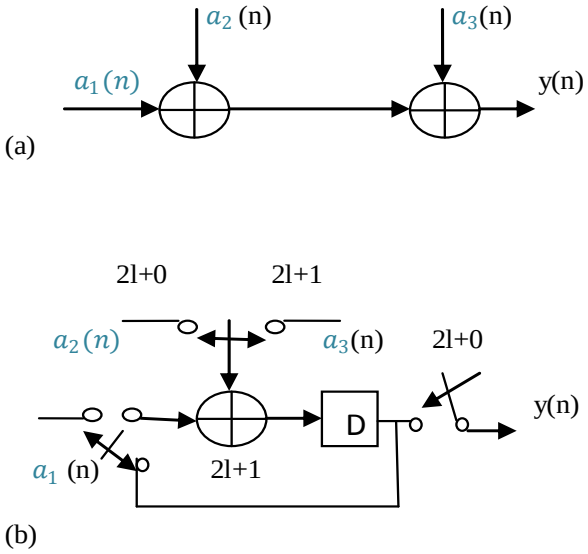

Figure 1. (a) A DSP program with 2 addition operations; (b) A folded architecture where the 2 addition operations are folded to a single pipelined adder.

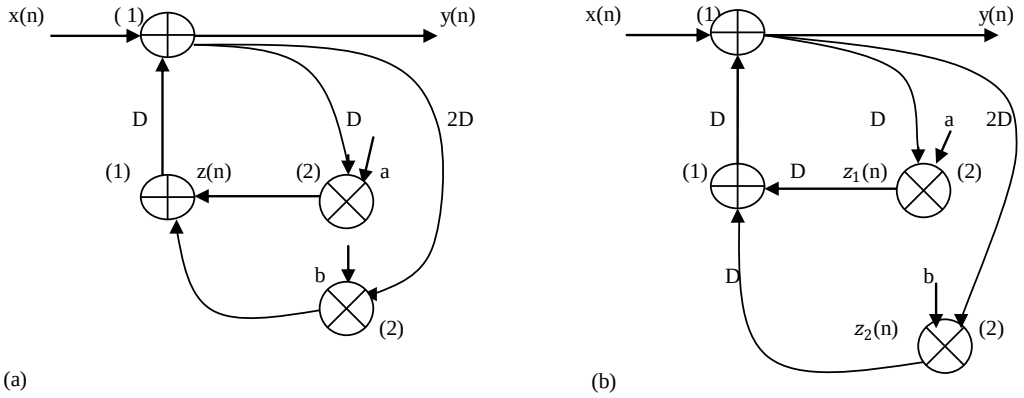

Figure 2. Two versions of an IIR filter and the computation times of the nodes are in parentheses.

architecture with low silicon area (Rajapadhy and Kiaei, 1991). This design optimization platform is designed using MATLAB/Simulink and Xilinx.

DESIGN OPTIMIZATION TECHNIQUE

Folding

This transformation technique helps to determine the control circuits in DSP system in which multiple algorithm operations are time multiplexed to a single functional unit which leads to the reduction of functional units (such as adders, multipliers) resulting with low silicon area. Figure 1a shows an example of a DSP program for adding two samples where the operation computes

$$Y(n) = a_1(n) + a_2(n) + a_3(n)$$

Here, one output sample is produced every 2 clock cycles and hence the input is valid for 2 clock cycles (2l+0 and 2l+1, where l is the iteration). In 0 cycle, $a_1(n)+a_2(n)$ is performed. In cycle 2l+1(second), $a_1(n)+a_2(n)$ is switch to the adder along with $a_3(n)$ and the sum is stored in the unit cycle 2. Folded architecture in which 2 addition operation are folded to a single pipelined adder is shown in Figure 1(b).

Retiming

It is used to change locations of delay elements without changing the input/output characteristic of the system which is illustrated using Figure 2a and b. The filter 2(a) is described by

z(n) = ay(n-1)+by(n-2)
y(n) = z(n-1)+x(n)
= ay(n-2)+by(n-3)+x(n)

And filter 2(b) is described by

z_1(n) = ay(n-1)
z_2(n) = by(n-2)
y(n) = z_1(n-1)+z_2(n-1)+x(n)
= ay(n-2)+by(n-3)+x(n)

These two filters are having the same input-output characteristics and can be derived from one another with the help of retiming, even though these filters are having delays at different locations.

Retiming can be used to increase the clock rate, to decrease the number of registers and to reduce the power consumption of a circuit (Keshab et al., 1992).

CHEBYSHEV FILTER

Type I Chebyshev filters are all-pole filters that exhibit equiripple behavior in the passband and monotonic characteristic in the stopband. By increasing the order N, the Chebyshev response approximates the ideal response. It has the property that they minimize the error between the idealized and the actual filter characteristic over the range of the filter. This type of filter is named after Pafnuty Chebyshev (John and Dimitris, 1996). The magnitude response of Chebyshev type I filter can be expressed as:

$$|H(j\Omega)| = \frac{A}{[1+\varepsilon^2\ C_N^2(\frac{\Omega}{\Omega_c})]^{0.5}}$$

Where A is the filter gain, ε is the constant, $\Omega_c$is the 3dB cutoff frequency. C_N(x) is the N^{th} order chebyshev polynomial defined as

C_N(x) = cos (N$\cos^{-1}x$), |x|≤ 1 (passband)

C_N(x)= cos(N$\cosh^{-1}x$), |x|> 1 (stopband) and the chebyshev polynomial is defined by the recursive formula:

$C_N(x)$ = 2x $C_{N-1}(x)$ - $C_{N-2}(x)$, N > 1

Where $C_0(x)$ = 1 and $C_1(x)$ = x

DATA FLOW GRAPH (DFG)

The operations of DSP algorithm are assumed to be executed repetitively. The DSP filter blocks needed to be optimized can be represented by DFG due to its easier, efficient and compactness. DFG is a directed graph G with sets of nodes/vertices V and sets of edges E (Edward, 1991; Rakshi et al., 2010). Each node in the DFG represents an algorithm operation and any arc *U → V with* w(e) delays states that the output of the l^{th} iteration of U is used to execute the $(l + w(e))^{th}$ iteration of V. The arc with and without delays represent the inter iteration and intra iteration precedence constraint, respectively (John and Dimitris, 1996).

DFG is used to described hardware architecture which depends on folding factor (N), number of operation folded to a single functional unit. Hu and Hv denote the operators that execute the operation U and V in the hardware DFG. Operations processed by the operators form a folding set S. Each folding sets contains N entries, some of which may be a null operations denoted as Ø. A delay or register elements in the hardware represents a storage unit.

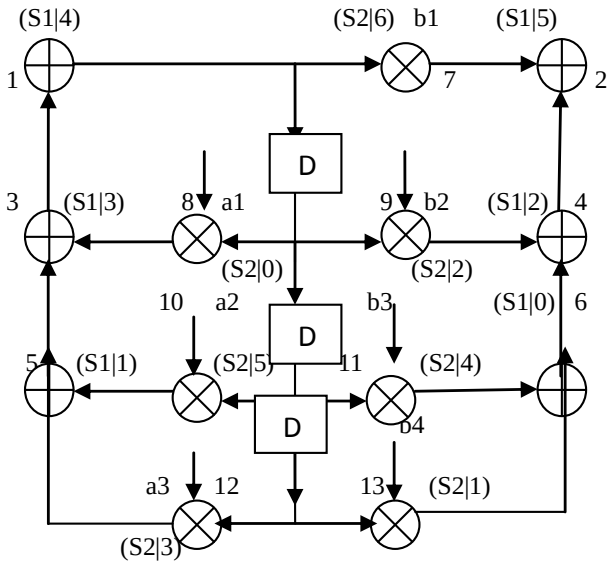

Figure 3. Direct form II, 3rd order Chebyshev I filter.

FOLDING EQUATIONS

Folding is a transformation technique used to reduce the silicon area by time multiplexing many algorithm operations into single functional units, such as adders and multipliers. It provides a systematic process to design control circuit for hardware. Folding is applied to the filter to reduce the chip area (Keshab, 2012). Consider an edge e connecting the nodes U and V with w(e) delays. Let the execution of l^{th} iteration of the nodes U and V be scheduled at the time units Nl+u and Nl+v, respectively, where u and v are the folding orders of nodes U and V that satisfy 0≤u, v≤N-1. Hu and Hv denote the functional unit that executes the nodes U and V. If Hu is pipelined by Pu stages, the l^{th} iteration of node U is available at time unit Nl+u+Pu. The result of l^{th} iteration of node U is used by $(l + w(e))^{th}$ iteration of the node V which is executed at N(l+w(e)) + v. Thus, the result must be stored for:

$$D_F(U \rightarrow V) = [N(l + w(e)) + v] - [Nl + Pu + u]$$
$$= Nw(e) - Pu + v - u \quad (1)$$

Time units, which is independent of l, a folding set is an ordered set of N operations executed by the same functional unit which depends on the folding order. The folding order of a node is the block of time to which the node is scheduled to execute the operation in the hardware. The folding sets of 3rd ordered Chebyshev filter is shown in Figure 3 and are given by

S_A= S1= {1, 2, 3, 4, 5, 6, Ø} and

S_M= S2= {7, 8, 9, 10, 11, 12, 13}

Using the above folding sets, the filter is folded with folding factor 6 which means that the iteration period of the folding architecture is 6 units of time (u.t). Here, each node of the filter is executed once every 6 u.t in the folded architecture that is the folded hardware executes six operations. The folding set S_A contains one null operation in Position 6 during which no operation is performed by the adder. The folding equations for each edge are given in Table 1

Table 1. Folding equations.

Edge	Folding equation
1→ 7	D_F(1→ 7) = 6(0)-1+6-4 = 1
1→ 8	D_F(1→ 8) = 6(1)-1+0-4 = 1
1→ 9	D_F(1→ 9) = 6(1)-1+2-4 = 3
1→ 10	D_F(1→ 10) = 6(2)-1+5-4 = 12
1→ 11	D_F(1→ 11) = 6(2)-1+4-4 = 11
1→ 12	D_F(1→ 12) = 6(3)-1+3-4 = 16
1→ 13	D_F(1→ 13) = 6(3)-1+1-4 = 14
8→ 3	D_F(8→ 3) = 6(0)-2+3-0 = 1
3→ 1	D_F(3→ 1) = 6(0)-1+4-3 = 0
10→ 5	D_F(10→ 5) = 6(0)-2+1-5 = -6
5→ 3	D_F(5→ 3) = 6(0)-1+3-1 = 1
12→ 5	D_F(12→ 5) = 6(0)-2+1-3 = -4
7→2	D_F(7→ 2) = 6(0)-2+5-6 = -3
9→ 4	D_F(9→ 4) = 6(0)-2+2-2 = -2
4→ 2	D_F(4 → 2) = 6(0)-1+5-2 = 2
11→ 6	D_F(11→ 6) = 6(0)-2+0-4 = -6
6→ 4	D_F(6→ 4) = 6(0)-1+2-0 = 1
13→ 6	D_F(13→ 6) = 6(0)-2+0-1 = -3

using Equation 1. Here, the equations are derived with an assumption that addition and multiplication operations require 1 and 2 units of time, respectively.

RETIMING

Basically, retiming is also a transformation technique used to change the location of the delay elements without affecting the input and output characteristic of the circuit. Retiming has to be performed before folding to forced causality of the system (Leiserson et al., 1986; Monteiro et al., 1993). The negative values of the above folding equations are made positive by using cutest retiming; a special case of retiming which only affects the weights of the edges of the cutest. It consist of adding k delays to each edge from disconnected subgraphs G1 to G2 and removing k delays from G2 to G1. Using retiming the weight of the edge U→ V is computed as:

$w_r(e)$= w(e)+r(V)-r(U) (2)

The retiming folding constraints are obtained using the relation

r(U)-r(V)≤ $\lfloor \frac{D_F(U \to V)}{N} \rfloor$, (3)

Where ⌊x⌋ is the floor of x, which is the largest integer less than or equal to x. The retimed folding constraints are:

r(1)-r(7)≤0, r(1)-r(8)≤0, r(1)-r(9)≤0

r(1)-r(10)≤2, r(1)-r(11)≤2, r(1)-r(12)≤3,

r(1)-r(13)≤2, r(8)-r(3)≤0, r(3)-r(1)≤0,

r(10)-r(5)≤-1, r(5)-r(3)≤0, r(12)-r(5)≤-1,

r(7)-r(2)≤0, r(9)-r(4)≤0, r(4)-r(2)≤0,r(11)-r(6)≤-1,
r(6)-r(4)≤0, r(13)-r(6)≤0

From these folding constraints, we can form the constraint graph. The inequalities can be solved using Floyd–Warshall algorithm and the final constraints after applying algorithm are:

r(1)=0, r(2)=0,r(3)=0,r(4)=0,r(5)=0,r(6)=0,

r(7)=0, r(8)=0, r(9)=0, r(10)=-1, r(11)=-1,

r (12)=-1, r(13)=0.

We can find the new retimed value using Equation 2. By applying the folding equations the new delays can be obtained and then cutest retiming is applied to have positive values from which the architecture can be derived.

REGISTER MINIMIZATION TECHNIQUE

The main objective here is to minimize the architectural area by minimizing the number of registers. The folded structure contains a higher number of register because the intermediate results need to be stored (Keshab, 2012; Parhi, 1992; Rajapadhy and Kiaei, 1991). This minimization process follows two steps:

(a) Lifetime analysis table and lifetime chart.
(b) Data allocation using forward and backward register allocation.

Table 2. Lifetime table.

Node	Tinput → Toutput
1	5→ 19
2	–
3	4 → 4
4	3 → 5
5	2→ 3
6	1→ 2
7	8 →11
8	2→ 3
9	4 →8
10	7→ 7
11	6→ 12
12	5 → 7
13	3 → 6

In lifetime analysis, a data sample (variable) is live from the time it is produced through the time it is consumed. It is dead, after the variable is consumed. When the variable is live, it occupies one register (Deepa and Vijaya, 2012). Here, the number of live variables at each time unit is computed and the number of registers needed by the folded architecture is computed. Lifetime table can be constructed by considering the two parameters and their relations:

T_{input} = u+P_u (Table 2).

T_{output} = T_{input} +max{D_F(U→ V)}

The linear lifetime chart is shown in Figure 4, which graphically represents the lifetime of each variable.

Here, the horizontal lines represent the clock cycle and vertical lines represent the lifetime of a variable. With the help of this chart, the resultant minimum number of registers is obtained as the maximum number of live variable at any time step. The maximum number of register is Max{0,0,1,1,2,3,4.4,3,4,4,5,5,5,5,4,5,5,6,6} = 6. After lifetime chart, the minimum number of register required to implement the architecture is found to be 6 and data are allocated to the registers. The registers are named as R1, R2, R3, R4, R5 and R6. This allocation scheme dictates how the variables are assign to registers (Figure 5).

Folded architecture

The folded architecture with respect to the folding equations and allocation table with a minimum of 6 registers is derived and shown in Figure 6.

RESULTS

Tables 3 and 4 show the comparison of unfolded and folded filter with respect to adders, multipliers and number of registers, and the device utilization for both the architecture. These architectures (unfolded and folded

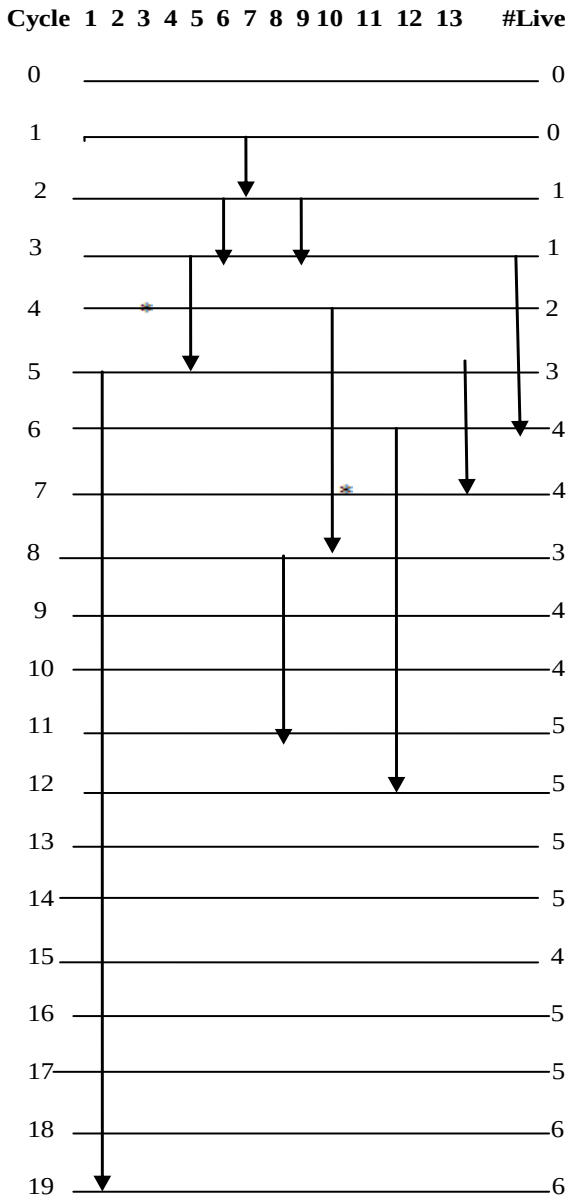

Figure 4. Lifetime analysis chart.

with register minimization) are synthesized using Spartan 3A/3AN device. Here the number of functional units such as adders and multipliers are reduced to 1 each, with 6 registers. In addition to these, the number of components namely slices, slice flip flop, look up tables (LTU) and input-output blocks (IOs), present in Spartan are reduced due to the reduction in functional units.

Conclusion

This paper addresses the challenges and opportunity of minimizing the filter architecture by the growing trend of VLSI DSP systems. It has been demonstrated that the

Cycle	i/p	R1	R2	R3	R4	R5	R6	o/p
0								
1	6							
2	5,8	6						6
3	4,13	5	8					5,8
4	3,9	13	4					3
5	1,12	9	13	4				4
6	11	1	9	13	12			13
7	10	11	1	9	12			10,12
8	7		11	1	9			9
9		7		11	1			
10			7		11	1		
11				7		11	1	7
12						1	11	11
13						1		
14						1		
15					1			
16						1		
17						1		
18					1			
19						1		1

Figure 5. The allocation table.

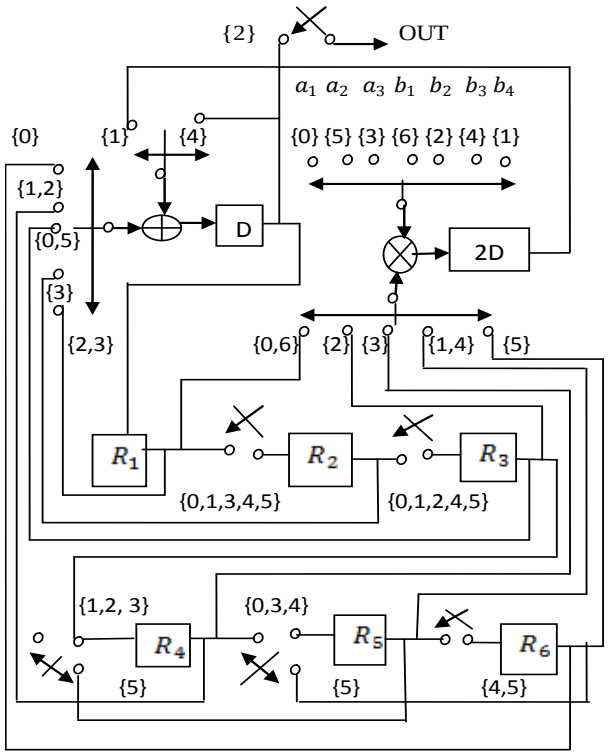

Figure 6. Folded architecture for Chebyshev I filter.

Table 3. Comparison between unfolded and folded filter.

Architecture	Adder	Multiplier	No. of register
Unfolded	6	7	3
Folded	1	1	6

Table 4. Comparison of unfolded and folded architecture.

Architecture	Unfolded	Folded
No. of Slices	112	9
No. of Slice flip flop	24	16
No. of 4 input LTUs	194	8
No. of IOs	76	68

Chebyshev I high pass filter architecture in terms of required number of functional unit such as adder and multiplier is substantially reduced from 6 adders to 1 and 7 multipliers to 1 by the folding and retiming with register minimization techniques. This context describes an effective and efficient heuristic and provides an optimized environment for digital filter. Our experimental results demonstrate that folding and retiming can significantly reduce the silicon area and therefore providing flexibility to the cost and effort of the designers.

Conflict of Interests

The author(s) have not declared any conflict of interests.

REFERENCES

Deepa Y, Vijaya K (2012). High Speed Digital Filter using register minimization retiming and Parallel Prefix Adders. IEEE 3rd International Conference on EAIT. pp. 449-453.
Edward AL (1991). Consistency in Data Flow Graph. IEEE Trans.

Parallel Distrib. Syst. 2:225-235.
Jackson LB, Keiser JF, Donald HS (2003). An approach to implementation of Digital Filters. IEEE Trans. Audio Electroacoust. 16(3):413-421. http://dx.doi.org/10.1109/TAU.1968.1162002
John GP Dimitris GM (1996). Digital Signal Processing Principles, Algorithms and Applications. Pearson Education (3rd ed.), Chapters 7 and 8.
Keshab KP (2012). VLSI Digital Signal Processing Design and Implementation. In Wiley Student (ed.), Chapters 4 and 5.
Keshab PK, Wang CY, Brown AP (1992). Synthesis of Control Circuits in Folded Pipelined Architecture. IEEE J. Solid State Circuit. 27(1):29-43. http://dx.doi.org/10.1109/4.109555
Leiserson C, Rose F, Saxe J (1986). Optimizing Synchronous Circuitry by Retiming. Third Caltech Conf. VLS I:87-116.
Monteiro DS, Ghosh A (1993). Retimimg Sequential Circuit for low power. In Proc. IEEE Int. Conf. Comput. Aided Design. pp. 398-402.
Parhi KK (1992). Synthesis of DSP data format converted using lifetime analysis and forward-backward register allocation. IEEE Trans. Circuit Systems-II. 39(7):423-440. http://dx.doi.org/10.1109/82.160168
Rajalakshmi K, Arumugam K, Priya MS (2013). Folded Architecture for Digital Gammatone Filter used in Speech Processor of Cochlear Implant. ETRI. J. 35(4).
Rajapadhy S, Kiaei S (1991). A folding transformation for VLSI IIR filter array design. Int. Conf. Acoust. Speed Sig. Process. 9:1237-1240.
Rakshi S, Premananda BS, Mahir NM (2010). Synthesis of DSP System using Data Flow Graph for silicon area reduction. IJCSIT. 1(5).337-341.
Salivahanan S, Vallavaraj A, Gnanapriya C (2010). Digital Signal Processing. (2nd ed.), Tata McGraw Hill.

academicJournals

Vol. 9(8), pp. 264-268, 30 April, 2014
DOI: 10.5897/SRE2013.5758
Article Numer: 6BB510844203
ISSN 1992-2248 © 2014

http://www.academicjournals.org/SRE

Scientific Research and Essays

Full Length Research Paper

Geometry optimization for heat sinks using thermography and finite element

I. J. Valencia Gómez[1], F. Hernández Hernández[1] , J. A. Duarte-Moller[2,3]*, O. Jiménez Sandoval[4], A. Marroquín de Jesús[1] and J. M. Olivares Ramírez[1]

[1]Universidad Tecnológica de San Juan del Río, Col. Vista Hermosa, Av. La Palma 125, San Juan del Río, Qro., C. P. 76800, México.
[2]Centro de investigación en Materiales Avanzados, S.C, Miguel de Cervantes 120 Complejo industrial Chihuahua, Chihuahua, Chihuahua 31109, México.
[3]Universidad Tecnológica de Querétaro. Av Pie de la Cuesta 2501. Col. Unidad Nacional Querètaro, Querétaro, 76148, México.
[4]Centro de Investigación y de Estudios Avanzados del Instituto Politécnico Nacional (Cinvestav), Unidad Querétaro, Apartado Postal 1-798, Querétaro, Qro.76001, México.

Received 28 November, 2013; Accepted 17 February, 2014

Cooling systems based on Peltier cells have great advantages to be energized by renewable energy sources. This paper describes the optimization of operation of a heat exchanger which was located in the side cool on Peltier Cell. For this work, we performed infrared shots of the experiment in order to establish and analyze the pattern of heat distribution. Infrared results as well as boundary conditions fueled our simulation model made in finite element. We analyzed the thermal and mechanical behavior of two commercial heat exchangers and presented a proposal for an improved geometry that optimizes by 50% the surface area of the heat exchanger.

Key words: Fins, Peltier and simulation.

INTRODUCTION

Nowadays the industry has many production processes that involve the thermal production of heat or steam through combustion of petroleum materials. These processes are not 100% efficient and therefore they have waste of heat or steam which are expelled to the environment. These wastes can be used for heat power in Peltier cells to obtain electric power. The use of wasted heat or steam in a useful project is considered as a contribution to the improvement of the environment as it helps to reduce problems related to global warming due to CO_2 effects. Another advantage is that avoiding the use of chlorofluorocarbon as a refrigerant has a serious impact on the reduction of the ozone layer (Darwish et al., 2008). The main advantage of cooling systems that use renewable energy is to delay of peaks oil.

The International Institute of Refrigeration estimated that approximately 10 to 20% of electricity production worldwide is consumed by cooling mechanisms and air

*Corresponding author. E-mail: alberto.duarte@cimav.edu.mx

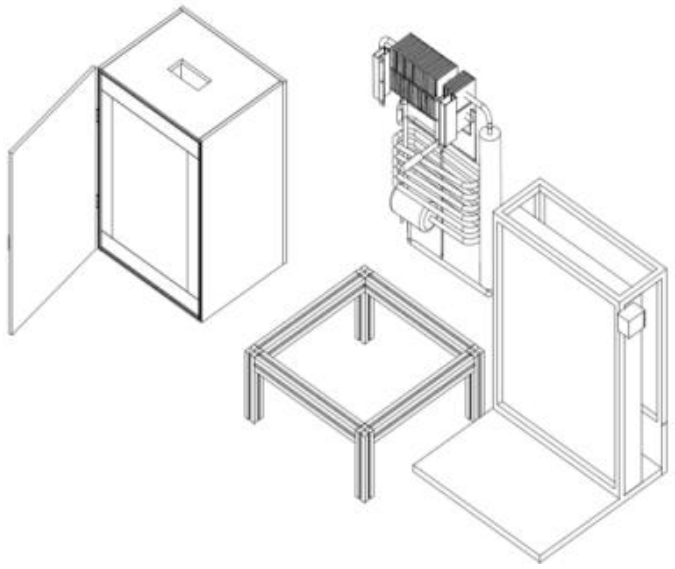

Figure 1. Control Volume refrigeration.

conditioning (Lucas, 1998; Helm et al., 2009; Erickson et al., 2004). Besides Kyoto Protocol nations urgently requested mitigate the negative impact of global warming (Chazournes, 1998).

Research has been conducted to optimize heat removal systems. Casano and Piva, (2011) reported the performance of thermoelectric modules used for electric power generation with sink plane. This device obtained 1.5 W at 60°C. Chen et al. (2012) performed experiments on heat transfer Peltier cells, and the results show the effects of flow pattern of heat sink and water flow rate on the performance to heat source; for the heat side the temperature plays an important role. Peltier cells have also been used to remove heat from photovoltaic cells obtained until 28% of reduction in the gradient of temperature at 77°C (Ari and Kribus, 2010).

Cosnier et al. (2008) conducted a numerical experimental heating and cooling air used in testing aluminum fins (3 groups of 101 channels) for heat dissipation. Obtained COP was up to 1.5 in the high temperature region 2 and the low temperature region with delta maximum temperature between a range of 5 to 10°C. Perez–Aparicio et al. (2012) examined the behavior of a Peltier mono-cell when acting as a cooler, using finite element simulation. The system is developed in three dimensions with nonlinear formulation using the quadratic dependence on temperature and material properties. Karamangil et al. (2010) conducted the study using a computer program, developing the simulation of the behavior of absorption refrigeration system of a stage. The developed software package includes: Selection of solution (H_2O-LiBr, NH_3-H_2O, NH_3-$LiNO_3$ or acetone-$ZnBr_2$), operating condition, where simulation results show the thermodynamic properties of solutions at each state point of cycle. Mazloumi et al. (2008) simulated a system of single-effect absorption, which is powered by a horizontally parabolic concentrator with an area of 57.6 m^2, and could provide 17.5 kW of cooling energy. This study aims to evaluate the heat transfer of aluminum sinks with commercial geometry (peaks and plain channels) attached to a Peltier cell a volume of air, in order to optimize their performance by design tools and finite element starting from the thermography acquisition, variations in temperature and speed to obtain 4°C within the control volume.

EXPERIMENTAL DETAILS

In the first stage we built a thermally isolated system (Figure 1) using polystyrene plates two inches thick; the dimensions of the internal volume being 0.42 m × 0.32 m × 0.26 m. This volume was internally coated stainless steel sheet caliber 22. At the top was placed a Peltier cell 48 W, which joined commercial heat exchangers (with fins plane and fins peaks) with heat sink grease SILICONE TEK ®.The fins of the heat sinks are exposed to natural convective flow, dimensions are shown in Figure 2. Heat triggers both fins plane and peaks were measured in an optical comparator Mitutoyo PJ3000 model. The size of their surface area was adjusted to a similar value of 0.066 m^2 as the new geometry (in this case, circular fins must have 0.033 m^2 in surface area).

Having equal surface area on all heat triggers (fins plane and fins peak) dismisses the possibility of better thermal performance, however with different surface areas or thicknesses in the volume of contact with Peltier, the cooling systems can have better thermal performance.

The bottom of the control volume has a removable area of 0.06 m × 0.06 m where an infrared camera was placed (Infrared 80T-IR probe temperature, 18 to 260°C, 3% error FLUKE trademark) with which thermographs were taken for 30 min at 1 min intervals. The second stage of the thermographic feed ANSYS'® thermal and fluid mechanical parts. The third step is the comparison of the simulation with experimental data allowing the design of new geometries, which will also be characterized thermographically.

RESULTS AND DISCUSSION

During the experiment, for both triggers the room temperature remained constant at 29°C to the shade. Both triggers were in contact with the Peltier cell which consistently reported a voltage of 11.5 V and 3 A, such that both experiments has an electric power of 34.5 W, however the cooling rates are different, where after 1 h of operation the temperature remains constant, existing temperature differential (DT) to sink plane and peaks were 12.4 and 10.2°C respectively. Relating the DT with heat output (Qc) in the graphs of Peltier cell manufacturer with data sheet (AA-100-24-22-00-00), different values of coefficients of Operation (COP) obtained for the plane fin heat sink is 0.32 and 0.41 for peak and therefore different values of power in the evaporator to the plane as well as 11.04 W to 14.26 W peak. This experiment corroborated

the hypothesis that even if numerical values have similar surface, the geometry of these impact the performance of the heat removal.

For the ANSYS simulation of the peaks trigger, geometry

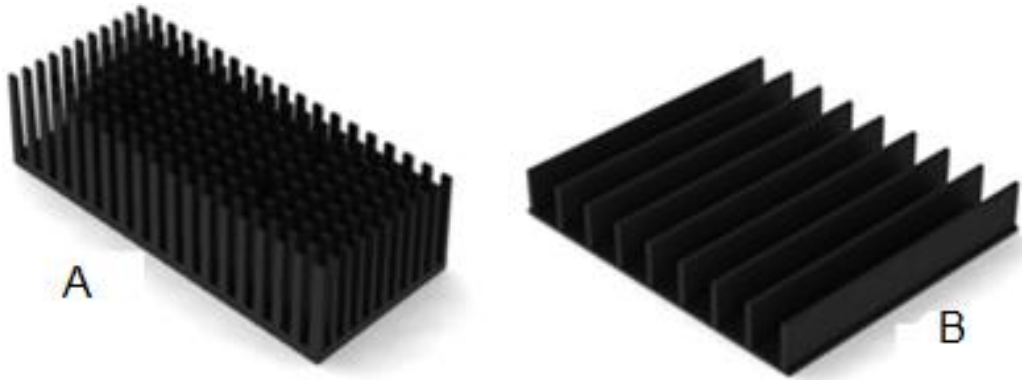

Figure 2. Details in mm. to Peak 1, Plain 2 and circular 3 fins.

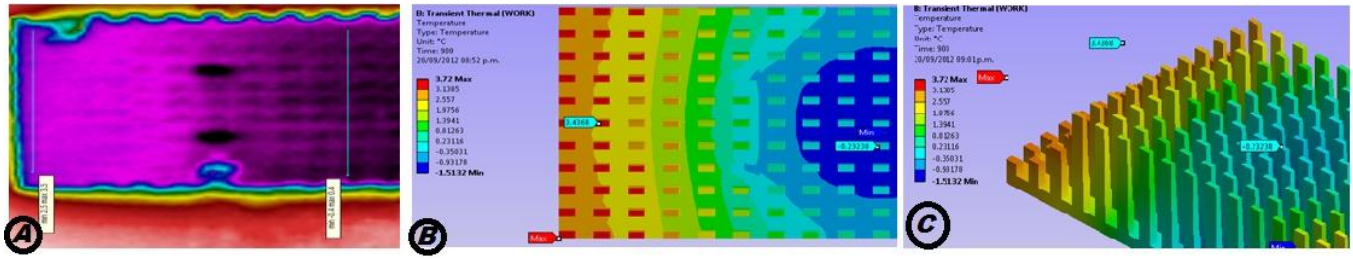

Figure 3. Thermography 1A, thermal map in ANSYS 1B and optimized trigger 1C.

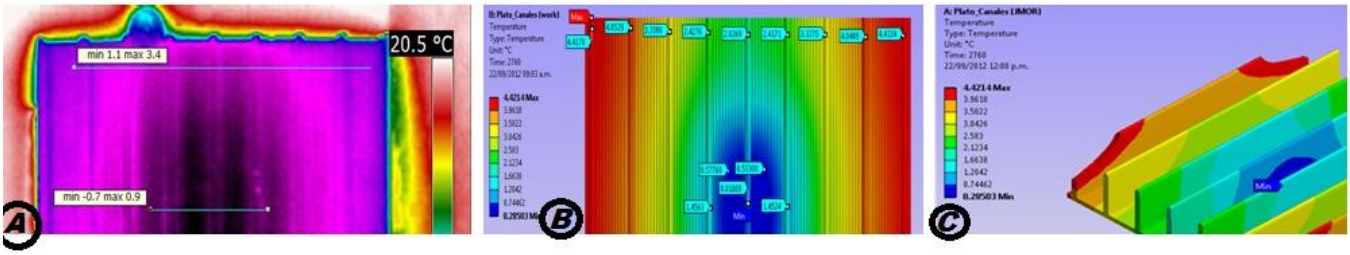

Figure 4. Thermography 2A, thermal map in ANSYS 2B and optimized trigger 2C.

was built in Design Modeler; thereafter we made a mechanical meshing at the tips. The model used was: transient thermal analysis for 3600 s, -14.26 W in the flow of heat of 10 W/m^2°C convection coefficients for surface and 13 W/m^2°C for vertical surfaces. The results of the simulation model are presented in Figure 3, where it can be seen that in the thermal extremes, the average temperature was 3.0°C and in the simulation was 3.503°C to the center of the trigger. Thermographically, the average temperature is 0.4°C and in the simulation was -0.232°C. In both cases, there is a variation of up to ±0.5°C; thus there is a lack of uniformity in the temperature distribution. Once validated the model in the simulator can make the cuts necessary to optimize the fin sink (Figure 3, part C). For the fins plane trigger (Figure 4), similar boundary conditions were taken in the simulator. The result for the thermographic evaluation at both ends revealed that the average temperature was 2.25°C and in the simulator was 3.32°C; in the center trigger, temperatures vary between 0.1 and 0.9°C for thermographic and simulator respectively. With the same boundary conditions, these are now built into the simulator 20 models by comparing their temperature profiles. The best performance is showing appointed round sink, which was constructed of aluminum same as fins peak and plane, but with half the surface area. The results show (Figure 5) to fin sink as circular thermographically, the average temperature at the ends

of 3.75°C and at the center of 2.75°C and with the simulator for the ends was 3.26°C and in central 2°C.

Figure 6 shows the performance of the three heat triggers, the experimental time was 60 min to be related

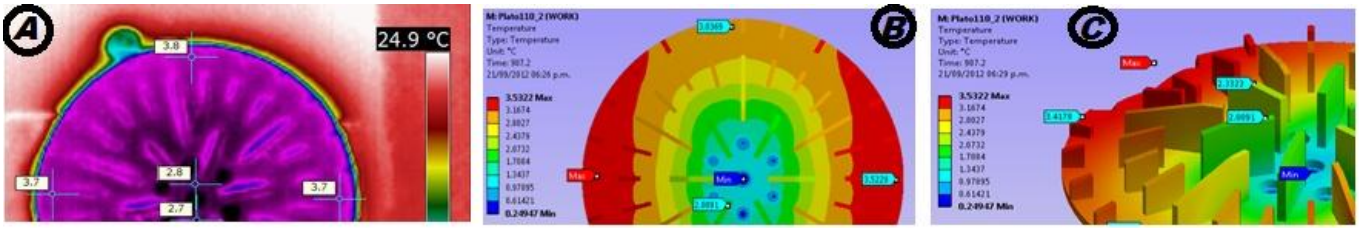

Figure 5. Thermography 3A, thermal map in ANSYS 3B and optimized trigger 3C.

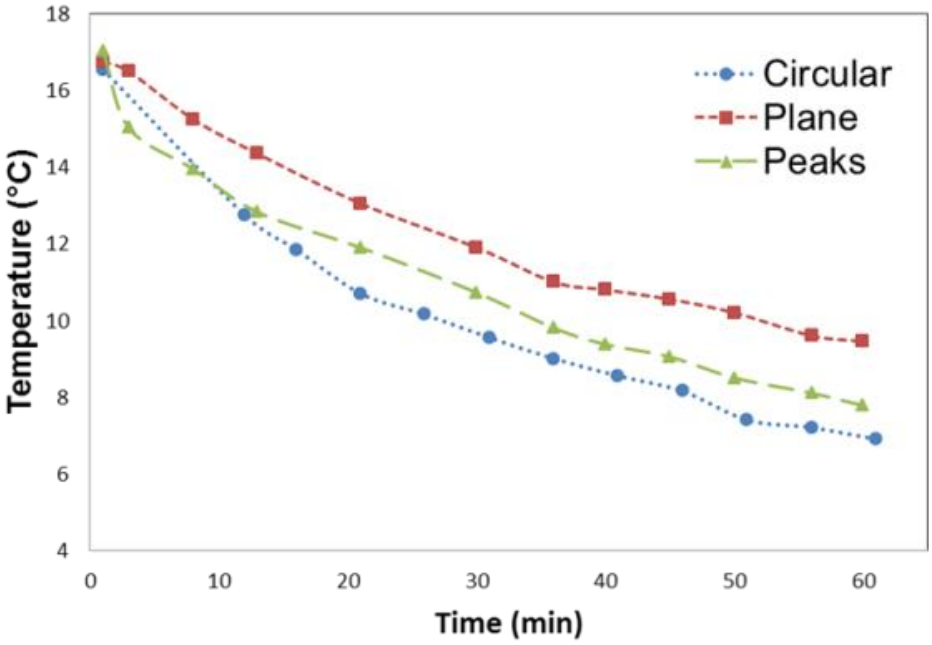

Figure 6. Heat sinks performance.

to the boundary conditions established for the ANSYS simulation, resulting that when fins are circular, the thermal performance is better. Finally, in the absorption system the circular trigger fins were inserted; the performance is shown in Figure 7, where after two hours of work, the temperature reaches 4°C. Four sensors were placed: one for ambient temperature (T4), on top (T2) and in contact with the circular heat trigger, and another half volume (T1) and one at the bottom (T3).

Conclusions

The analytical methodology used to obtain an optimized heat trigger, was satisfactory, as with half of the total area on circular heat trigger attached to the evaporator resulted in a heat transfer similar to that of commercial triggers fins plane and peaks.

The temperature difference between the center and the ends is 3, 2.65 and 1°C, for peak, plane and circular, respectively. These temperature differences are those that allow developing better or worse thermal performance.

When we are able to use geometries in which the temperature distribution is uniform, the surfaces have better thermal performance.

The programs can be used to simulate the behavior of systems, saving time, financial resources, and otherwise for this research would have required the machining of 19 heat sinks with their respective experimentation.

Conflict of Interests

The author(s) have not declared any conflict of interests.

ACKNOWLEDGEMENTS

This paper was developed with the project FOMIX of CONACYT; “Desarrollo de capacidades, tecnologías e innovación para el aprovechamiento de energías renovables en el sector agroindustrial del Estado de Querétaro”.

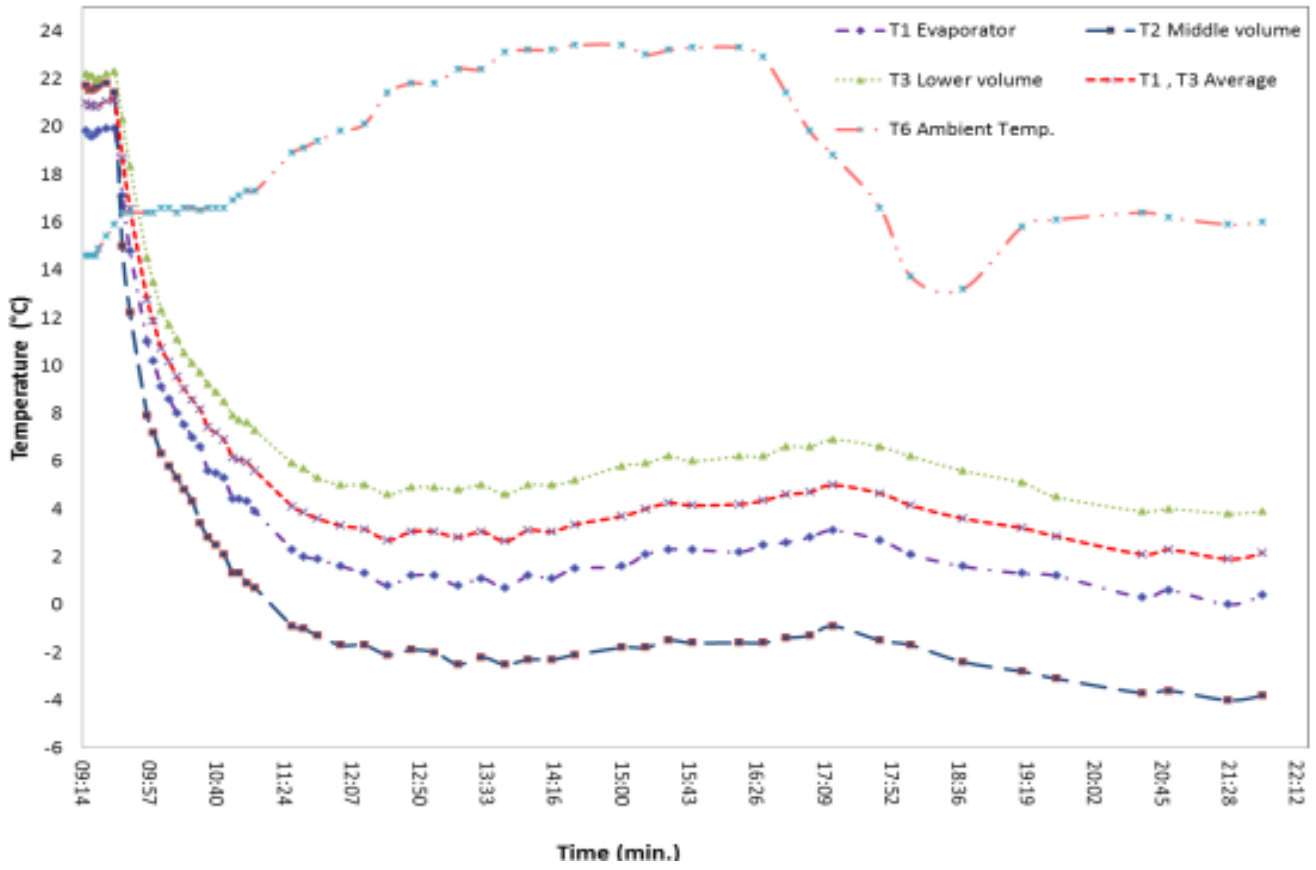

Figure 7. Heat sink circular thermal performance.

REFERENCES

Ari N, Kribus A (2010). Impact of the Peltier effect on concentrating photovoltaic cells. Solar Energy Mater. Solar Cells, 94(12):2446-2450. http://dx.doi.org/10.1016/j.solmat.2010.08.015

Casano G, Piva S (2011). Experimental investigation of the performance of a thermoelectric generator based on Peltier cells. Exp. Therm. Fluid Sci. 35(4):660-669. http://dx.doi.org/10.1016/j.expthermflusci.2010.12.016

Chazournes LB (1998). Kyoto Protocol to the United Nations Framework Convention on Climate Change. UN's Audiovisual Library of International Law http://untreaty. (http://legal.un.org/avl/ha/kpccc/kpccc.html)

Chen WH, Liao CY, Hung CI, Huang WL (2012). Experimental study on thermoelectric modules for power generation at various operating conditions. Energy 45(1):874-881. http://dx.doi.org/10.1016/j.energy.2012.06.076

Cosnier M, Fraisse G, Luo L (2008). An experimental and numerical study of a thermoelectric air-cooling and air-heating system. Int. J. Refrig. 31(6):1051-1062. http://dx.doi.org/10.1016/j.ijrefrig.2007.12.009

Darwish NA, Al-Hashimi SH, Al-Mansoori AS (2008). Performance analysis and evaluation of a commercial absorption–refrigeration water–ammonia (ARWA) system. Int. J. Refrig. 31(7):1214-1223. http://dx.doi.org/10.1016/j.ijrefrig.2008.02.005

Erickson DC, Anand G, Kyung I (2004). SYMPOSIUM PAPERS-AN-04-07 Absorption/Sorption Heat Pumps and Refrigeration Systems-Heat-Activated Dual-Function Absorption Cycle. ASHRAE Trans. Am.Soc. Heat. Refrig. Air cond. Eng. 110(1):515-524.

Helm M, Keil C, Hiebler S, Mehling H, Schweigler C (2009). Solar heating and cooling system with absorption chiller and low temperature latent heat storage: Energetic performance and operational experience. Int. J. Refrig. 32(4):596-606. http://dx.doi.org/10.1016/j.ijrefrig.2009.02.010

Karamangil MI, Coskun S, Kaynakli O, Yamankaradeniz N (2010). A simulation study of performance evaluation of single-stage absorption refrigeration system using conventional working fluids and alternatives. Renew. Sustain. Energy Rev. 14(7):1969-1978. http://dx.doi.org/10.1016/j.rser.2010.04.008

Lucas L (1998). IIR news. Int. J. Refrige. 21(2):87-95. http://dx.doi.org/10.1016/S0140-7007(98)90000-7

Mazloumi M, Naghashzadegan M, Javaherdeh K (2008). Simulation of solar lithium bromide–water absorption cooling system with parabolic trough collector. Energy Convers. Manage. 49(10):2820-2832. http://dx.doi.org/10.1016/j.enconman.2008.03.014

Perez–Aparicio JL, Palma R, Taylor RL (2012). Finite element analysis and material sensitivity of Peltier thermoelectric cells coolers. Int. J. Heat Mass Transf. 55(4):1363-1374. http://dx.doi.org/10.1016/j.ijheatmasstransfer.2011.08.031

academicJournals

Vol. 9(8), pp. 269-279, 30 April, 2014
DOI: 10.5897/SRE2014.5825
Article Number: BC843CE44207
ISSN 1992-2248 © 2014

http://www.academicjournals.org/SRE

Scientific Research and Essays

Full Length Research Paper

4F_C: A conceptual framework for understanding architectural works

Saleem M. Dahabreh

Department of Architecture, Faculty of Engineering and Technology, University of Jordan, Amman 11942, Jordan.

Received 29 January, 2014; Accepted 10 March, 2014

This paper presents a conceptual framework for understanding an architectural building by qualitatively discerning the complex issues involved in building design and systematically integrating them into a theoretical construct. The premise behind this framework is that, in design, a better understanding of what to design leads to a more informed understanding of how to design, resulting in a more structured and innovative architectural work. Using a grounded theory method, this paper postulates an ontological framework that recasts the Vitruvian triad of *utilitas, venustas*, and *firmitas* into spatial, intellectual, and structural form, respectively. More importantly, it expands this triad to include architectural thinking manifested as a formative concept as an integral component of any architectural work, and situates a design in its related context. Thus, this paper aims to close a gap in many architectural frameworks. The framework provided here offers a level of robust understanding of architecture that can become a foundation for a more effective and rational architectural design practice. This foundation can be used as a basis for structuring architectural forms, as well as describing and analyzing existing works of architecture. Its value exceeds theory framing and extends toward architectural pedagogy as a theoretical framework in teaching design studio.

Key words: Conceptual framework, architectural form, intellectual form.

INTRODUCTION

As a social phenomenon characterized by complexity and linked to multiple bodies of knowledge, architecture belongs to diverse disciplines. Architectural design in particular typifies a multidisciplinary design domain since architecture, engineering, and construction, each dealing with a particular feature of building design and each with its own concepts and interpretations, come together as one (Roseman and Gero, 1997). Furthermore, architectural design is an integrative and interdisciplinary process that calls for a deep understanding of 'what' to design in order to better inform 'how' to design, therefore involving complex requirements of material and immaterial knowledge (Friedman, 1992, 2003). A better understanding of such phenomena requires a multidisciplinary approach that distills concepts across domains and organizes them into a coherent structure, creating what is known as a conceptual framework (Jabareen, 2009). Developing a conceptual framework elucidates the basic concepts of a certain domain and helps to develop a common language within that domain,

E-mail: saleem.dahabreh@ju.edu.jo. Tel: +96265669224. Fax: +96265669224.

Table 1. Variations of the Vitruvian triad.

Vitruvius	Wotton	Gropius (Modern functionalism)	Norbert-Schulz	Steele
Utilitas	Commodity	Function	Building Task	Task Instrumentality, Shelter and security Social contacts
Venustas	Delight	Expression	Form	Symbolic identification Pleasure
Firmitas	Firmness	Technics	Technics	Growth

providing the uniformity necessary to a better understanding of the phenomena (Shields and Rangarajan, 2013).

This paper postulates such a conceptual framework for understanding 'what' a work of architecture is through the development of a meta-level integration of various conceptions of architectural form. This framework facilitates an understanding of architectural form by expounding its underlying constituents and integrating them into a coherent whole, thus, allowing for a more structured description, interpretation, and generation of proposed works for study, and, consequently, a more structured discourse of architectural design.

Many researchers and theoretician have attempted to formulate a definition of architecture through a determination of its ruling principles (Gharibpour, 2012). However, most of these attempts can be traced back to one of the oldest and most enduring sets of architectural principles, proposed by Vitruviusin his treatise *De Architectura* in the first century BC: *venustas* (beauty), *firmitas* (firmness), and *utilitas* (commodity) (Stein and Spreckelmeyer, 1999). Associated with aesthetics, structure and technology, and function, these three concepts have played an important role in the history of architecture. Different theoreticians have used the same triad with different cultural and historical gradations (Lang, 1987). Among these are Wotton (1624, 1897), Gropius (1947), Norberg-Schulz (1965), and Steele (1973), among others, as summarized in Table 1.

Researchers tend to emphasize one or more of these aspects and use them as a base for understanding architecture. Semper (1851, 2011), for example, emphasized the technical aspects of architecture, explaining its origins and history with four distinctive elements and stages: hearth, roof, enclosure, and mound. Frankl (1973) analyzed architectural styles based on spatial composition, treatment of mass and surface, treatment of optical effects such as light and color, and the relation of design to social function. Researchers in other fields, such as artificial intelligence and design computing, have also proposed schemas to characterize design artifacts. Stiny and Gips (1978), for example, presented anaesthetic algorithm machine for the analysis and generation of designs in art and architecture. Stiny and March (1981) created algorithmic design machines to model the design process. Gero (1990) presented a function-behavior-structure (FBS) framework to describe the three variables of a designed object. Tzonis (1992), similarly, developed the POM system, emphasizing performance, operation, and morphology as representative of the precedents, principles, and rules of architecture. Extending the design machine of Stiny and March (1981), Economou and Riether (2008) also presented a 'Vitruvian machine,' which maps Vitruvius's triad of *venustas*, *firmitas*, and *utilitas* into a formal structure. Dahabreh (2014) presented the AD_M machine emphasizing design desiderata, formal design languages, design thinking, technology, and context as a framework for structuring architectural design knowledge.

However, most of these models do not account for the crucial components of an architectural work and thus cannot be used as a conceptual framework for architecture. First, as a building symbolic performance is inseparable from time and place (Piotrowski, 2001), the relation of the work to its context and the dynamic role of the context in shaping the building's architectural form and design process are of extreme importance. Accordingly, the context becomes an integral component for understanding what a particular work of architectural design is and must be incorporated within any conceptual framework for architecture. More importantly, architectural design is a reflexive process-in other words, it involves critical reflection on the part of all the constituents of a design situation. Through an internalized design process, designers add to a design situation according to their concepts and reflections (Peponis, 2005), framing it within a context that goes beyond beauty, firmness, and commodity and eventually affecting the final form of a work. Accordingly, design reframing is accomplished through conceptual thinking. This not only affects the structure of the design constituents but also becomes embedded within the form of a work itself, making it imperative to introduce design concepts as part of an answer to what an architectural work is.

Through a qualitative description of a work of

architecture, this paper aims to develop an architectural framework that clarifies the basic concepts involved in any work of architecture and incorporates the context and these design concepts. By no means is this framework intended to be a fully detailed account of what architecture is; rather it lays out the key concepts and constructs and posits some relationships among them. These concepts are the building blocks with which designers reason about architectural form; thus, they govern design intelligence. The framework structures existing academic debates about architecture in terms of a basic taxonomy of concepts and propositions and accordingly allows for sensible debate to take place.

MATERIALS AND METHODS

Jabareen (2009, p. 51) defined a conceptual framework as "a network, or 'a plane,' of interlinked concepts that together provide a comprehensive understanding of a phenomenon or phenomena. "The aim of a conceptual framework is to provide an organizing scheme for a phenomenon through the organized structuring of concepts that constitute that phenomenon (Shields and Rangarajan, 2013). The constituent concepts that articulate the respective phenomena support one another and establish a framework-specific philosophy. Conceptual frameworks are based on ontological aspects (that is, what they are), epistemological aspects (that is, how they are), and methodological aspects (that is, how assumptions about them are formed) (Guba and Lincoln, 1994). Of interest here is the ontological aspect of a conceptual framework. In the field of design computing, ontologies are structured conceptualizations of a domain that are defined in terms of the entities in that domain and their relationships (Gero and Kannengiesser, 2007). They present a knowledge set about a subject, and describe the basic objects, classes, properties, and characteristics and the relations between them (Aksamija, 2009).

One of the strongest features of conceptual frameworks is that they assimilate knowledge from several disciplines and integrate them into a theoretical construct (Jabareen, 2009). As such, they are an excellent mechanism for understanding multidisciplinary domains such as architectural design-where art, theory, engineering, and construction, among other disciplines, come together. As conceptual frameworks are formed through qualitative analysis, they do not provide knowledge of hard facts but offer soft interpretations of intentions or concepts (Levering, 2002). They aim neither at providing explanations nor at predicting outcomes that address questions of how and why. Rather, they provide an understanding of what constitutes a certain phenomenon.

Jabareen (2009) proposed building conceptual frameworks from multidisciplinary literature through conceptual framework analysis. A conceptual framework analysis is composed of: 1) identifying and mapping selected data sources; 2) identifying and naming the main concepts within the identified literature or source of data; 3) deconstructing and categorizing the concepts in order to identify the concepts' main attributes, characteristics, assumptions, and roles; and 4) consequently organizing and categorizing the concepts according to their features. The result is an integration of concepts into constructs or mega concepts and the synthesis of these into a conceptual framework. This paper follows the same methodology in constructing the proposed conceptual framework for architecture.

Understanding architecture: Identifying concepts

According to Ulrich (1988), the ability to reason about an artifact depends upon the ability to abstractly categorize that artifact and provide a minimal description of its salient structural aspects. For Tzonis (1992), any intelligent design system should describe the most significant aspects of how artifacts work, how they are made, what they do in respect to what is expected, how they fit into the surrounding environment, and how all these aspects are interrelated. Describing architectural works, however, is not an easy task; buildings can be described according to the context in which they operate, according to their features and properties as designed artifacts, and/or according to the functions they need to perform. Hillier et al. (1984) defined buildings as cultural artifacts that can be regarded as material constructions, spatial arrangements, and objects in a particular style. The fundamental function of spatial organization, labeled by the German theorist, Frankl (1973) as spatial form, is to accommodate human activities that respond to the needs and values of different individuals, groups, and institutions. According to Hendrix (2012), the modern connotation of the word function with respect to buildings is related to the building's use or utility for housing human activities. By designating a projected building to house a certain institution, an architect gives the building a label (e.g. hospital), which defines its functional type. According to Markus (1987), for any building to function effectively (that is, accommodate the functions required by an institution occupying the space of the building), the building must organize people, objects, and activities into meaningful relationships within a space. This spatial form represents what a building does. Thus, it can be inferred that the primary function of a building is the organization of space through the building's formal configuration.

As projected buildings do not exist in reality, building programs are the means through which building sponsors or owners describe and/or prescribe their future buildings to designers and communicate them to users and other stakeholders in the projected building. According to Capille and Psarra (2013), the program is both a trans-spatial and a spatial manifestation: *"The transpatial aspect defines purposes, activities and roles for different groups of people. In this sense, the program can be understood as a social script. The spatial dimensions of program refer to the ways in which this social script is embedded in space through a pattern of distribution, affordances and labeling "*(p. 18). The division of the space inside a building is not adhoc; many buildings have explicit rules about how people, objects, and activities are disposed in space so that the spatial embodiment of these dispositions represents the particular practices or knowledge in a certain field. This insures proper functioning of the institution or building (Markus, 1987). These rules impose restrictions on the location (e.g. adjacencies and proximity, zoning of different functions, accessibility, and movement between spaces). Accordingly, housing functions inside the building are arranged into zones and spatial relations are organized according to the rules that govern the functioning of the institution. A building's operation and performance are also associated with a building's function. Building operations refer to how the form of a building controls, maintains, or channels people, objects, and equipment associated with activities (Tzonis, 1992). According to Zarzar (2003), a building's performance is determined by the functions that the building was intended to carry out.

The material construction (that is, the structural form) shapes the space and signifies how to construct the physicality of the building. The material construction of the building involves engineering and construction aspects (Rosenman and Gero, 1997): structural engineering addresses concepts of stability and support of the building and accordingly is concerned with various structural systems, materials, and technology. Mechanical and electrical engineering are concerned with the operation of a building. They intersect with the functionality of the building in terms of serviceability and the provision of suitable conditions for functioning. Accordingly, mechanical and electrical engineering are concerned with electromechanical systems. The materialization of

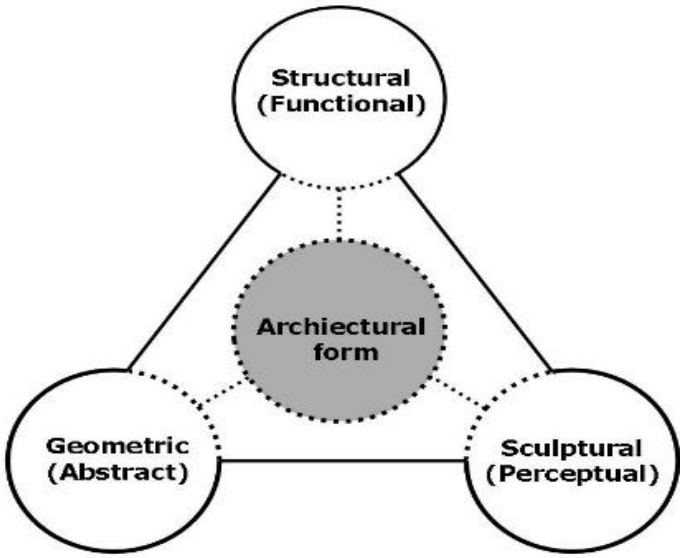

Figure 1. The components of architectural form as proposed by Vitruvius.

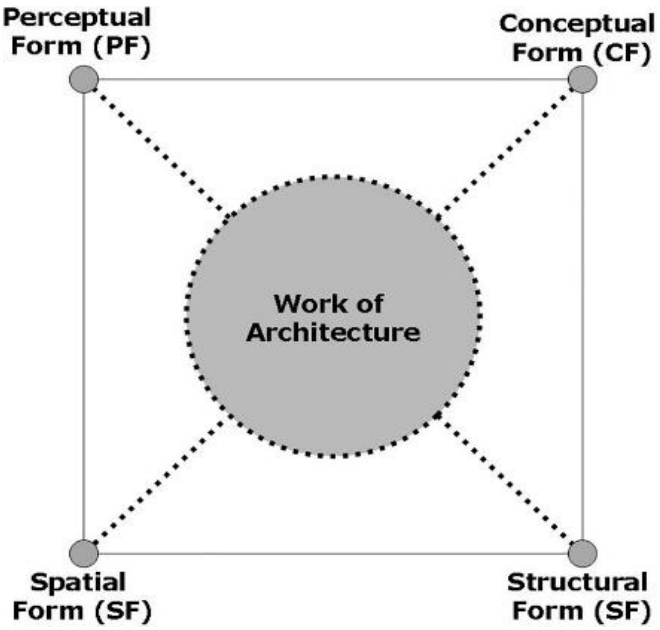

Figure 2. Four types of form defining a work of architecture.

architectural work into built form is the responsibility of contractors and involves the process of transforming raw materials by means of engineering knowledge and technical know-how. Contractors are concerned with constructability, the relationships between physical elements, and the operations and sequence of operations required to construct the building. In other words, contractors concern themselves with concepts such as availability, composition, stability, time, place, and so on.

Material construction also has visual qualities that depend on the materials used, the color, and the surface texture, as well as aspects of construction and detailing that characterize space such as moldings, grooves, changes in materials, and so on. These elements add cultural significance and aesthetic appeal. Through material construction, buildings organize and structure space and transmit social meaning through their physical form. This point confirms with what Hiller's (2007) statement that:

"A building then becomes socially significant . . . in two ways: first, by elaborating spaces into socially workable patterns to generate and constrain some socially sanctioned-and therefore normative-pattern of encounter and avoidance; and second, by elaborating physical forms and surfaces into patterns through which culturally and aesthetically sanctioned identities are expressed." (p. 24)

Material constructions have formal attributes such as design elements, architectural vocabulary, design principles, and so on that not only are material in nature but also have a cognitive, conceptual, and affective dimension (Peponis, 2005). In that sense, material constructions have abstract and architectonic aspects, usually expressed geometrically (Unwin, 2003), that signify how to logically and formally structure the materiality of the building. In this sense, architecture can be regarded as an intellectual activity consisting of underlying conceptual systems (Unwin, 2008) that structure the building elements and organize the material construction. These generate the formal properties of the building and accordingly subdivide the space of the building into a spatial pattern. The distinction between the abstract and the material was made 500 years ago by Alberti in the 15th century in his *Ten Books on Architecture*. He distinguished between a building's geometry and material construction where the function of geometry (lineaments in Alberti's terms) is to *"prescribe, and appropriately place, exact numbers, a proper scale, and a graceful order for whole buildings and each of the constituent parts"* (as cited in Dahabreh, 2006, p. 179).

Consequently, the form of the material construction can be read as a structural form of utilitarian nature that supports the building's or structure's space, a perceptual form related to the articulation of surfaces and pertaining to sensory perception and experience, and a conceptual or logical form that orders the elements and regulates the material form. These three kinds of forms are related to the material structure described by Vitruvius's model of the structural, sculptural, and geometric, as identified by Agudin (1995) (Figure 1).

The spatial form of an architectural building and its structural, perceptual, and conceptual forms are interrelated and cannot be separated. Each affects and conditions the other, and all exist simultaneously in every work of architecture. Together they constitute architectural form (Figure 2). It should be noted that the categorical distinction between spatial and physical form, or between the two aspects of physical form (that is, structural and intellectual), is not intended to capture two or more kinds of organization. Rather this distinction recognizes the different aspects of a building that become important depending upon the kinds of questions one asks (Bafna, 2012).

Hendrix (2012) distinguished between two functions of form in architecture: a communicative function, which involves expression and representation as fulfilled by perceptual and conceptual forms, and an instrumental function, which is expressed in terms of utility and technology through spatial and structural forms, respectively. Accordingly, the constituent forms of architecture can be regrouped into three forms: spatial, which is related to utility; intellectual, which combines conceptual and perceptual forms and relates to the agency of the intellect; and structural, which relates to technology and construction (Figure 3).

These three forms are synthesized through the design process, which can be defined as an intentional process that begins with a conceptual description of a situation requiring action and develops toward a concrete, syntactic description of an artifact as a response to that situation (Meyer and Fenves, 1992). This process involves critical reflection upon the situation, framing it in a way that goes

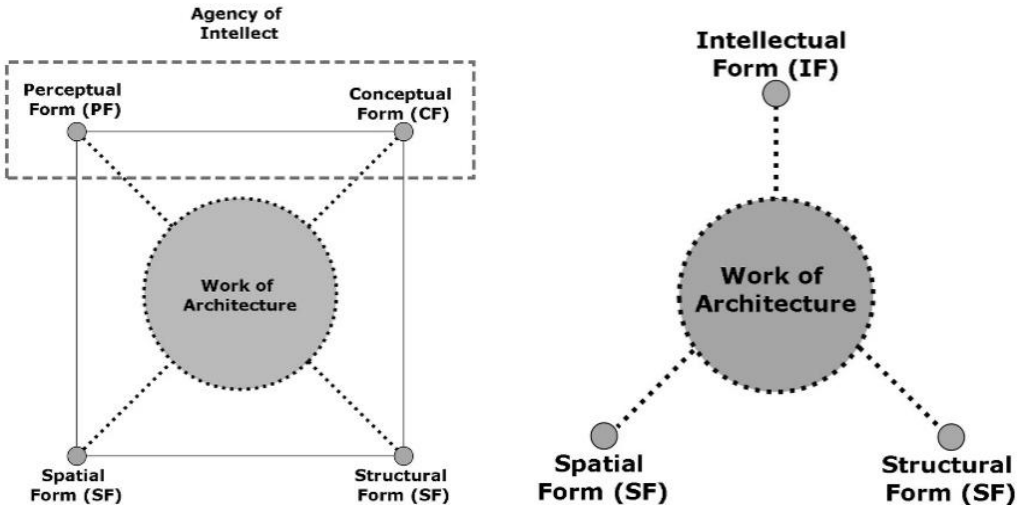

Figure 3. Architectural work understood as spatial, intellectual, and structural forms.

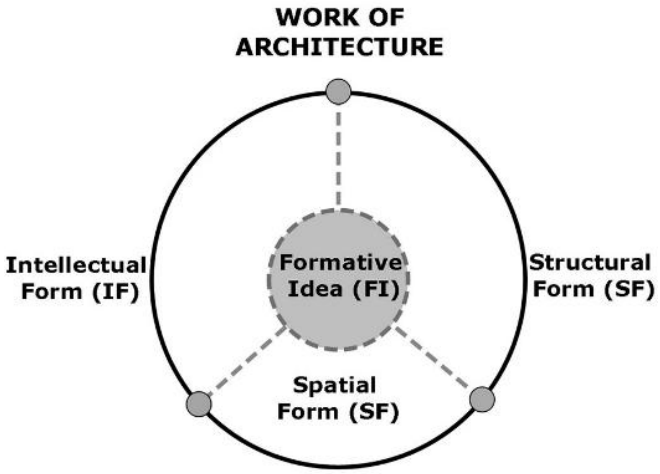

Figure 4. Intellectual form as the integrator of architectural work.

beyond the immediate conditions and leads to new understanding (Dahabreh and Ghanimeh, 2012). This new understanding necessitates the reformulation of several design constituents (e.g., structural form, instrumental form, and spatial form) in an innovative manner to address the conditions of the new situation. Moreover, the synthesized architectural form becomes an object in its own right requiring investigation and examination.

This process of reformulation involves the exploration of aesthetic aims through the manipulation of form and evaluation of the proposal against the design desiderata (Peponis, 2005). This type of thinking is known in architectural design literature as the design concept. It refers to *"how the various aspects of the requirements of a building can be brought together in a specific thought that directly influences the design and its configuration"* (McGinty, 1979, p. 215). As such, design concepts are formative ideas that designers use to influence or give form to design (Clark and Pause, 1996). Formative ideas include additional aims or inflections of aims brought about by designers in the course of design, as well as the aims of design as intrinsic to the designed object; therefore they cannot be initiated before the design process begins (Peponis and Wineman, 2002). According to Schumacher (2011), this type of theoretical reformulation and innovation differentiates architecture from mere building. This theoretical intent manifests itself in the choices made in the design process and is embedded in the final form of the building. Essentially, one can detect in the form of the building the conceptual input. Consequently, an architectural building has an abstract and conceptual aspect (that is, a formative idea) that integrates the spatial, structural, and intellectual forms into a unified whole, providing a logical order that governs and organizes the material construction and expressing how a designer reasons about the design situation and what he or she has added. Thus, the diagram of architectural form in Figure 3 can be recast to integrate the formative idea as the heart of any architectural work (Figure 4).

Kolodner (1993) defined a case as "a contextualized piece of knowledge representing an experience that teaches a lesson fundamental to achieving the goals of the reasoner" (p. 13). In light of Kolodner's statement that reasoning about any case cannot be separated from context (that is, the situation under which the case evolved and took place), the final constituent of the conceptual framework is the context under which architectural work was conceived and in which it exists. The inclusion of context as part of the understanding of a work of architecture stems from the fact that humans exist in a natural physical environment and operate in a socio-cultural one that prescribes their values and goals. Both of these environments establish human needs, whether perceived or real, physical or nonphysical. When the surrounding conditions do not meet the needs of humans, designers "devise courses of action aimed at changing existing situations into preferred ones" (Simon, 1998. p. 112), accordingly, creating new artifacts that belong to a techno-physical environment (Rosenman and Gero, 1998). Thus, the satisfaction of human needs belonging to one or more of the contextual environments becomes the motivation behind the initiation of the architectural design process. These motivations become the goals the work is designed to accomplish. They define the requirements that state what properties-functional or constructional-an artifact should have from the perspective of the goals of the stakeholders (Greefhorst and Poper, 2011).

Additionally, context plays a proscriptive role in architectural design. By being constrictive in terms of its physical or techno-physical nature (e.g., topography and climate) or controlling by setting rules and regulations for design (e.g., building codes and

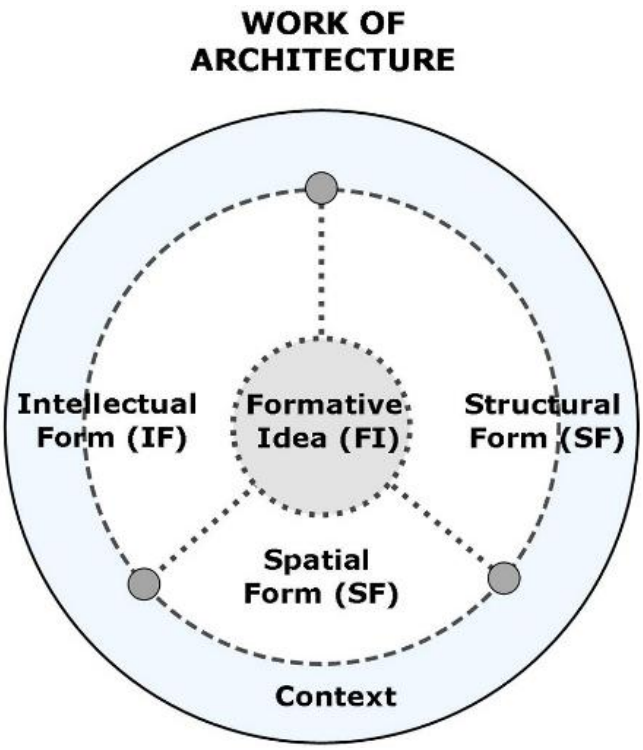

Figure 5. Architectural work as an integration of the five concepts.

Figure 6. The Smith house.

zoning), context constrains the design, specifying what should not or cannot be done. Finally, building operation and performance are conditioned by the circumstances of the surrounding context. As such, understanding what a work of architecture is cannot be complete without understanding the conditions under which conception, formation, and materialization take place. The final conceptual framework is presented in Figure 5.

According to the conceptual framework presented in this paper, an architectural building can be understood as a material construction molded though a formative idea, structured by intellectual requirements, that regulates functional requirements and mathematical and physical necessities (technology and construction)-all within the constraints of a context. In order to elaborate on the practical application of this framework, a case study is described and analyzed using the main components of the framework.

Case study: Smith house

The Smith House (1965, 1967) was built as a vacation house for Fredrick and Carole Smith and their two children. Overlooking the Long Island South, the house stands as a white, painted, stand-alone rectilinear block on one-and-a-half acres along the rocky coastline of Darien, Connecticut. It is constructed of vertical wood siding, steel Lally columns, and glass with brick for the chimney (Figure 6). The three floors of the house (Figure 7) are occupied by a two-story living room and dining room, which open to outdoor terraces; a kitchen with service areas on the ground floor; an entrance area, a master bedroom and accompanying bathroom, two individual bedrooms and a bathroom, a guestroom, and library/play balcony overlooking the living room. The house is topped by an outdoor roof deck.

Intellectual, spatial, and structural forms, along with the formative idea presented earlier, are used to structure the description and analysis of the Smith House, both qualitatively and visually. The generic antecedent of the house is a rectilinear block. The intellectual form of the house encompasses both perceptual and conceptual forms. Conceptually, the house was conceived as a rectilinear block configured by manipulation of the most basic architectural elements: column, plane, and mass. The block's inherent geometric order of axes, regulating lines, and symmetry structure the relationships between elements and the spatial and physical massing of the house. The allocation of walls, columns, subdivisions, and additions, as well as the overall massing, is based on ideal geometries and is disciplined through Meier's use of modules and proportional systems such as the 1:√2 ratio. Externally, however, the block does not remain in its platonic state. Meier articulates the mass through additions and subtractions: one side of the block is partially subtracted to emphasize the main stairs whereas two masses are subtracted from the opposite side to create terraces on the ground and first floors. A vertical chimney stands opposite the entrance ramp, and a stair projects outside the block in diagonal relation to the main stairs inside (Figure 8). Perceptually, Meier affirms the dominance of an ideal and abstract aspect of his design through the colorlessness and a-contextualization of the free-standing mass of the house. The wood framing is painted in white, giving the impression of a totally white mass. The outer skin is articulated by window fenestration on one side and the expansive use of glass on the other (Figure 9).

The interior volume of the house is articulated into a distinctive spatial form. Horizontally, the volume is split into three sub-volumes using two planes. Vertically, the interior space is split into two volumetric systems. First, there is a dynamic and expansive volumetric system created by subtracting and interlocking slabs, thus, generating spatial interpenetrations and double volumes (Figure 10a). Second, there is a static volumetric system made of compact and cellular small volumes (Figure 10b). As these cellular volumes are expressed individually-and can only be experienced through sequential progression from one volume to another or via a

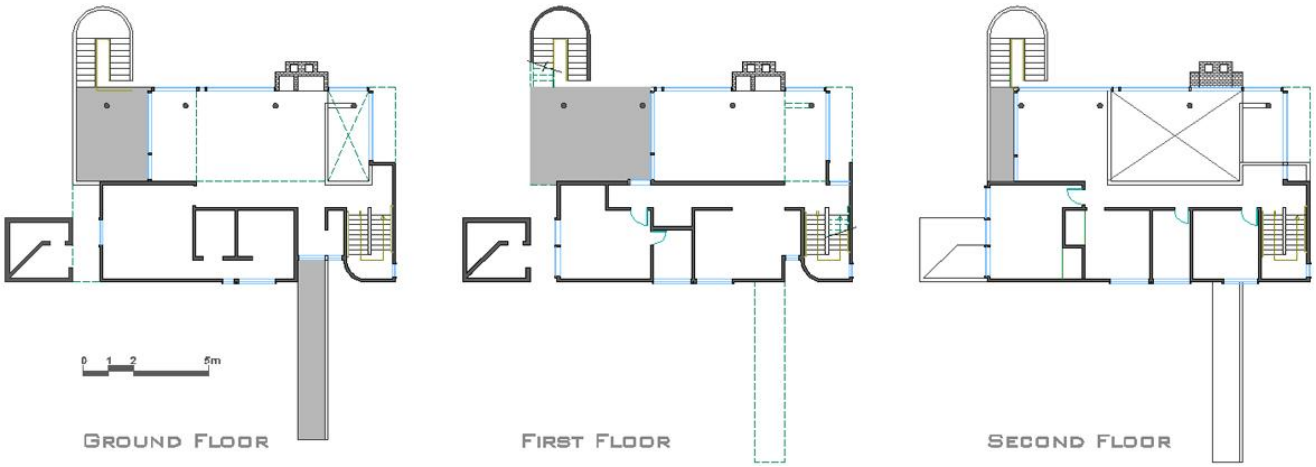

Figure 7. The layout of the Smith house. Redrawn by Author.

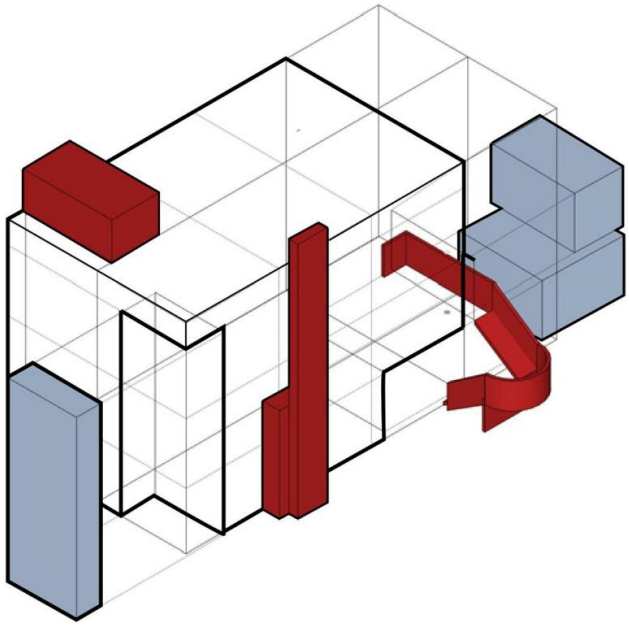

Figure 8. Animation and articulation of the house.

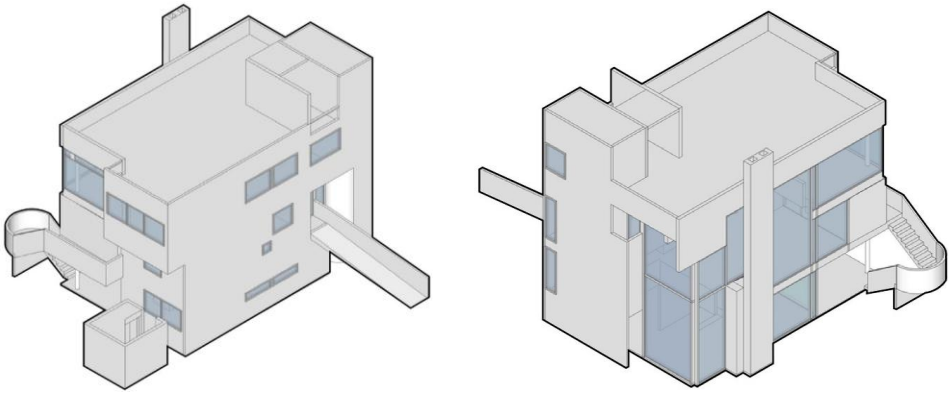

Figure 9. The dual treatment of the outer skin.

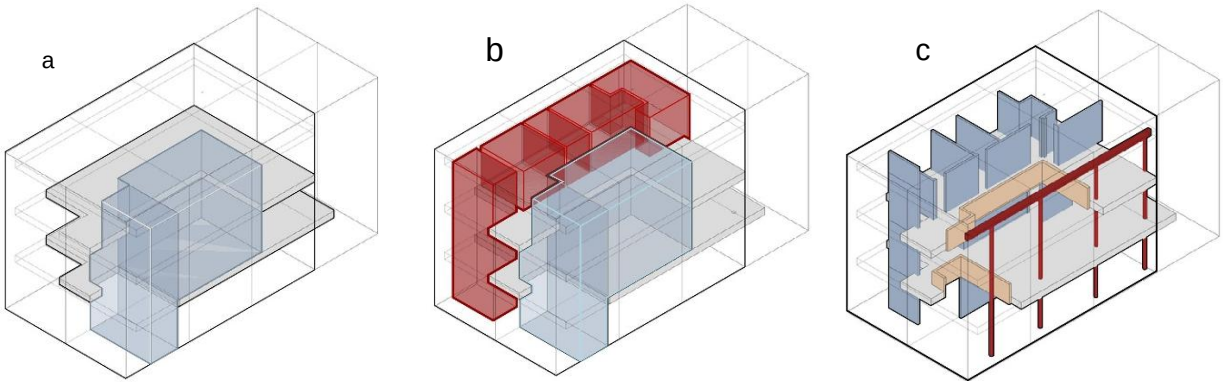

Figure 10. The internal volumetric subdivision of the house.

connecting volume-Meier organized them linearly and inserted a transitional volume that connects the separate volumes and mediates between the cellular and expansive systems. These linearly layered volumetric systems are demarcated by columns and walls (Figure 10c). Inside the house, they express a programmatic separation of the public and private. The cellular volumetric system houses the private activities such as the bedrooms, bathrooms, kitchen, and service areas whereas the expansive zone houses the open spaces such as living areas, the library, and the dining area. The corridor running parallel to the main axis of the house mediates these functional zones on each floor.

The structural form of the house enables the creation of the volumetric systems through the use of a dual structural system. Wood-framed bearing walls surround and support the enclosed cellular system while steel columns and support beams form the structure of the continuous volumetric system (Figure 10c). Meier designed the house in direct contrast with the context such that the whiteness and machine aesthetic of the mass contrasts with the natural green setting of the house. Through this contrast, Meier creates a state of tension and reconciliation between the natural and the man-made, a composite order such that the man-made points to the natural and acts as a stage for appreciating nature.

The question that remains is, Why did Meier design the house in this manner? A partial answer to this question can be traced back to commentary by Colin Rowe (1975), who saw the design of the house as a dialectic scheme between the ideal and abstract (which have to do with formal design systems and principles) and the real and analytic (which have to do with design desiderata made up of constraints drawn from the site and program, circulation and entrance, and structure and enclosure). Thus, the basic formative idea of the house can be identified as the duality of binary oppositions, a duality that divides functions into public and private, enabling the reading of a single block intellectually as mass and surface. It also structures the spatial form into cellular and open volumes, necessitating the use of a dual structural system, and creates a state of tension between the natural and man-made. Table 2 summarizes the description and analysis of the house.

RESULTS AND DISCUSSION

Table 2 shows the theoretical density and repleteness of the Smith House are unraveled and made discrete through the application of the conceptual framework. The constituents of the framework provide an explicit and systematic review of specific concepts related directly to the design of the house. They constitute the main categories according to which the house is described and analyzed, and they frame and structure the qualitative description, stipulating the type of representations needed to express the description. Furthermore, the conceptual framework provides two added values. First, the use of spatial form instead of function or utility as in the Vitruvian triad shifts the focus toward the quality and geometry of space in terms of 3-D volume and visual articulation, away from the qualitative description of activities housed within a space. This enables a better description, both verbal and geometric (that is, diagrammatic), of the functionality of the house and provides a more formal, representative means for manipulation and design in projected future designs. In other words, the provision of functions as 3-D volumes facilitates the formal manipulation and design of projected spaces. Second, the transfer from aesthetics in the Vitruvian triad, which involve appreciation of sensible characteristics of an object or an emotional response to these characteristics, to the intellectual form of an object signifies an intellectual shift toward seeing beyond the sensible appearance and accessing the principles of creation and underlying logic through the application of intelligence. Accordingly, the description and analysis of the Smith House here is concerned with identifying the elements of its design, their relationships, and the principles governing these relationships instead of describing the physicality of the house.

More importantly, a description and analysis of the house based solely on the Vitruvian triad would not address the concept behind the design of the house. The concept of duality guides the design of the house, giving rise to some of the house's properties, which structure the interaction of the intellectual, spatial, and structural forms, uniting them in the final form of the building. Identifying the formative idea of duality explains why the house took its final form and how intellectual, spatial, and structural forms were integrated to express the concept in the built form. By explaining why, the formative idea addresses

Table 2. Summary of the description and analysis of the Smith house.

Conceptual framework		Questions asked	
Formative idea		How did the final form come about and how was everything integrated and reflected upon?	Duality of binary oppositions
Intellectual form	Conceptual form	What are the architectonics of the building in terms of elements, principles, and transformation processes?	Single block Columns, planes, and mass
	Perceptual form	What is the materiality of the building and visual expression in terms of construction and final finish?	Single abstract form with machine-like detailing
Spatial form		What functions are housed and expressed volumetrically with their relationships?	Private/cellular volumetric system Public/continuous volumetric system
Structural form		How was the building constructed and supported?	Load-bearing walls Column and beam
Context			Contrast and tension

the issue of what the designer is trying to achieve over and above the constraints of the functional requirements and particularities of the design language. In that sense, buildings can be perceived as formations with systematic formal aspects such that the various elements that make up their form are not circumstantially brought together but are organized under the systemizing influence of a formative idea.

As seen from the case study, addressing a work of architecture through forms, allows the construction of a framework which answers questions that deal with what to design, how to design it, and how to construct it. The framework categorically identifies the kind of knowledge needed for each question, including the substantive knowledge necessary for understanding what to design, the procedural knowledge addressing how to design, and the reflexive knowledge related to concept formation and critical thinking.

Thus, within the conceptual framework, the Smith House can be understood as a material construction formed by the concept of duality, which structures a specific form comprised of platonic forms juxtaposed in asymmetrical but balanced composition and animated by the use of the basic architectural elements such as point, line, plane, and mass. This form regulates functional requirements into private and public zones, expressed as cellular and continuous volumes that are constructed by a dual structural system of load-bearing walls, columns, and beams. The well-crafted form is then set in contrast with a natural, all-green setting.

Conclusions

This paper proposed a conceptual framework for understanding architectural works. The conceptual framework comprised spatial form, intellectual form, structural form, formative idea, and context. The bridges between the different domains present a structure of the different concepts that constitute an architectural work and enable the understanding of what is a work of architecture. The main thrust of this framework is that it expands the traditional triad of *venustas*, *firmitas*, and *utilitas* to include how to conceptually think about an architectural work. The framework reintroduces context as an integral concept in understanding what a work of architecture is. As such, through its main constituents, the framework answers five basic questions pertaining to analyzing, synthesizing, and evaluating any architectural work: What does a building do and what is the logic of its spatial organization? How is a building physically constructed? How is a building intellectually (that is, formally) structured? Why does a building take its final form? Finally, under what conditions does it take this form? By presenting the basic concepts of designing any work of architecture as forms, this framework avoids the ambiguity of terms such as function and aesthetics and refocuses the attention of the designer on the geometry and visual representations of forms that can be visually expressed, manipulated and articulated.

In that sense, using forms to abstract the materiality of a work of architecture, captures underlying ideas and concepts and represents them visually. The visualization and expression of these forms diagrammatically enables the framework to act as a posteriori framework for architectural analysis and criticism by providing a systematic description and interpretation of built works of architecture. Such a framework can also be used a priori structure to support architects in the conceptual stages of design where it draws the attention of designers to the

basic aspects that need addressing at the beginning of the design process. As such, it is of pedagogical value as a didactic tool for teaching in a design studio or as a framework for architectural morphology.

The 4F_C framework, through the clarification of concepts, depicts the underlying status quo of an architectural work and enables communication between interested communities. By explicating the status quo, this paper offers a platform for structured debate concerning the nature of architecture and architectural works. Further, the shortfalls in the existing body of knowledge open up venues for further reflection and investigation.

Finally, the conceptual framework is a generic, meta-level framework that only describes generalized concepts of relevant and interrelated knowledge necessary for architectural design. This framework provides a new foundation for the development of a more intelligent knowledge-based design model that is relevant for architectural design. Furthermore, each of the concepts within the framework can be further broken down into smaller and more detailed schemas and frames for investigation and modeling.

Conflict of Interests

The author(s) have not declared any conflict of interests.

ACKNOWLEDGEMENT

This research has been made possible by a research grant from the University of Jordan.

REFERENCES

Agudin LM (1995). The concept of type in architecture: An inquiry into the nature of architectural form. PhD dissertation,Swiss Federal Institute of Technology, Zurich, Switzerland.

Aksamija A (2009). Computational representations of architectural design for tall buildings. Complexity 15(2):45-53. http://dx.doi.org/10.1002/cplx.20271

Bafna S (2012). The imaginative function of architecture: A clarification of some conceptual issues. In: Greene M, Reyes J, Castro A (eds.), Proceedings: Eighth International Space Syntax Symposium Santiago, Chile, pp. 1-19.

Capille C, Psarra S (2013). Space and planned informality: Strong and weak program categorization in public learning environments. In: YO Kim, Park HT, Seo KW (eds.),Proceedings of the Ninth International Space Syntax Symposium, Sejong University,Seoul, Korea, pp. 009:1-22.

Clark RH, Pause M (1996). Precedents in architecture (2nd ed.), Van Nostrand Reinhold, New York, NY.

Dahabreh SM (2006). The formulation of design: The Case of the Islip Courthouse by Richard Meier, PhD dissertation, Georgia Institute of Technology, Atlanta, GA, USA.

Dahabreh SM, Abu GA (2012). Design as formulation: From application to reflection. Disegnare idee immagini, 45:76-88.

Dahabreh SM (2014). The architectural design machine (AD_M): Integrating architectural knowledge. Int. J. Appl. Eng. Res. 9(4):483-493.

Economou A, Riether G (2008). The Vitruvian machine. In Proceedings of the 13th International Conference on Computer-Aided Architectural Design: Beyond computer-aided design Chiang Mai, Thailand, pp. 522-528.

Frankl P (1973). Principles of architectural history. Trans. J. F. O'Gorman: MIT Press, Cambridge, MA, (Original work published 1914).

Friedman K (1992). Strategic design taxonomy. Oslo, Norway: Oslo Business School.

Friedman K (2003). Theory construction in design research: Criteria, approaches, and methods. Des. Stud. 24:507-522. http://dx.doi.org/10.1016/S0142-694X(03)00039-5

Gero JS (1990). Design prototypes: A knowledge representation schema for design. AI Magazine 11(4):26-36.

Gero JS, Kannengiesser U (2007). A function-behavior-structure ontology of processes. Artif. Intell. Eng. Des. Anal. Manuf. 21:379-391. http://dx.doi.org/10.1017/S0890060407000340

Gharibpour A (2012). Definition of architecture: Rethinking the Vitruvian triad. Int. J. Arch. Urban Dev. 2(4):51-58.

Greefhorst D, Poper E (2011). A conceptual framework for principles: The cornerstones of enterprise architecture. Springer Verlag, Berlin, Germany, Vol. 4.

Gropius W (1947). Design Topics. Mag. Art 40:229-244.

Guba EG, Lincoln YS (1994). Competing paradigms in qualitative research. In N. K. Denzin & Y. S. Lincoln (eds.), Handbook of Qualitative Research, Thousand Oaks, CA, pp. 105-117.

Hendrix J (2012). Theorizing a contradiction between form and function in architecture. South Afr. J. Art Hist. 27:9-28.

Hillier B (2007). Space is the machine: A configurational theory of architecture. London, UK: Space Syntax.

Hillier B, Hanson J, Peponis J (1984). What do we mean by building function. In J. A. Powell et al., Designing for building utilization. London, UK: Spon.

Jabareen Y (2009). Building a conceptual framework: Philosophy, definitions, and procedure. Int. J. Qual. Meth. 8(4):49-62.

Kolodner J (1993). Case-based reasoning. Morgan Kaufmann, San Francisco, CA.

Lang J (1987). Creating architectural theory: The role of behavioral sciences in environmental design. VNR, New York, NY.

Levering B (2002). Concept analysis as empirical method. Int. J. Qual. Meth. 1(1):35-48.

Markus T (1987). Buildings as classifying devices. Environment and Planning B: Plan. Des. 14:467-484. http://dx.doi.org/10.1068/b140467

McGinty T (1979). Concepts in architecture. In J. C. Snyder & A. J. Catanese (eds.), Introduction to architecture, McGraw-Hill, New York, NY, pp. 208-235.

Meyer S, Fenves SJ (1992). Adjacency structures as mappings between function and structure in discrete static systems (Report no. 45). Carnegie Mellon University Department of Civil and Environmental Engineering, Pittsburgh, PA.

Norberg-Schulz C (1965). Intentions in architecture. MIT Press, Cambridge, MA

Peponis J (2005). Formulation. J. Arch.10(2):119-133.

Peponis J, Wineman J (2002). The spatial structure of environment and behavior. In R. Bechtel & A. Churchman (eds.), Handbook of Environmental Psychology, Wiley, New York, NY. pp. 271-291.

Piotrowski A (2001). On the practices of representing and knowing architecture. In A. Piotrowski & J. Williams Robinson (eds.), The discipline of architecture, University of Minnesota Press, Minneapolis, pp. 40-60.

Rosenman MA, Gero JS (1997). Collaborative cad modelling in multidisciplinary design domains. In: Maher ML, Gero JS, Sudweeks F (eds.), Formal aspects of collaborative computer-aided design, University of Sydney, Sydney, Australia, pp. 387-403.

Rosenman MA, Gero JS (1998). Purpose and function in design: From the socio cultural to the techno-physical. Des. Stud. 19(2):161-187. http://dx.doi.org/10.1016/S0142-694X(97)00033-1

Rowe C (1975). Five architects. Oxford University Press, Oxford, UK.

Schumacher P (2011). The autopoiesis of architecture (Vol. 1): Wiley, Chichester, UK.

Semper G (2011). The four elements of architecture and other writings.

Trans. H. F. Mallgrave & W. Herrmann, Cambridge University Press, Cambridge, UK.(Original work published 1851).
Shields PM, Rangarajan N (2013). A playbook for research methods: Integrating conceptual frameworks and project management. Stillwater, OK: New Forums Press.
Simon H (1998). The sciences of the artificial (3rd ed.). Cambridge, MA: MIT Press.
Steele F (1973). Physical setting and organizational development. Cambridge, MA: Addison Wesley.
Stein JM, Spreckelmeyer KF (1999). Classic readings in architecture. New York, NY: WCB/McGraw-Hill.
Stiny G, Gips J (1978). Algorithmic aesthetics: Computer models for criticism and design in the arts. University of California Press, Berkeley.
Stiny G, March L (1981). Design machines. Environ. Plan. B. 8:245-255. http://dx.doi.org/10.1068/b080245
Tzonis A (1992). Huts, ships and bottleracks: Design by analogy for architects and/or machines. In Cross N, Dorst K, Roozenburg N (eds.), Research in design thinking, Delft University Press, Delft, Netherlandspp. 139-164
Ulrich KT (1988). Computation and pre-parametric design (Report No. 1043). Cambridge, MA: MIT Artificial Intelligence Laboratory.
Unwin S (2003). Analyzing architecture (2nd ed.). London, UK: Routledge.
Unwin S (2008). An architecture notebook (3rd ed.). London, UK: Routledge.
Wotton SH (1897). The elements of architecture. Springfield, MA: F. A. Basstte. (Original work published 1624).
Zarzar KM (2003). Use and adaptation of precedents in architectural design: Toward an evolutionary design model PhD dissertation, Delft University Press, Delft, Netherlands.

academicJournals

Related Journals Published by Academic Journals

- International NGO Journal
- International Journal of Peace and Development Studies